Soft Tissue Sarcomas

3

David M. Parham, Sue C. Kaste, Anand Raju, and M. Beth McCarville

Overview and Classification

Soft tissue tumors can be broadly defined as neoplasms that arise within connective tissue and supporting structures such as blood vessels, nerves, muscle, and adipose tissue. However, this fails to convey the principle that these lesions may arise within viscera as well as soft tissue, and that most of the tumefactions of connective tissue represent reactive or inflamed tissue rather than autonomous growths.

WHO Classification

In 2005, 2013 [1], the World Health Organization (WHO) included cell types updated a classification system of soft tissue neoplasms that was based on two factors: supposed cell of origin (or phenotype), and behavior, the latter separated into benign, borderline, and malignant lesions. Table 3.1 lists the WHO classification as published at that time, although a few modifications have since been suggested [1]. Most of these lesions affect children and adolescents of various ages, and even the ones that primarily occur in adults will occasionally arise in pediatric patients. This classification has great value in systematizing diagnosis and predicting behavior, but it suffers from the fact that there are a great number of heterogeneous entities, few of which occur with sufficient regularity to perform prospective therapeutic trials in a timely fashion, even in large multi-institutional trials such as run by the Children's Oncology Group (COG).

Grading

The problem of treating a large, heterogeneous group of diagnoses, most being rare entities, has been partially solved by the COG with the use of sarcoma grading. In 1987, the Pediatric Oncology Group (POG) began a prospective trial testing the value of grading in prognosis and stratification of childhood soft tissue sarcomas other than rhabdomyosarcoma or Ewing tumors. A system based on both histological diagnosis and more traditional factors such as mitotic count and necrosis was devised [2] (Table 3.2) and effectively separated patients with good and bad outcomes [3].

A sarcoma grading system was also devised by Coindre et al. for the Fédération Nationale des Centres de Lutte Contre le Cancer (FNLCC) [4] and is based on scoring of three parameters: mitoses, necrosis, and differentiation (Table 3.3). In a retrospective study of POG patients, this system also predicted tumor behavior of pediatric sarcomas [5].

Morphologic Classification

Pediatric soft tissue tumors can be separated into broad morphological categories, as an aid for differential diagnosis and ancillary testing. However, tumors overlap considerably among categories; for example rhabdomyosarcoma may be a round cell, spindle cell, epithelioid, or myxoid neoplasm, and there are fibroma-like variants of epithelioid sarcoma.

A list of round cell soft tissue neoplasms appears in Table 3.4. These lesions comprise blastemal neoplasms with little or no differentiation, so that a large panel of ancillary tests may be necessary for diagnosis. The initial approach with these lesions is to consider the most commonly occurring ones—rhabdomyosarcoma, Ewing sarcoma, lymphoma, and

D.M. Parham, M.D. (✉)
Department of Pathology and Laboratory Medicine, Children's Hospital Los Angeles/University of Southern California, 4650 Sunset Blvd., #43, Los Angeles, CA 90027, USA
e-mail: daparham@chla.usc.edu

S.C. Kaste, D.O.
Radiological Sciences, St. Jude Children's Research Hospital, 262 Danny Thomas Place, Memphis, TN 38105-3678, USA
e-mail: sue.kaste@sdude.org

A. Raju, M.D. • M.B. McCarville, M.D.
St. Jude Children's Research Hospital, Memphis, TN, USA
e-mail: beth.mccarville@stjude.org

D.M. Parham et al. (eds.), *Pediatric Malignancies: Pathology and Imaging*,
DOI 10.1007/978-1-4939-1729-7_3, © Springer Science+Business Media New York 2015

Table 3.1 WHO classification of soft tissue neoplasms

Adipocytic neoplasms
Fibroblastic/myofibroblastic neoplasms
Fibrohistiocytic neoplasms
Smooth muscle tumors
Pericytic tumors
Skeletal muscle neoplasms
Vascular neoplasms
Chondro-osseous neoplasms
Neoplasms of indeterminate histogenesis

Table 3.2 Pediatric oncology group grading system for childhood sarcomas

Grade 1
Myxoid and well-differentiated liposarcoma
Well-differentiated or infantile (<4 years old) fibrosarcoma
Well-differentiated or infantile (<4 years old) hemangiopericytoma
Well-differentiated malignant peripheral nerve sheath tumor
Angiomatoid malignant fibrous histiocytoma
Deep-seated dermatofibrosarcoma protuberans
Extraosseous myxoid chondrosarcoma
Grade 2
<15 % of the surface area shows necrosis
Mitotic count <5 mitotic figures/10 hpf with 40× objective
Nuclear atypia is not marked
The tumor is not markedly cellular
Grade 3
Pleomorphic or round-cell liposarcoma
Mesenchymal chondrosarcoma
Extraskeletal osteogenic sarcoma
Malignant triton tumor
Alveolar soft part sarcoma
Any other sarcoma not included in grade 1 and showing >15 % necrosis and/or >4 mitotic figures/10 hpf with 40× objective

Table 3.3 FNLCC system for grading sarcomas

Differentiation score
1: Closely resembles normal adult mesenchymal tissues
2: Resembles normal mesenchymal tissues but not closely
3: Embryonal, undifferentiated, or indeterminate histogenesis
Mitotic count (hpf, a hpf measures 0.1734 mm^3)
1: 0–9/10
2: 10–19/10
3: >19/10
Geographic necrosis
0: None
1: <50 % of tumor
2: >49 % of tumor
Grade
1: Total score of 1–3
2: Total score of 4–5
3: Total score of 6–8

Table 3.4 Round cell neoplasms

Rhabdomyosarcoma
Lymphoma/leukemia
Neuroblastoma
Ewing sarcoma
Desmoplastic small round cell tumor
Synovial sarcoma
MPNST
Germinoma
Round cell liposarcoma
Small cell osteosarcoma
Mesenchymal chondrosarcoma
Undifferentiated sarcoma
Histiocytic lesions such as giant cell tumor of tendon sheath
Organ-based embryonal tumors such as Wilms tumor and hepatoblastoma

Table 3.5 Spindle cell soft tissue tumors

Nodular fasciitis
Proliferative fasciitis/myositis
Fibromatosis of various types
Myofibrosarcoma
Inflammatory myofibroblastic tumor
Dermatofibrosarcoma protuberans
Juvenile xanthogranuloma/benign fibrous histiocytoma
Infantile fibrosarcoma
Adult-type fibrosarcoma
Monophasic spindle cell synovial sarcoma
Solitary fibrous tumor
Myxoinflammatory fibroblastic sarcoma
Spindle cell rhabdomyosarcoma
Undifferentiated sarcoma, particularly pleomorphic sarcoma (“MFH”)
Gastrointestinal stromal tumor (GIST)
Leiomyosarcoma
Schwannoma
Neurofibroma
MPNST
Angiomatoid fibrous histiocytoma
Plexiform fibrohistiocytic tumor
Dedifferentiated liposarcoma

neuroblastoma—and then to tailor the immunostain panel to exclude these lesions. Positively staining lesions may be confirmed by genetic tests, and if discrepancies or unresolved results occur, a wider test panel can be used for less common tumors.

Spindle cell neoplasms are listed in Table 3.5. Unlike round cell neoplasms, many in this group are benign, but they may be locally aggressive and frequently recurrent. Many of the malignant lesions are relatively common in adults but rare in children. Often, they comprise fibroblastic tumors, for which immunostains may have limited utility after myogenic and neural neoplasms have been excluded.

Table 3.6 Epithelioid soft tissue neoplasms

Epithelioid sarcoma
Vascular tumors
Epithelioid rhabdomyosarcoma
Epithelioid GIST
Rhabdoid tumor of soft tissue
Epithelioid MPNST
Myomelanocytic tumors of soft tissue (PEComas)
Monophasic epithelial cell synovial sarcoma
Alveolar soft part sarcoma
Clear cell sarcoma of soft tissue
Myoepithelial tumor of soft tissue (parachordoma)
Perineurioma
Sclerosing epithelioid fibrosarcoma

Table 3.7 Myxoid soft tissue neoplasms

Intramuscular myxoma
Lipoblastoma
Myxoid liposarcoma
Well-differentiated liposarcoma/atypical lipomatous tumor
Pleomorphic liposarcoma
Myxoinflammatory fibroblastic sarcoma
Myxofibrosarcoma
Myxoid DFSP
Giant cell fibroblastoma
Schwannoma
Neurofibroma
Extraskeletal myxoid chondrosarcoma
Embryonal rhabdomyosarcoma
Myxoid leiomyosarcoma
Myxoid solitary fibrous tumor
Low-grade fibromyxoid sarcoma

Epithelioid neoplasms, are listed in Table 3.6, but with the exception of hemangiomas comprise an uncommon group of entities. Some, like perivascular epithelioid cell tumors (PEComas) and alveolar soft part sarcoma, have no non-neoplastic cellular counterpart. Others, like epithelioid sarcomas, myoepithelial tumors, or clear cell sarcomas of soft tissue, represent mesenchymal counterparts of carcinomas, pleomorphic adenomas, or melanomas respectively. Still others represent rare variants of other soft tissue sarcomas such as malignant peripheral nerve sheath tumor, rhabdomyosarcoma, or synovial sarcoma. All are characterized by cells with abundant, variably eosinophilic cytoplasm, cell junctions, and variable staining for epithelial markers like cytokeratin and epithelial membrane antigen.

Myxoid neoplasms are listed in Table 3.7. These all contain variable, often predominant, amounts of loose, mucoid stroma rich in proteoglycans. This category contains lesions that have traditionally been difficult to diagnose and hard to predict, but current genetic testing has eased much of this burden, and new tests are described on a regular basis. Most of these are benign neoplasms, intermediate tumors, or low-grade sarcomas, but they may progress to high-grade lesions. For example, myxoid liposarcoma is a low-grade sarcoma that has a high-grade counterpart, round cell liposarcoma. Similarly, low-grade fibromyxoid sarcomas may progress into cellular, aggressive lesions upon recurrence.

Approach to Imaging of Soft Tissue Tumors

Evaluation of soft tissue tumors often begins with obtaining a clinical history and performing a physical evaluation, with the patient's age being critical in narrowing the differential diagnosis. The presenting concern is often a palpable mass, with larger lesions frequently presenting with pain. Important clinical information includes the presence of any pre-existing conditions, location, duration, growth pattern of the lesion, overlying skin abnormalities, changes in appearance of the mass, and any associated systemic symptoms [6].

Imaging studies are usually required when the clinical and physical examination findings do not completely define the diagnosis. Imaging is used to determine tumor extent and relation of the mass to surrounding anatomic structures. Imaging can also differentiate the origin of the mass from bone or soft tissues when this cannot be delineated on physical examination.

When soft tissue lesions are small and superficial, ultrasound is usually the investigation of choice because it is readily available, relatively easy to perform, lacks ionizing radiation, has no contraindications, is low cost, and does not require sedation or general anesthesia. High-frequency linear array transducers should be used to evaluate soft tissue masses, with the complimentary use of convex array transducers for larger and deeper lesions. Ultrasonography is particularly helpful in distinguishing solid from cystic lesions. Routine use of spectral and color Doppler is necessary to determine whether intra-lesional blood flow exists and to assess the amount of flow within the lesion [6]. The ability to show blood flow by color Doppler increases the specificity of the diagnoses of vascular and inflammatory lesions. The specificity of gray-scale ultrasonography in the diagnosis of soft tissue tumors is only about 40 %; however, ultrasound is useful in planning further imaging [6, 7].

Despite being expensive and sometimes requiring sedation or general anesthesia, magnetic resonance imaging (MRI) is the imaging modality of choice for evaluating pediatric soft tissue masses because of its high tissue contrast and multiplanar capabilities, and it is an excellent modality for most large and deep lesions. MRI is particularly important in presurgical management of soft tissue tumors to determine the soft tissue extension and the relationship of the tumor to the bone, neurovascular structures, and the joint. This modal-

ity is also used to monitor the response of soft tissue tumors to therapy. Combining T1- and T2-weighted imaging forms the basis of MRI. Fat-suppressed images are helpful in evaluating lesions in subcutaneous tissues. Most soft tissue masses have similar features on MR images: hypointense on T1-weighted (T1W) images, hyperintense on T2-weighted images, and a pseudocapsule.

Gadolinium-enhanced MR imaging is important in evaluating tumor viability and perilesional soft tissue edema. While MRI may be of limited utility in determining a particular diagnosis it can help in differentiating benign from malignant processes. Malignant MRI characteristics include heterogeneous signal, neurovascular encasement, invasion of bone, and asymmetric margins. MRI is crucial for verifying the extent of the lesion, which helps in determining resectability [7]. Multiplanar capabilities allow delineation of the 3-dimensional relationship of a soft tissue mass to adjacent structures.

The role of other modalities, including plain radiography and computed tomography (CT), is very limited. Plain radiography may be used to evaluate and assess the bony involvement of a soft tissue mass or the osseous origin of a presumed soft tissue lesion. The role of CT in evaluating soft tissue tumors is limited because tissue characterization is not well defined by CT. However, CT is helpful in detecting calcification or ossification within a lesion but is usually used with MRI when this is in question. CT should rarely be used as the primary imaging modality because it requires radiation exposure to the patient and yields less tissue contrast than does MRI [6–8].

Positron emission tomography (PET) has a growing role as an imaging modality that is used with MR and CT imaging to detect the primary site, assign stage, and direct management of sarcomas. PET imaging with F^{18}-fluorodeoxyglucose (FDG-PET) and FDG-PET/computed tomography (PET-CT) are increasingly important imaging techniques in the noninvasive evaluation and monitoring of known or suspected malignant disease in children. The advent of dual-modality PET/CT imaging systems has added unprecedented diagnostic capability by revealing the precise anatomic location of metabolic information, thus allowing metabolic characterization of normal and abnormal structures [9].

Fibroblastic Tumors

Pediatric fibroblastic tumors comprise a heterogeneous array of diverse lesions that must be discriminated from reactive processes. Pediatric reparative tissues often contain exuberant proliferations of fibroblasts and myofibroblasts, necessitating careful observation and clinical correlation. Quasineoplastic lesions may show abnormal fibroblastic growth, such as IgG4 plasma cell proliferations, soft tissue HHV8, mycobacterial, or Histoplasma infections, or poorly understood lesions such as sclerosing mediastinitis. However, some lesions formerly considered reactive "inflammatory pseudotumors" have now been shown to be clonal proliferations derived from specific genetic mutations or translocations.

Fibroblastic Tumors of Intermediate Malignancy

Infantile Fibrosarcoma

Definition: Infantile fibrosarcoma is a low-grade but locally invasive fibroblastic neoplasm that typically arises in the extremities of newborns. It contains a characteristic chromosomal translocation shared by morphologically and clinically diverse infantile neoplasms.

Clinical Features and Epidemiology

Infantile fibrosarcomas are relatively uncommon lesions, comprising about 10 % of pediatric sarcomas in many series [2, 10]. However, they comprise a substantial component of congenital and infantile soft tissue sarcomas [11]. As such they generally arise in very young infants and are one of the most common forms of soft tissue sarcoma in this age group. These lesions usually form large, bulky, expansile tumors that extensively invade adjacent tissues, including bone. They most commonly arise from the distal portions of the extremities, particularly the forearm and lower leg, but unexpected origins such as heart and lung have been reported [12].

Imaging Features

Infantile fibrosarcoma (IFS) often presents as a rapidly enlarging soft tissue mass in an extremity at or shortly after birth. These tumors may cause a violaceous skin discoloration similar to hemangiomas. Superficial skin ulcerations communicating with large draining veins can result in life-threatening bleeding. The most common plain radiographic finding of IFS is a soft tissue mass that grows rapidly on follow-up imaging. There have been no reports of tumor ossification or matrix calcification (Fig. 3.1a) [13, 14]. The adjacent bone may show deformity and cortical thickening with failure of normal tubulation. Destruction of bone is rare and associated with extensive soft tissue tumors that may cause widespread bony erosion. Bone destruction, when present, is usually well defined and associated with periosteal reaction only very late in the process [13, 15]. There are only a few reports of the sonographic appearance of IFS [15–17]. In one report this tumor appeared as a homogenous hyperechoic mass, while others report a mass with solid and

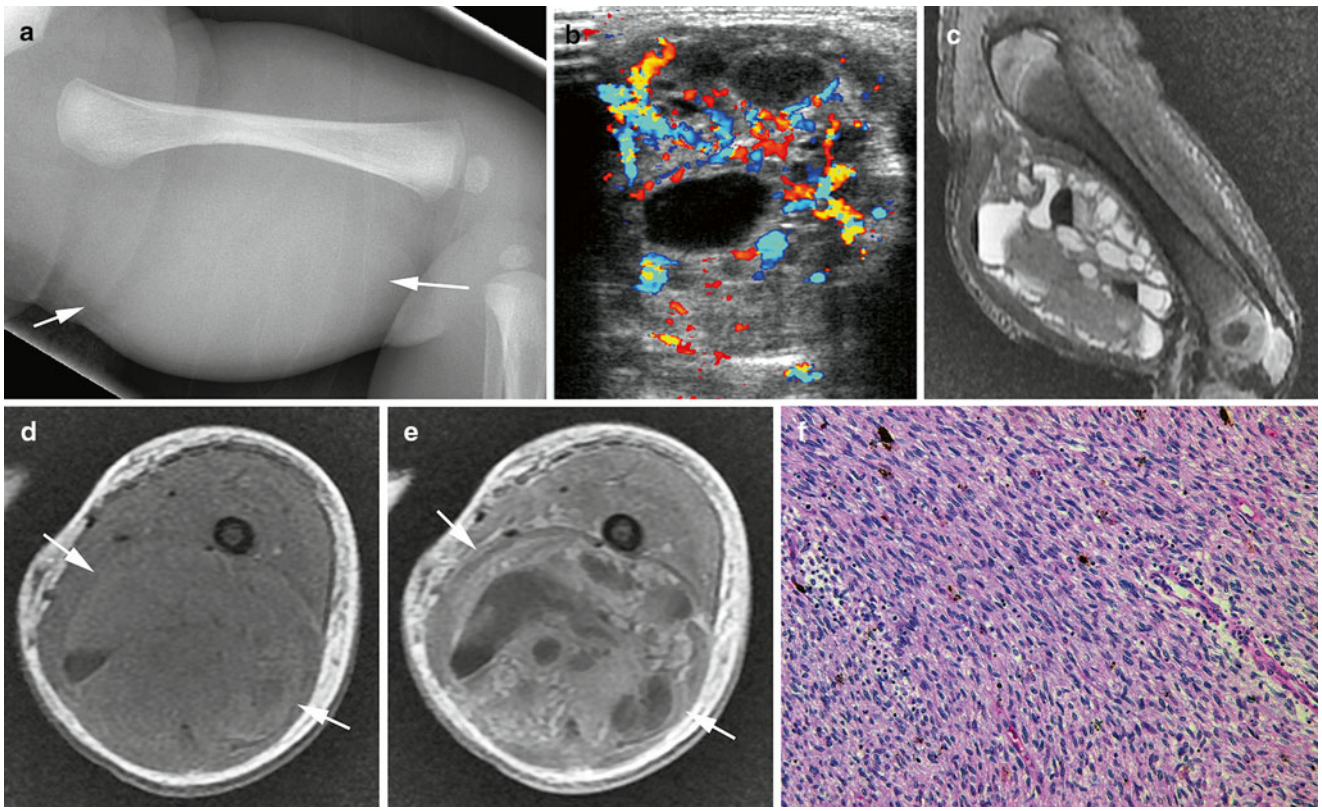

Fig. 3.1 Infantile fibrosarcoma. A 2-month-old boy presented with right thigh swelling subsequently diagnosed with infantile fibrosarcoma. (**a**) Lateral radiograph shows large soft tissue mass (*arrows*) without matrix calcification or bone involvement. (**b**) Transverse Doppler ultrasound image shows a hypervascular mass with cystic and solid components. (**c**) Sagittal T2W MR image shows a large, well-circumscribed, solid and cystic soft tissue mass without bone involvement. Note fluid-fluid levels and variability of signal within cysts due to blood products. (**d**) Axial T1W MR image shows a heterogeneous mass (*arrows*) that (**e**) enhances heterogeneously after contrast administration. (**f**) Histologically, infantile fibrosarcoma comprises streaming dense fascicles of spindle cells resembling the "herring bone" pattern of adult fibrosarcoma

cystic components and mixed echogenicity or a mass that was isoechoic with muscle. Doppler ultrasound may demonstrate the hypervascular nature of these tumors (Fig. 3.1b). CT has the advantage of demonstrating bony involvement; however, it exposes the patient to the potentially harmful effects of radiation.

MRI is the preferred cross-sectional imaging modality because it avoids radiation and provides superior soft tissue characterization and delineation of tumor margins, features important in surgical planning. When tissue planes are violated, or neurovascular involvement is present, surgical resection alone is unlikely to provide local control [13, 14]. On MRI these tumors appear as mixed solid and cystic masses due to internal necrosis and hemorrhage (Fig. 3.1c, d). Initially the solid components appear intermediate or hypointense on T1W images and hyperintense on T2W images due to a high cellular content. As tumors mature they may appear more hypointense on T2W images due to increasing collagen accumulation within areas of fibrosis. Tumors typically demonstrate a heterogeneous pattern of contrast enhancement (Fig. 3.1e) [13, 14, 17]. Conventional or MR angiography will show tumor hypervascularity with disorganized vessels and large draining veins [13, 15, 18, 19].

Molecular Genetics

Infantile fibrosarcomas contain a reciprocal translocation, the t(12;15)(p16;q25) [20], which fuses the *TEL* (or *ETV6*) proto-oncogene on chromosome 12 with the *NTRK3* on chromosome 15. These genes are located on the distal long arms of the two chromosomes and were not discovered until relatively recently compared with other established translocations [20]. Also known as *ETV6*, *TEL* encodes a helix-loop-helix DNA transcription factor that is often dysregulated in childhood acute lymphoblastic leukemia [21]. *NTRK3*, alias *TRKC*, encodes neurotrophin 3, a signal transduction molecule activated by nerve growth factor and expressed by some neuroblastomas [22]. The fusion transcript produced by this translocation acts as an aberrant tyrosine kinase capable of transformation of multiple cell lineages [23]. Neoplasms associated with the *TEL-NTRK3* fusion include infantile fibrosarcoma, cellular mesoblastic nephroma, congenital bronchopulmonary myofibroblastic tumor, and secretory carcinoma of the breast [24].

Gross and Microscopic Features

Infantile fibrosarcomas produce bulky, invasive, fibrous masses that have a whorled, pale grey, nonencapsulated appearance like that of other fibrous lesions. Microscopically, the tumor extensively infiltrates and destroys adjacent fat, connective tissue, muscle, underlying bone, and overlying skin. Lesional cells display plump to elongated spindly profiles with a high degree of cellularity and mitotic activity (Fig. 3.1f). In spite of these factors and the presence of geographic necrosis, these lesions should be considered grade 1 sarcomas [2]. The tumor cells form whorled arrays, often with the classic herringbone pattern, or they may display a hemangiopericytomatous appearance reminiscent of infantile myofibroma [25].

Immunohistochemistry and Other Special Stains

Ancillary stains have limited value in the diagnosis of infantile fibrosarcoma. As expected, vimentin, smooth muscle actin, and occasionally desmin are positive, reflecting their myofibroblastic content. Trichrome stains highlight intercellular collagen, and reticulin stains reveal investment of the tumor cells by a fine lacework of reticulin fibers, characteristic of fibrosarcoma and hemangiopericytoma.

Molecular Diagnostic Features and Cytogenetics

Besides the t(12;15) described above, infantile fibrosarcomas often contain extra copies of chromosome 8, 11, 17, and 20 [26], particularly chromosome 8, but these are common in other sarcomas. Both Fluorescence In-situ Hybridization (FISH) and Reverse Transcriptase-Polymerase Chain Reaction (RT-PCR) can be profitably used to diagnose lesions with *TEL-NTRK3* fusions [27, 28]. This testing has recently been utilized to define new categories of non-fibrosarcomatous infantile sarcoma [29] and to diagnosis infantile fibrosarcoma in unexpected locations [12].

Prognostic Features

In spite of its ominous appearance, infantile fibrosarcoma generally shows only local aggressiveness and infrequently metastasizes [30]. However, its destructive nature frequently leads to radical local surgery, such as amputation, but preoperative chemotherapy may decrease its size and allow a more conservative approach [31].

Sclerosing Epithelioid Fibrosarcoma

Definition: Sclerosing epithelioid fibrosarcoma is a low-grade fibrosarcoma containing fibroblastic cells embedded in a dense collagenous stroma.

Clinical Features and Epidemiology

Sclerosing epithelioid fibrosarcoma is a rare neoplasm recognized only recently and primarily occurring in young adults, but with an age range that includes adolescents [32]. The lesions most commonly occur in the lower extremities, but diverse sites have been reported [33]. Approximately one-third have metastasized at presentation, and about 85 % eventually metastasize, belying the low-grade histological appearance. Only 89 patients had been reported by 2008 [33]. Lesions may arise in bone as well as soft tissue [34].

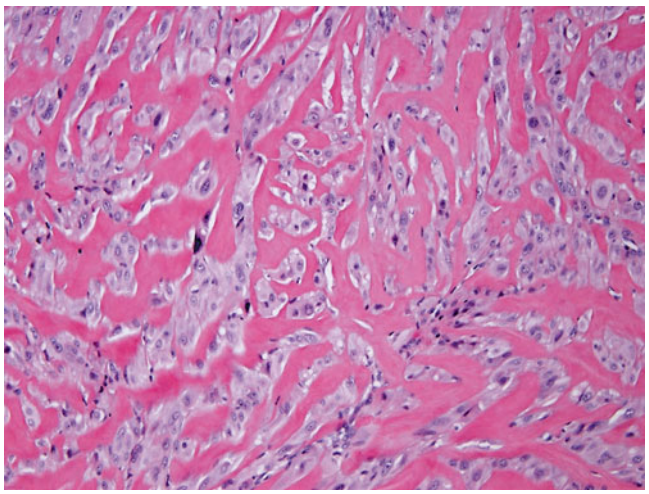

Fig. 3.2 Sclerosing epithelioid fibrosarcoma. Dense strands of thick, osteoid-like collagen intersect cords of epithelioid fibroblasts

Imaging Features

The imaging features of sclerosing epithelioid fibrosarcoma have not been well described.

Molecular Genetics

Sclerosing epithelioid fibrosarcomas contain rearrangements of the *FUS* gene similar to those occurring in low-grade fibromyxoid sarcoma (see below) [35, 36]. This suggests that it represents a variant of that tumor and not a separate, distinct entity.

Gross and Microscopic Features

Sclerosing epithelioid fibrosarcomas are densely fibrous, invasive lesions with destruction of adjacent tissues, including bone. This latter feature may lead to confusion as to whether it has a bony or soft tissue primary site [34]. Microscopically this leads to difficulty in diagnosis, as the tumor contains a densely sclerotic collagenous stroma resembling osteoid (Fig. 3.2). The stroma invests bland appearing, monomorphic, epithelioid cells [32] that form nests and cords resembling carcinoma.

Immunohistochemistry and Other Special Stains

Immunohistochemistry has limited value in the diagnosis of sclerosing epithelioid fibrosarcoma. EMA, S100, and cytokeratin positivity may be seen [32].

Molecular Diagnostic Features and Cytogenetics

Cytogenetic analysis of sclerosing epithelioid fibrosarcoma may reveal multiple chromosomal rearrangements [37]. *FUS* rearrangement may be detected by FISH [35].

Prognostic Features

Unfortunately, in spite of its low-grade appearance, sclerosing epithelioid fibrosarcoma is an aggressive lesion that shows chemoresistance [34]. Therefore, survival is linked to the adequacy of excision. Head and neck lesions appear to fare worse than those in other sites, and overall survival is about one-third at 3.5 years, with approximately the same number surviving with disease [33].

Myofibrosarcoma

Definition: Myofibrosarcoma, also known as low-grade myofibroblastic sarcoma [38], is a neoplastic with features intermediate between fibrosarcoma and leiomyosarcoma. It is generally a low- to intermediate-grade sarcoma that is locally aggressive but showing limited capacity for distant spread [39].

Clinical Features and Epidemiology

Myofibrosarcoma is an uncommon lesion that occurs in both children and adults, primarily the latter. In children, it has a predilection for the head and neck region [40]. It is a locally invasive lesion that may involve the bone of the maxilla or mandible.

Imaging Features

There is limited literature regarding the imaging features of myofibrosarcoma. In one case report the tumor arose from the nasal bone in a 4-year-old girl and was a small, solid, well-defined mass causing bone thinning on CT imaging. On MRI it appeared as a homogenous solid mass, isointense to muscle on T1W images and hyperintense on T2W images. After administration of gadolinium contrast the tumor demonstrated homogenous enhancement [41].

Molecular Genetics

At present, there are no genetic features that distinguish myofibrosarcoma.

Gross and Microscopic Features

Grossly, myofibrosarcomas form infiltrative, pale grey lesions with invasion and destruction of adjacent tissues. Microscopically, they contain whorls and bundles of cells with fusiform nuclei and moderate amounts of pink to purple cytoplasm (Fig. 3.3). The tumor cells may form storiform arrays. These lesions are composed of myofibroblasts, which are ultrastructurally defined by the presence of ergastoplasm, peripheral microfilaments, and anchoring filaments (fibronexus junctions) [42].

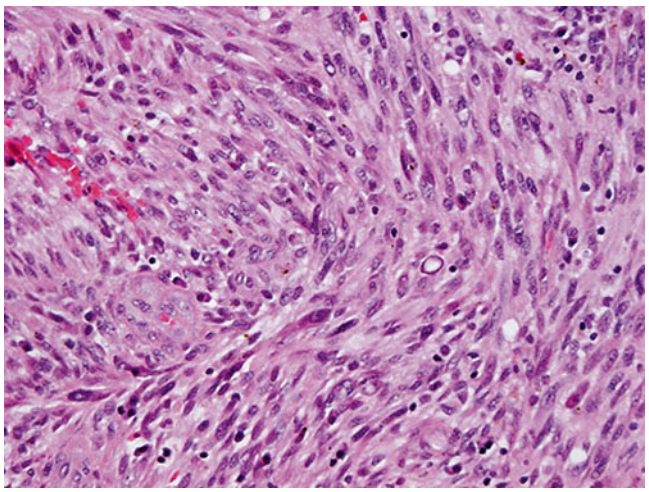

Fig. 3.3 Myofibrosarcoma. Dense, whorled bundles of plump spindle cells contain mildly enlarged fusiform nuclei and tapering purplish cytoplasm

By convention, low-grade myofibrosarcomas show moderate atypia and mitotic activity [38]. With higher grade features, one should consider the diagnosis of pleomorphic undifferentiated sarcoma ("malignant fibrous histiocytoma") [43, 44]. Myofibroblastic sarcomas thus exhibit a range of histological appearances.

Immunohistochemistry and Other Special Stains

As with ultrastructure, the combination of a smooth muscle and fibroblastic phenotype defines myofibrosarcoma. Thus, all lesions are vimentin-positive, most are smooth muscle actin- or muscle-specific actin-positive, and some are desmin-positive [39]. However, they are negative for calponin, separating them from leiomyosarcoma [45], and for myogenin or MyoD, separating them from rhabdomyosarcoma [46].

Molecular Studies

Molecular testing in myofibrosarcoma is primarily an exercise in exclusion, as they have no distinguishing features. However, their lack of ALK or TEL rearrangements separates them from inflammatory myofibroblastic tumor or infantile fibrosarcoma, respectively [43, 47], and they do not show the beta catenin pathway alterations typical of desmoid fibromatosis [48].

Prognostic Features

Myofibrosarcomas are relatively low-grade, indolent sarcomas that infrequently metastasize, so the major feature that predicts behavior is the adequacy of excision. They frequently recur, with untoward consequences in head and neck locations [40].

Low-Grade Fibromyxoid Sarcoma

Definition: Low-grade fibromyxoid sarcoma, a very descriptive term, is a connective tissue neoplasm of intermediate malignancy and mixed fibrocollagenous and mucinous stromal content.

Clinical Features and Epidemiology

In the pediatric age spectrum, low-grade fibromyxoid sarcoma mostly arises in adolescents, and it also occurs in young adults [49]. It usually arises in the lower extremity and groin but may affect unusual sites such as the big toe [50]. It is a rare lesion, but it is consistently included in large retrospective reviews of fibrosarcomatous lesions [51].

Imaging Features

A recent review of the imaging of 22 patients with low-grade fibromyxoid sarcoma found that most tumors arose in the deep soft tissues of the lower extremity and had an average size of about 6 cm. Tumors were solitary at diagnosis but multiple at local recurrence. On plain radiography tumors were visible as soft tissue masses without calcification or bone involvement. On sonography tumors were solid with intralesional nodules and predominantly hypoechoic at the periphery and hyperechoic centrally. Arterial flow was evident by Doppler evaluation. On non-contrast enhanced CT the tumors were heterogeneous but predominantly hypodense to muscle with internal isointense areas. After contrast administration most tumors contained peripheral or internal enhancing areas. On CT several tumors had internal calcifications that were puntate or linear and several showed bone erosion. On MRI most tumors were hypo- or isointense to muscle on T1W images and were hyperintense on T2W sequences. Many displayed a unique brain gyriform pattern of alternating folds of hypo- and hyperintense signal intensity or had intralesional nodules evident on T2W sequences. Contrast enhancement was variable and felt to reflect high cellularity of fibrous tissue, which appeared hypointense on T2W sequences and enhanced intensely, and non-enhancing myxoid tissue that appeared hyperintense on T2W imaging [52].

Molecular Genetics

A reciprocal translocation affecting chromosome 16, the t(7;16)(q33;p11) or the t(11;16)(p11;p11), characterizes low-grade fibromyxoid sarcoma [36] and respectively fuses *CREB3L1* or *CREB3L2* with *FUS*. *FUS* encodes a protein involved in transcriptional activation and protein/RNA binding. Both CREB3L1 and CREB3L2 belong to the leucine zipper family of transcription factors and normally activate stress proteins in the endoplasmic reticulum.

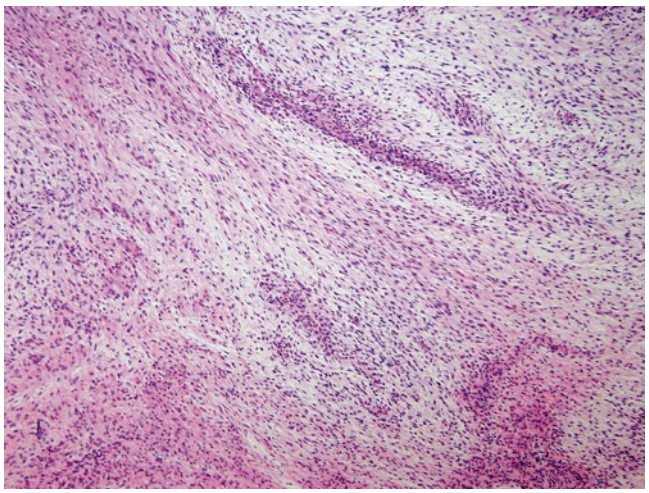

Fig. 3.4 Low-grade fibromyxoid sarcoma. Bundles of fibroblastic cells enmeshed in collagen alternate with relatively hypocellular strands of myxoid stroma

Gross and Microscopic Features

Low-grade fibromyxoid sarcoma forms deceptively well-circumscribed but nonencapsulated masses, with well-contoured, fibrous to myxoid cut surfaces [49]. Low power magnification reveals contrasting areas of myxoid and fibrous stroma, containing cells arrayed in a swirling growth pattern (Fig. 3.4) [53]. The tumor cells have a deceptively bland appearance and consist of fibroblasts and occasional myofibroblasts [49]. However, with progression and recurrence the lesions can become increasingly cellular with moderate pleomorphism [53].

Some low-grade fibromyxoid tumors contain foci of giant rosettes with collagenous cores rimmed by round to oblong nuclei. This lesion was originally described as a separate neoplasm, "hyalinizing spindle cell tumor with giant rosettes" [54]. However, it is now considered a variant and not a distinct entity, as it bears the molecular abnormalities of low-grade fibromyxoid tumor.

Immunohistochemistry and Other Special Stains

As with most fibroblastic neoplasms, immunohistochemistry has limited value in diagnosis of low-grade fibromyxoid sarcoma, which mostly stains with nonspecific markers such as vimentin but with occasional positivity for cytokeratin and actin [49]. Of note, the cells surrounding rosettes stain for neural markers such as S100, neuron-specific enolase, and Leu 22 [54]. Because of the characteristic gene fusions, there is overexpression of MUC4, which can be used for ancillary diagnosis [55, 56].

Molecular Diagnostic Features and Cytogenetics

Molecular studies offer confirmation of the diagnosis of low-grade fibromyxoid tumor and separate it from other fibrocollagenous and myxoid neoplasms [57, 58]. FISH is a suitable means for detecting FUS rearrangement [59], and RT-PCR detects most tumors [60], with the caveat that fusion variants may not be detected in a single probe study.

Array studies of low-grade fibromyxoid sarcoma show a characteristic gene expression pattern, with upregulation of *FOXL1* and *CD24* [56].

Prognostic Features

Accurate prediction of low-grade fibromyxoid sarcoma behavior requires years of follow-up, as recognized in the initial reports of this lesion [53]. Most deaths do not occur until after 5 years, as the tumor appears to pursue a slow, relentless course if not completely excised at initial surgery. On the other hand, long-term survival is possible even with metastasis [49].

Malignant Fibroblastic Neoplasms

"Adult-Type" Fibrosarcoma

Adult-type fibrosarcomas are distinguished from infantile fibrosarcomas not only by the obvious age difference but also by molecular features and clinical behavior. As fibroblastic neoplasms have become increasingly subcategorized, the entity of adult-type fibrosarcomas has become vanishingly rare, particularly in the pediatric age group [51], so they will not be further discussed. Rare childhood cases may occur as second malignant neoplasms or post-irradiation sarcomas [61].

So-Called Fibrohistiocytic Tumors

The term "fibrous histiocytoma" has been the source of considerable debate in recent years, as many of these tumors are derived from neither fibroblasts nor histiocytes. Benign and intermediate lesions in this category often have features of dermal dendrocytes [62, 63], whereas malignant lesions have been a "wastebasket" category for a wide variety of pleomorphic, undifferentiated sarcomas [64, 65]. However, this category of lesions persists because of its historical stature and its familiarity among pathologists and clinicians, largely because of its characteristic storiform histology.

Intermediate Fibrohistiocytic Neoplasms

Dermatofibrosarcoma Protuberans (DFSP)/ Giant Cell Fibroblastoma

Definition: Dermatofibrosarcoma protuberans (DFSP) and giant cell fibroblastoma comprise a spectrum of low-grade malignancies characterized by a *COL1A1/PDGFB* fusion and typically occurring in superficial soft tissues.

Clinical Features and Epidemiology

Both DFSP and fibrosarcoma most commonly occur in dermal and subcutaneous tissues, which they expand in a plaque-like fashion. Although they are locally invasive, they rarely metastasize. DFSP more commonly occurs in young adults, whereas giant cell fibroblastoma more commonly occurs in young children. Some tumors show both histologies or convert subtypes with recurrence. Occasionally, lesions occur in deep soft tissues.

Imaging Features

Gross imaging characteristics of DSFP demonstrate involvement and location in the skin and subcutaneous adipose tissue with rare involvement of the underlying muscle. Radiographically, a nodular or multinodular soft tissue mass lacking calcifications is seen [66–69]. Typically, bony infiltration and periosteal reaction are absent [66]. Rarely, these tumors demonstrate more aggressive behavior with violation of dermal planes, bony infiltration [66], and intracranial extension [70, 71].

Because of the typically superficial location of these nodular/multinodular lesions, ultrasound can provide important information regarding the size, dermal and fascial plane involvement, and, in cases of involvement into the deep soft tissue layers, tumor effect on adjacent tissues and structures (Fig. 3.5a). Ultrasound characteristics vary from decreased echogenicity through iso-echogenicity and hyperechogenicity relative to adjacent soft tissues [72, 73]; lesions may demonstrate heterogeneous echotexture [74]. Moderate to increased vascularity may be demonstrated [72, 75]. Histopathologic correlation revealed hypoechoic areas to be composed of tumor cells and those of heterogeneous echogenicity to be composed of fibrous tissues intermixed with tumor cells [76].

DFSP lesions may be multiple small nodules or coalesce into a plaque. Linear extensions along the skin and satellite lesions may be demonstrated. Tumor attenuation is similar to or greater than that of muscle [67]. These lesions lack calcifications by CT, may be lobulated [72], and demonstrate enhancement with intravenous contrast administration [72].

MR signal characteristics are nonspecific and on T1- and T2-weighted sequences are similar to or slightly less intense than muscle and similar to or more intense than fat on T1- and T2-weighted sequences, respectively (Fig. 3.5b–d). On short tau inversion recovery (STIR) or fat suppressed T2-weighted sequences (Fig. 3.5b–d), signal is typically increased but may be heterogeneous in the presence of necrosis or hemorrhage; cystic areas and fluid-fluid levels may result [74, 77, 78]. DSFP lesions enhance moderately with gadolinium contrast administration [68, 69, 77]. MR is particularly useful for preoperative planning [69, 78–80]. One case report suggests that a negative choline peak on (1H) MR spectro sccopy (MRS) may be useful in suggesting the diagnosis of DFSP in a highly vascular subcutaneous mass [81].

DFSP are known to recur and are typically readily identifiable clinically. Limited experience suggests that 18F FDG PET imaging is useful in detecting small sites of disease recurrence [82].

Molecular Genetics

COL1A1 PDGFB fusions characterize both DFSP and giant cell fibroblastoma [83]. DFSPs typically contain ring chromosomes with multiple copies *COL1A1/PDGFB* [84], whereas giant cell fibroblastomas more often contain a reciprocal t(17;22)(q22;q13) [85]; some contain an unbalanced translocation [86]. Pigmented DFSP (Bednar tumor) and myxoid DFSP also contain the *COL1A1/PDGFB* fusion [83].

Gross and Microscopic Features

Grossly, both DFSP and giant cell fibroblastoma form grey-tan fibrous lesions with nonencapsulated, infiltrative borders, with the latter having a looser appearance. Myxoid variants of DFSP have a somewhat gelatinous appearance, whereas the pigmented variant may be brown or brownish-yellow.

Microscopically, DFSP contains distinctive pinwheel-shaped bundles of spindle cells arranged in a storiform pattern, resembling the weave in a wicker-bottom chair (Fig. 3.5e). A rich microvasculature usually nourishes these lesions. Modest mitotic activity, up to 5 mitoses per 10 high power fields, is typically present. The borders of DFSP characteristically infiltrate adjacent soft tissues, entrapping collagen bundles, nerves, and vessels and showing no hint of encapsulation. Sometimes this phenomenon imparts a somewhat neural appearance, with a suggestion of waviness and streaming.

Some lesions contain similar plump spindle cells, but with a marked reduction in cellularity and increase in myxoid stroma. These myxoid variants may contain larger, pleomorphic giant cells that segue into giant cell fibroblastoma. Pigmented lesions, known as Bednar tumors, contain melanin. Some DFSPs have a fibrosarcomatous component with greater cellularity, larger, more pleomorphic cells arranged in a herringbone pattern, and more mitoses [51].

Giant cell fibroblastomas have much less cellularity and contain loose bundles of collagen separated by ectatic blood vessels and slender, wavy tumor cells. Sprinkled within this matrix are scattered multinucleated cells with large round nuclei and inconspicuous nucleoli, arrayed around the ectatic vessels or distributed haphazardly (Fig. 3.5f). Giant cell fibroblastoma may also contain zones of higher cellularity that resemble DFSP, and vice versa [87].

Immunohistochemistry and Other Special Stains

Of all stains for confirmation of DFSP/giant cell fibroblastoma, the most useful is CD34, whose positivity in these tumors usually separates them from similar tumors like deep fibrous histiocytoma or juvenile xanthogranuloma [88, 89]. CD34 staining may be lost in foci of secondary fibrosarcoma [90]. Histiocytic markers like CD163, CD68, or Factor XIIIa are expressed by a minority of DFSPs [91].

Molecular Diagnostic Features and Cytogenetics

With DFSP/giant cell fibroblastoma, cytogenetics may demonstrate a ring chromosome or the t(17;22), and RT-PCRT or FISH can show *COL1A1/PDGFRB* fusion [86, 92].

Prognostic Features

DFSP and giant cell fibroblastoma are low-grade sarcomas with a metastasis rate of less than 10 % [93]. Local recurrence is common after incomplete resection [94]. Lesions with fibrosarcomatous change do not necessarily indicate a worse prognosis, particularly with complete excision [90, 93]. Because of involvement of the PDGF axis, aggressive tumors may be susceptible to therapy with imatinib [95].

Angiomatoid Fibrous Histiocytoma

Definition: Angiomatoid fibrous histiocytoma is a low-grade, cystic neoplasm occurring in subcutaneous tissues and containing blood-filled spaces surrounded by cells resembling histiocytes.

Clinical Features and Epidemiology

Angiomatoid fibrous histiocytomas usually occur in older children and adolescents. In the original series [96], the median age was 13 years. Originally, these lesions were considered adolescent variants of "malignant fibrous histiocytoma," but because of their indolent behavior the term "malignant" was later dropped [97]. They occur only rarely and comprise 0.3 % of all soft tissue neoplasms [98]. Occasionally patients present with constitutional symptoms, such as fever, anemia, elevated erythrocyte sedimentation rate, and even polyarteritis nodosa [99]. Lesions mostly occur in extremities but may include areas bearing lymphoid tissue, such as the antecubitus, axilla, inguinum, and supraclavicular region [100].

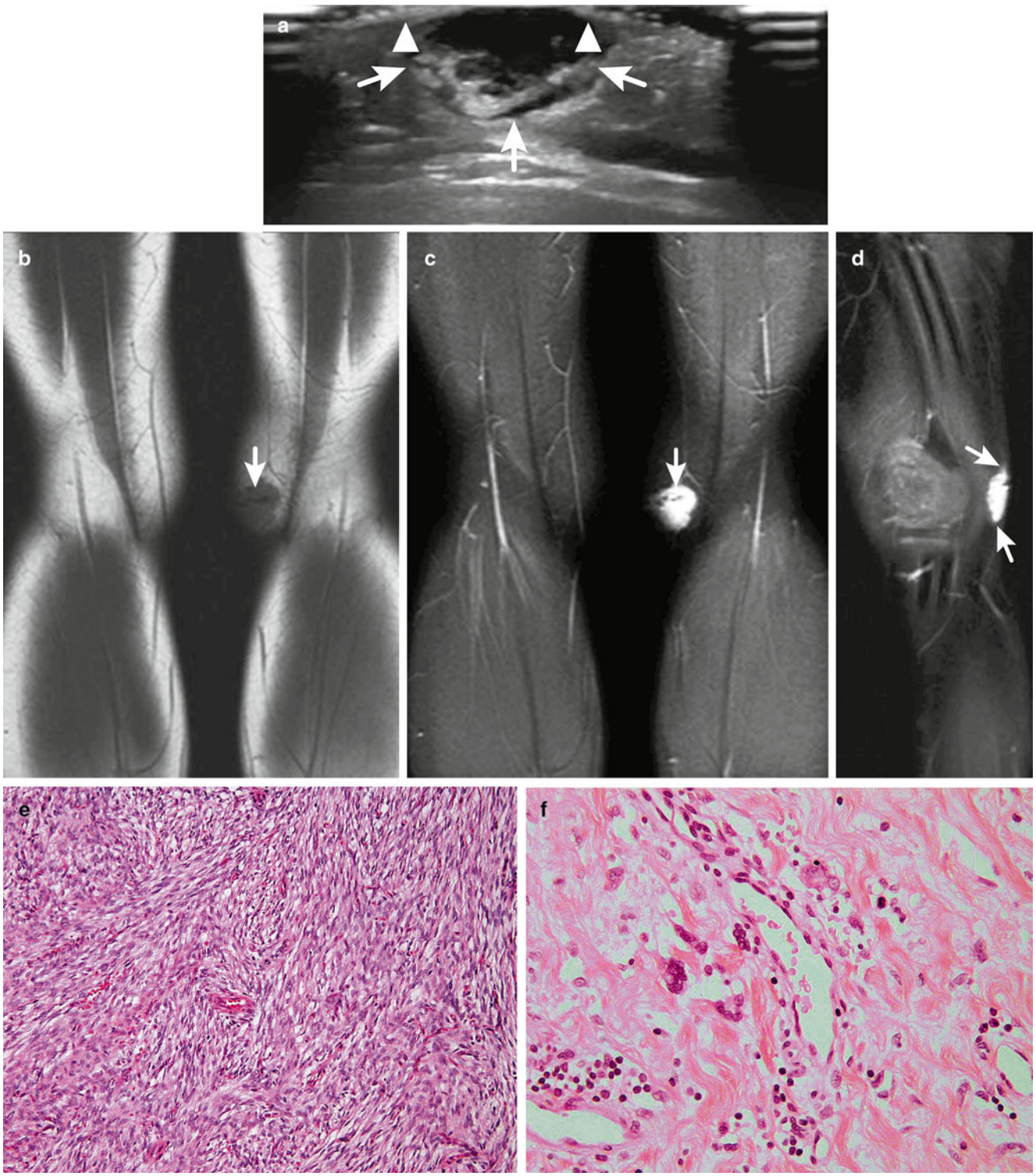

Fig. 3.5 Dermatofibrosarcoma protuberans. (**a**) A 4-year-old boy with a 2×1.8×7 cm mass in the left popliteal fossa, post-incisional biopsy. Longitudinal ultrasound image demonstrates an irregular, heterogeneous nodular soft tissue mass (*arrows*), just deep to the skin (*arrowheads*). (**b**) Coronal non-contrast T1-weighted MR shows the irregular margins of the mass within the subcutaneous fat; the mass is isointense with muscle. (**c**) Short tau inversion recovery (STIR) image shows increased signal emanating from the mass. The horizontally oriented *dark line* (*arrow*) through the mass is the healed surgical scar from prior incisional biopsy. (**d**) The mass enhances briskly with administration of intravenous contrast material on this sagittal contrast-enhanced T1-weighted image with fat suppression. Also note, the tiny strands of enhancing soft tissue extending superiorly and inferiorly (*arrows*) into the adjacent subcutaneous fat. (**e**) Classical dermatofibrosarcoma protuberans containing swirling, tightly interlaced, storiform bundles of spindle cells. (**f**) Giant cell fibrosarcoma with loose collagenous stroma, ecstatic vessels, and multinucleated fibroblasts

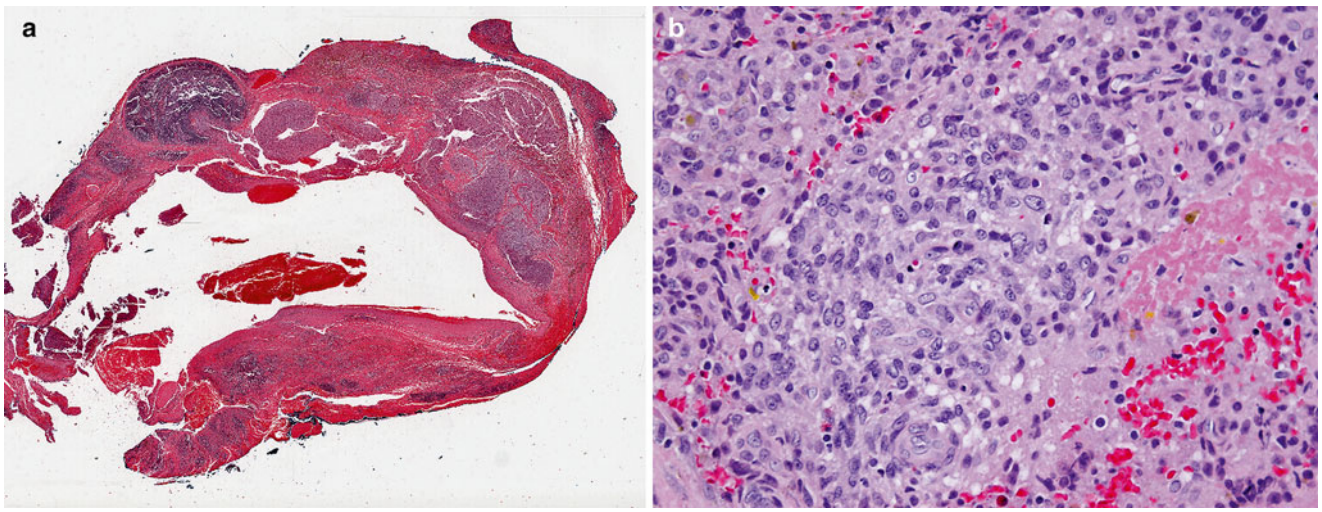

Fig. 3.6 Angiomatoid fibrous histiocytoma. (**a**) Blood-filled cystic spaces and a peripheral shell of lymphocytes characterize the low power appearance of this lesion. (**b**) High power view illustrating plump, histiocytoid tumor cells, moderately pleomorphic nuclei, and scattered erythrocytes and siderophages

Imaging Features

The imaging appearances of angiomatoid fibrous histiocytoma have not been well defined. Several reports, however, describe a striking MRI feature of multiple cystic areas with fluid-fluid levels within a soft tissue mass. These cystic areas and fluid levels correspond to the blood-filled spaces seen histopathologically. While this MR feature may be characteristic of angiomatoid fibrous histiocytoma it is not specific to it. On MR these tumors tended to be well defined by a fibrous pseudocapsule that appeared dark on both T1 and T2W sequences and demonstrated prominent contrast enhancement [101]. A single case of angiomatoid fibrous histiocytoma of bone has been reported. This tumor markedly expanded the bone but did not disrupt the cortex. It contained very large cystic areas with fluid-fluid levels, an appearance similar to aneurysmal bone cyst. However, the cystic areas of angiomatoid fibrous histiocytoma were larger than those typically seen in aneurysmal bone cyst and the septal enhancement was less pronounced. The bone tumor also had a fibrous pseudocapsule similar to that described above for soft tissue angiomatoid fibrous histiocytoma [102].

Molecular Genetics

Angiomatoid fibrous histiocytoma either contains a fusion of *EWSR1* with *ATF1* on chromosome 12, analogous to clear cell sarcoma [103, 104], or more frequently, *EWSR1* with *CREB1*. The latter occurs more frequently, and alternate *FUS-ATF1* fusions may be seen [105].

Gross and Microscopic Features

Angiomatoid fibrous histiocytomas usually occur in superficial soft tissues but occasionally arise in deep locations [103]. They typically form relatively small masses, 2–4 cm in diameter [98]. These form well-circumscribed firm nodules containing blood-filled, cystic spaces (Fig. 3.6a). Microscopically, the nodules contain a peripheral fibrous pseudocapsule with abundant lymphocytes, often bearing germinal centers and creating a strong resemblance to nodal metastases. Central spaces contain blood but do not have a true endothelial lining. Occasional lesions lack cystic spaces but still exhibit the reactive lymphoid shell [100]. Chronic hemorrhage with hemosiderin-laden macrophages is frequent. Single or multiple aggregates of ovoid to plump spindle cells with bland nuclei and amphophilic to lightly eosinophilic cytoplasm comprise the neoplastic component of the tumor (Fig. 3.6b). Occasional lesions show prominent nuclear pleomorphism and mitotic activity [106].

Immunohistochemistry and Other Special Stains

Angiomatoid fibrous histiocytomas often express myoid markers such as desmin and calponin, and occasionally actin and caldesmin, but not MyoD or myogenin [100, 107]. CD99 and CD68 are positive in many cases, but of note, histiocytic/dendritic cell markers like lysozyme, CD21, S100, and CD35 are negative [100].

Molecular Diagnostic Features and Cytogenetics

Break-apart FISH for *EWSR1* may be used for diagnosis of angiomatoid fibrous histiocytoma [108], particularly in cases with atypical histology [106]. Rare lesions lack *EWR1* fusions but show *FUS* rearrangement [108]. Neither FISH nor RT-PCR distinguishes angiomatoid fibrous histiocytoma from clear cell sarcoma, but S100 immunostains may be of value [100].

Prognostic Features

Angiomatoid fibrous histiocytoma is generally an indolent lesion. Metastases occur in less than 5 % of tumors [98]; recurrence is rare in lesions <5 cm [109]. Aggressive behavior

has been associated with adult onset, larger size (>5 cm), deep location, recurrence, and atypical mitoses [109, 110]. Metastases may grow rapidly and show chemoresistance [111]. Predictors of bad outcome include head and neck location and deep invasion, but not histologic parameters like mitotic rate and pleomorphism [97].

Plexiform Fibrohistiocytic Tumor

Definition: Plexiform fibrohistiocytic tumor (PFT) is a borderline neoplasm composed of small nodules of fibrohistiocytic cells and arising in the deep dermis and soft cutis.

Clinical Features and Epidemiology

PFT primarily affects children and young adults, with a median age of 14 years reported in the first large series [112]. However, a wide age range exists within children, and the lesion occasionally arises in infants [112–114]. It preferentially involves the upper extremities, particularly the hand and wrist, but it may also arise in the trunk, lower extremities, and head [115, 116]. Typically PFT arises in the subcutaneous tissues, but sometimes it occurs only in the dermis [117].

PFTs occur relatively rarely, with only occasional examples reported in COG studies. Only 123 cases were reported in the 2007 review by Taher and Pushpanathan [116]. It preferentially affects females, with a female:male ratio of 6:1 [118], but no racial or geographic predilection has been reported [116].

Generally, PFTs present as deep-seated solitary rubbery nodules that raise the overlying skin. They grow slowly and insidiously, often with a long delay in diagnosis of months to years [112].

Imaging Features

The imaging features of this tumor have not been well described.

Molecular Genetics

There have been few genetic or cytogenetic analyses of PFT, probably because of their relative circumscription and presentation. One study reported a 46,X,del(X)(q13), in a single case, but no molecular or cytogenetic features have been described as typical of this lesion [114].

Gross and Microscopic Features

Grossly, PFTs typically form a nonencapsulated, firm, pale grey mass in the deep dermis or subcutis, with an average size of 2.5 cm (range 0.5–8.0 in one series [118]. They may invade underlying skeletal muscle [118].

Microscopically, sections of PFTs exhibit a characteristic multinodular, infiltrative appearance, with small nodules of tumor separated by intervening fibroconnective tissue (Fig. 3.7). The nodules comprise small collections of epithelioid macrophage-like cells or plump spindle cells, in variable proportions. Variable numbers of multinuclear cells infiltrate these foci. Mitotic activity is generally low, <3 per 10 high power fields, and atypical mitoses or significant atypia are unusual features [118].

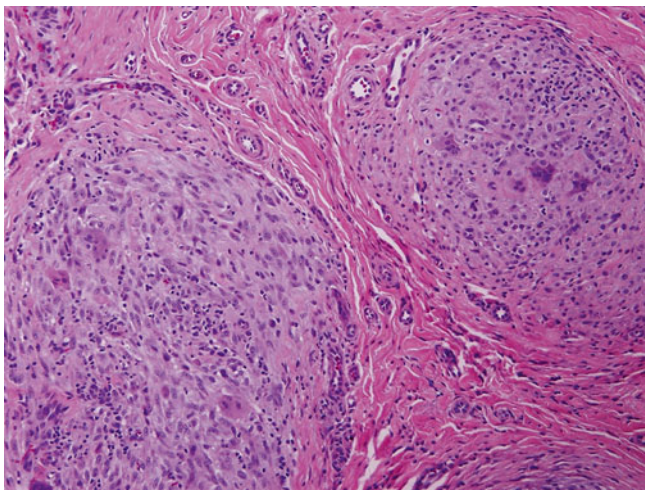

Fig. 3.7 Plexiform fibrohistiocytic tumor. The lesion comprises nodules of spindle cells, monocytoid cells, and giant cells, separated by deep dermal collagen

Immunohistochemistry and Other Special Stains

PFTs express a limited palette of antigens, typically vimentin and smooth muscle actin, with CD68 in epithelioid giant cells. Important negative stains include Factor XIIIa, CD34, NK1C3, and beta-catenin [119].

Molecular Diagnostic Features and Cytogenetics

Genetic studies of PFT have been limited, and no recurring abnormalities are reported [114].

Prognostic Features

Initial studies of PFT suggested that it only rarely metastasized to lymph nodes and never to distant sites [120]. However, newer reports of pulmonary metastasis have appeared. Because of a tendency to recur locally, complete marginal excision of PFT is recommended [116].

Malignant Fibrohistiocytic Neoplasms

Undifferentiated Pleomorphic Sarcoma

Definition: Undifferentiated pleomorphic sarcoma (UPS; formerly called malignant fibrous histiocytoma) is a high-grade, spindle cell sarcoma containing pleomorphic cells that resemble macrophages and showing no more than fibroblastic or myofibroblastic differentiation.

Clinical Features and Epidemiology

Although once the most common adult sarcoma, the incidence of UPS has waned with the advent of molecular and immunological techniques. It is even rarer in children and generally occurs in adolescents [109]. Most commonly, the lesion arises in the extremities, but the head, neck, or trunk may also be primary sites [109]. There appears to be a particular predilection to the head in children [121], who may have a history of prior irradiation [109].

UPS in children differs from that in adults in that most pediatric cases are in the dermis and soft tissues of the head and neck region rather than in the extremities.

Imaging Features

UPS are usually multinodular, well circumscribed, and lobulated. Calcification or ossification may be seen in some tumors. The role of plain radiography is very limited and nonspecific in evaluating these tumors and may show deep, soft tissue swelling, calcification, or underlying osseous involvement (Fig. 3.8a) [122, 123].

On gray-scale ultrasound images, a hypoechoic lesion that is well encapsulated can be seen in the deep soft tissues. Discrete intratumoral echogenic areas with acoustic shadowing may be seen if calcification is present. Intratumoral hemorrhage may be present and usually appears as an echogenic area without acoustic shadowing.

MRI is the modality of choice for evaluating these tumors, which may have varying signal characteristics due to variations in myxoid contents and cellularity. UPS is usually isointense to slightly hyperintense to muscle on T1-weighted images and has heterogeneous signal intensity on T2-weighted images (Fig. 3.8b–d). T1- and T2-weighted images of these tumors may have low-signal internal septations because of fibrous bands or acellular streaks [122, 123].

Molecular Genetics

The molecular features of pediatric UPS mirror those of adult tumors [124]. Particularly noteworthy is amplification of chromosome 12q13-14, containing protooncogenes such as *CHOP, SAS, MDM2,* and *CDK4* [124]. However, this finding suggests that these lesions are dedifferentiated liposarcomas [125, 126].

Gross and Microscopic Features

UPS typically forms bulky, infiltrative masses that may have a fibrous, grey-tan cut surface or contain areas of hemorrhage and necrosis. They often arise within musculature, but subcutaneous and fascial tissues may be involved.

UPS by definition is a pleomorphic spindle cell sarcoma, usually containing variably plump spindle cells arrayed in a storiform pattern (Fig. 3.8e). The tumor cells range from plump spindle cells to epithelioid cells with variable, often striking, degrees of nuclear pleomorphism, atypia, and hyperchromasia. Also by definition, there should be no identifiable line of differentiation other than fibroblasts or myofibroblasts; otherwise, the lesion is best considered a dedifferentiated form of another tumor type. Mitoses are generally frequent, with atypical forms (Fig. 3.8e), and geographic necrosis is often present.

Immunohistochemistry and Other Special Stains

This diagnosis requires a panel of stains to rule out dedifferentiated tumors of other types. One should exclude pleomorphic or dedifferentiated variants of rhabdomyosarcoma, leiomyosarcoma, liposarcoma, and nerve sheath tumors, as well as lymphoma, carcinoma, and melanoma [64]. Otherwise there are nonspecific positive reactions to vimentin and CD68, with weak and variable smooth muscle actin positivity.

Vascular Tumors

Intermediate Vascular Tumors

Kaposiform Hemangioendothelioma

Definition: Kaposiform hemangioendothelioma (KH) is a locally aggressive vascular lesion containing immature endothelial cells arranged in bundles and fascicles, often with platelet trapping.

Clinical Features and Epidemiology

KH typically occurs in young children, often infants, although cases in older children and adults have been recognized. It arises in superficial soft tissue but often involves deep soft tissues, bone, or viscera. Often, patients show signs of consumptive coagulopathy as a result of platelet trapping within the lesion (Kasabach–Merritt syndrome), and lesions may bleed profusely following initial biopsy or incomplete attempts at excision.

Imaging Features

There are few articles describing the imaging features of KH. In one review of 21 children, the main MRI findings were diffuse enhancement after contrast administration, poorly defined tumor margins, skin thickening, stranding of subcutaneous fat, blood product deposits within the tumor and small feeding and draining vessels (Fig. 3.9a, b) [127]. The tumor is locally invasive and there are reports of secondary bone erosion and cortical destruction [128–130]. Tumors grow rapidly and are often associated with skin discoloration [131]. There may be local-regional nodal spread but distant metastasis has not been reported. Common primary sites include the cervicofacial area, extremities, peritoneum, and retroperitoneum [131, 132]. These clinical and imaging features in a patient with Kasabach–Merritt phenomenon should suggest a diagnosis of KH.

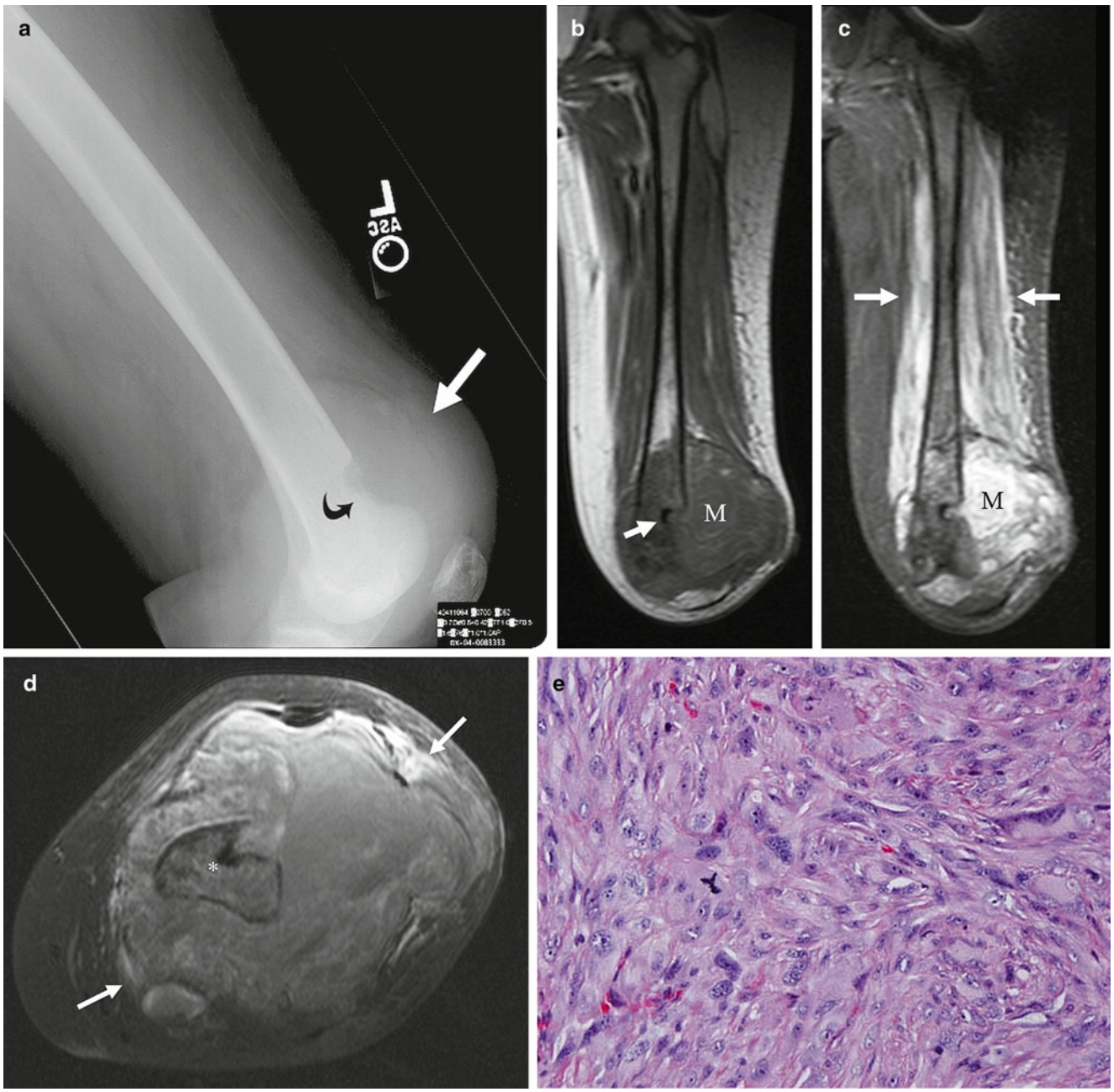

Fig. 3.8 Undifferentiated pleomorphic sarcoma (malignant fibrous histiocytoma) in an 18-year-old boy with primary site in the left thigh. (**a**) This lateral radiograph demonstrates a non-calcified, soft tissue mass (*straight arrows*) that destroys the distal femoral cortex (*curved arrow*). (**b**) On this coronal T1W, non-contrast-enhanced image the mass (*M*) is heterogeneous but predominantly isointense to muscle. Direct invasion of the distal femur is evident (*arrow*). (**c**) The tumor (*M*) is heterogeneous on this T2W coronal image. Involvement of the distal femur is again evident. Extensive surrounding soft tissue edema appears as bright signal throughout the thigh muscles (*arrows*). (**d**) This post-contrast T1W axial image shows heterogeneous but fairly minimal enhancement of tumor (*arrows*) perhaps due to ischemia. Adjacent bone invasion (*asterisk*) is again noted. (**e**) The lesion contains dense, storiform fascicles of pleomorphic cells with large, pleomorphic nuclei and atypical mitosis

Gross and Microscopic Features

Kaposiform hemangioendothelioma forms a hemorrhagic, fibrous mass with poorly circumscribed borders. It comprises small slit-like vascular channels surrounded by spindle to epithelioid cells and arranged in lobules or discrete nodules (Fig. 3.9c). Some lesions contain more discrete, rounded open channels, resembling a hemangioma or bloody lymphangioma, particularly at the periphery. Platelet rich microthrombi, highlighted by CD31, may be seen within nests of pericytes and epithelioid tumor cells. Erythrocyte fragments and hemosiderin may also be conspicuous.

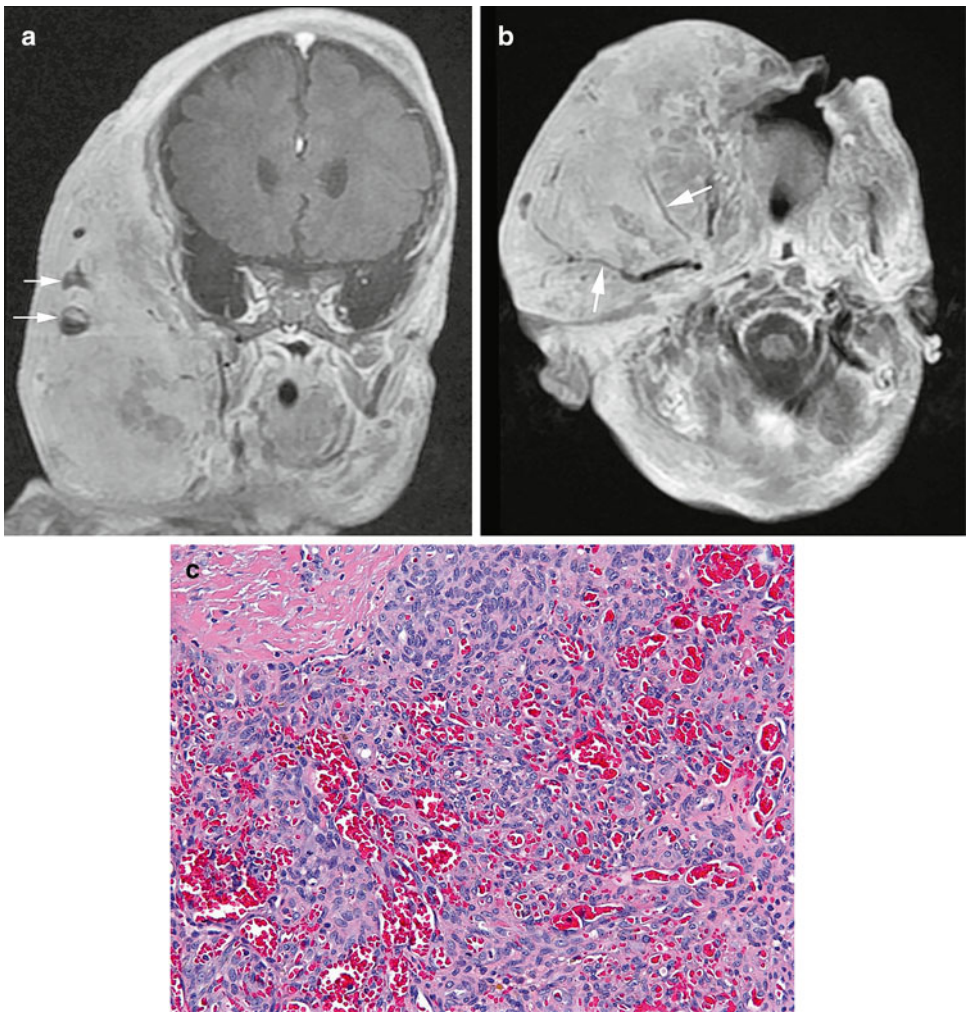

Fig. 3.9 Kaposiform hemangioepithelioma. A 3-week-old with Kasabach– Merritt syndrome and large cervico-facial lesion. (**a**) Coronal T1W contrast-enhanced magnetic resonance image shows an extensive, diffusely enhancing mass involving the right face and neck. Several cystic foci with fluid-fluid levels are due to blood products (*arrows*). (**b**) T1W axial post-contrast image shows diffuse enhancement and numerous small vessels (*arrows*) coursing throughout the tumor. (**c**) Histologically, Kaposiform hemangioendothelioma comprises irregular vascular channels lined by clusters of epithelioid and spindle cells

Immunohistochemistry and Other Special Stains

KH generally shows expression of both lymphatic and blood vascular endothelial markers. These factors appear to be upregulated by Prox-1, a transcription factor that induces programming of blood vessels into lymphatics as well as promoting invasiveness and aggressive behavior [133]. Prox-1 appears to be a good immunomarker of KH and tufted angioma, a rare related tumor [134]. In addition, KH shows biphenotypic expression of CD31, CD34, podoplanin (D2-40), and (variably) factor VIIIa related antigen (von Willebrand factor) [134, 135].

Prognostic Features

KH can be cured with complete excision, but incompletely excised lesions may cause significant bleeding and result in the patients' demise. A variety of medical options are available, including chemotherapy, immune modulators, and radiation [135].

Malignant Vascular Tumors

Angiosarcoma

Definition: Angiosarcoma is an invasive, malignant neoplasm composed of neoplastic endothelial cells forming irregular vascular channels.

Clinical Features and Epidemiology

Angiosarcomas are quite rare in children, but a few published series exist [136–138]. These relatively small series show a wide age range, from infancy through adolescence, with a median of 11 years. The viscera, particularly the heart, are affected among deep lesions [137], and superficial lesions tend to involve the extremities of girls [138]. Lesions may present as cutaneous ecchymoses that are confused with hematoma [138]. A significant proportion have an underlying

genetic defect, such as neurofibromatosis 1 (NF1), hemihypertrophy, or Aicardi syndrome, and there may be a history of prior irradiation [137, 138]. Kasabach–Merritt syndrome is not typically present.

Imaging Features

Imaging characteristics of angiosarcomas, regardless of their location, readily reflect the vascular aggressive nature of this tumor (Fig. 3.10a–e). Most imaging publications describe these tumors in liver and spleen but they may occur elsewhere. Organomegaly [139, 140] and metastatic disease [139, 141] are common findings at the time of diagnosis.

By ultrasound, angiosarcoma and its metastases appear as heterogeneous solid masses with varying degrees of cystic areas that likely represent hemorrhage or necrosis [139, 141].

By CT, angiosarcoma may be nodular or diffuse and it may reveal satellite nodules or punctate calcifications [139–141] (Fig. 3.10a, d, e). It may be mass-like or an en plaque subcutaneous lesion within a lymphedematous extremity. By MR, it has a nonspecific appearance with increased T2 and intermediate T1 signal intensity. Non-enhancing areas of hemorrhage may be seen in areas with increased T1 signal [77, 142] (Fig. 3.10b, c). MR signal characteristics reflect the vascularity and hemorrhage of the lesions. Heterogeneous enhancement that progresses and persists on delayed images can be shown using dynamic contrast-enhanced techniques [143]. Hemosiderin-laden nodules may appear as low-signal intensity foci on all sequences [141, 144].

When angiosarcoma occurs in the extremities, MR can delineate tumor nodules from surrounding lymphedematous soft tissues. It comprises a lobulated mass of low to intermediate signal by T1-weighted imaging. Because of fibrous stroma, these tumors also have decreased signal on T2-weighted sequences. The administration of intravenous contrast results in diffuse or heterogeneous tumor enhancement [72, 142]. Fluid-fluid levels may be present [145].

Though experience is limited, 18F FDG PET appears to have a developing role in grading [146] and staging [147, 148] angiosarcoma. 18F FDG may potentially be useful for distinguishing angiosarcoma from cavernous hemangiomas, as the latter has been reported to have low FDG avidity [149].

Gross and Microscopic Features

Angiosarcomas form hemorrhagic, nodular masses with varying size, often with ill-defined borders resembling hematoma. Histologically, they contain aggregates of irregular vascular channels lined by atypical cells with large, irregular, nuclei (Fig. 3.10f). Both epithelioid and spindle cells form cords, strands, and nests that slice into adjacent fibrofatty or muscular tissue. The vascular channels exhibit irregular, anastomosing profiles with sinusoidal features. Necrosis and mitotic activity are frequent.

Immunohistochemistry and Other Special Stains

Due to the rarity of pediatric angiosarcomas, immunohistological data is sparse, but the tumors express vascular markers such as CD31, CD34, and factor VIII-related antigen (von Willebrand factor). Podoplanin expression is generally absent [137], but cytokeratin expression is not unusual.

Prognostic Features

Pediatric angiosarcomas are usually high-grade sarcomas that exhibit aggressive local invasion and metastasis. Local control is difficult, and the lesions do not respond to traditional chemotherapy [136]. However, there are some survivors [137] particularly among superficial, easily accessed lesions [138].

Malignant Adipose Tumors

Myxoid/round Cell Liposarcoma

Definition: A malignant tumor composed of malignant lipoblasts embedded in an abundant myxoid stroma (myxoid liposarcoma) or forming dense cellular aggregates (round cell liposarcoma).

Clinical Features and Epidemiology

Although liposarcomas now comprise the most common adult sarcoma group, they occur relatively infrequently in children. Nevertheless, they rank first among adult-type sarcomas occurring in the pediatric age group. In one relatively large series of 82 cases [125], there was a roughly 1:2 male:female ratio, and ages ranged from 5 to 22 years, with a median of 15.5 years. The tumors occurred in a wide array of locations, mostly in the soft tissue of extremities. Conventional myxoid and round cell liposarcomas constituted 71 % of cases.

Imaging Features

Myxoid liposarcoma contains prominent myxoid tissue, branching capillaries, and less than 10 % fat, but usually lacks necrosis [72, 150]. Extremity lesions are typically intermuscular [151, 152].

Ultrasound interrogation is useful to characterize the lesion and readily demonstrates its complex, solid nature [77, 152] and hypervascular areas [72]. Decreased attenuation of the lesion as seen on CT may mimic a cyst but can usually be differentiated using ultrasound [152].

CT and MR of myxoid liposarcoma are very similar. It forms a large, usually well-defined lobulated mass when located in soft tissues and has mixed lytic and blastic characteristics when located within the skeleton [151]. Lesions often lack fat signal and demonstrate findings of increased water content [142, 151]. MR typically demonstrates the

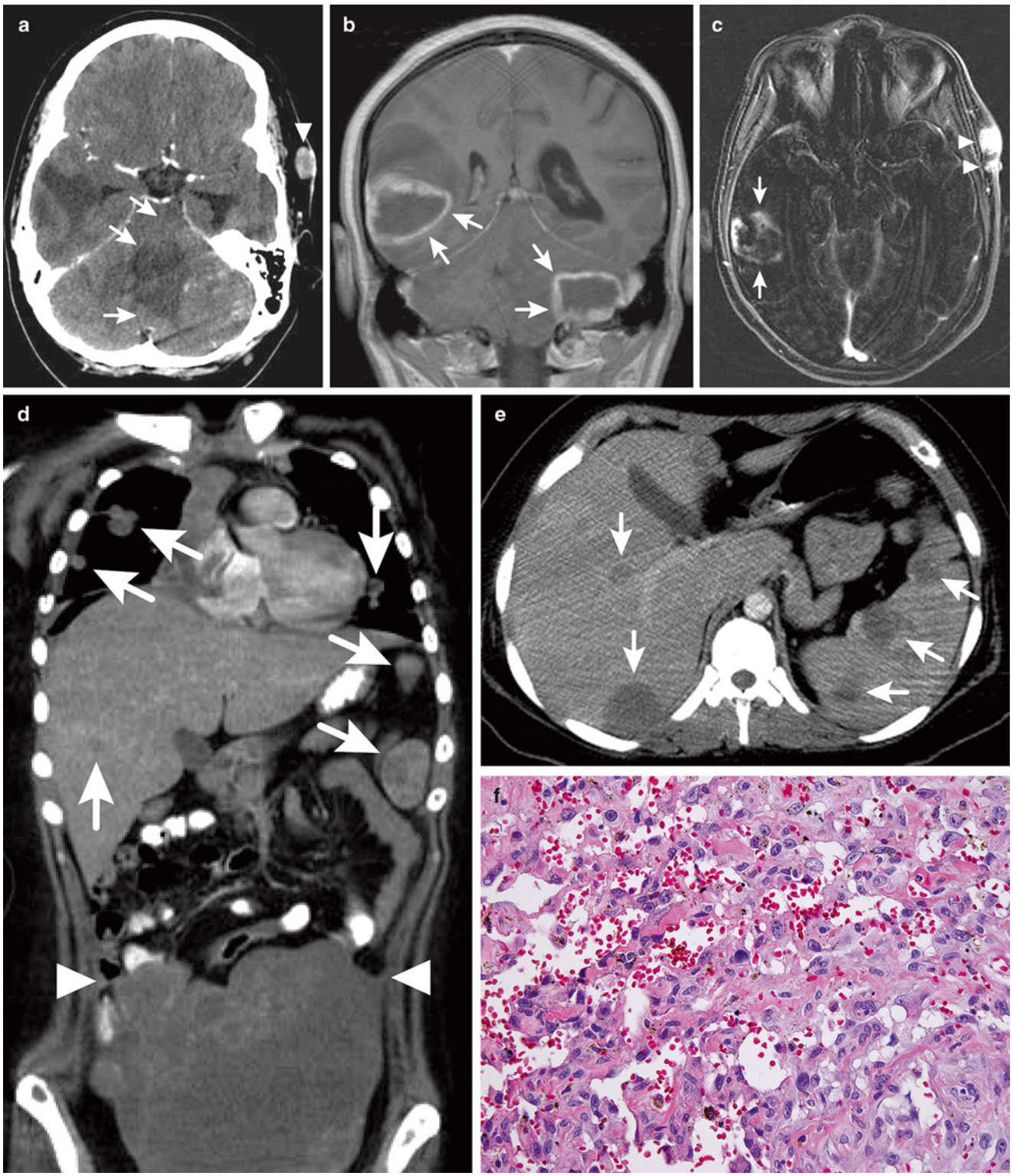

Fig. 3.10 Angiosarcoma. (**a**–**c**). A 19-year-old girl presented with headaches, exacerbated by turning her head, nausea and vomiting. She was subsequently diagnosed with metastatic angiosarcoma. (**a**) Axial contrast-enhanced CT through the temporal lobes. (**b**) Coronal contrast-enhanced T1-weighed MR through the midline brain. (**c**) Axial contrast-enhanced subtracted MR through the temporal lobes images shows multiple heterogeneously enhancing intracranial metastases (*arrows*) associated with vasogenic and effacing the CSF spaces. Note the briskly enhancing subcutaneous nodules in the left temporal region (*arrowheads*). (**d**) Coronal reformatted contrast-enhanced CT showing multiple metastases (*arrows*) involving the lungs, pleura, liver, and spleen. The large heterogeneously pelvic mass enhances heterogeneously and has extension to the adjacent peritoneal surface (*arrowheads*). (**e**) Axial contrast-enhanced CT image through the upper abdomen demonstrates multiple low-density metastases throughout the liver and spleen (arrows). (**f**) A histological section of pediatric angiosarcoma contains irregular vascular channels lined by epithelioid endothelial cells with enlarged, hyperchromatic nuclei

large size and well-defined multilobulated contours [72, 150, 151, 153] (Figs. 3.11a–d). MR characteristics may vary according to the histologic makeup of the lesions [153]. Lesions may mimic a cyst due to the high water content, evidenced on MR by decreased T1- and markedly increased T2-signal intensity [150]. Adipose tissue may be seen as small nodules or located within septations. Intravenous contrast administration may aid by demonstrating enhancing septations in cysts and solid components within sarcomas [72, 150, 153–155]. The extent and distribution of enhancement varies with the distribution of nodularity (peripheral, central, or diffuse) [77] and location (soft tissues or skeleton) [151]. Mucinous areas lack enhancement, leading to a heterogeneous pattern [150]. Areas of round cell proliferation may demonstrate more diffuse enhancement [77]. Areas of hemorrhage may also occur [72].

Molecular Genetics

Myxoid and round cell liposarcoma contain a characteristic t(12;16)(q13;p11) [156] that fuses the *CHOP* and *FUS* genes and creates a chimeric gene product showing transformative properties and affecting transcription of adipogenic genes [157, 158].

Gross and Microscopic Features

Liposarcomas form bulky masses that have lobular contours and yellow to white cut surfaces that resemble fat.

Myxoid liposarcomas contain relatively bland appearing lipoblasts with cytoplasm vacuoles, enmeshed in an abundant myxoid stroma (Fig. 3.11e). Thin arcuate capillaries course through this mileau and recreate an appearance akin to pulmonary edema. Round cell liposarcomas, in contrast, form aggregates and sheets of primitive lipoblasts that resemble other round cell sarcomas (Fig. 3.11f). A mixture of round cell and myxoid foci often occurs. In addition to these classic histologies, Alaggio et al. [125] describe variant forms with large pleomorphic nuclei, giant cells, and atypical mitoses resembling pleomorphic liposarcoma.

Immunohistochemistry and Other Special Stains

Immunohistochemistry has limited value in diagnosis of liposarcoma, but like normal adipocytes these tumors generally express S100.

Molecular Diagnostic Features and Cytogenetics

The *FUS-CHOP* fusion may be detected by RT-PCR, and a *FUS* or *CHOP* rearrangement may be demonstrated by break-apart FISH [159]. *EWS* replaces FUS as the fusion partner of *CHOP* in about 10 % of cases [160] and should be tested by FISH in cases with typical histology and no *FUS* rearrangement.

Prognostic Features

Myxoid liposarcoma is a low-grade malignancy (Grade 1 in the POG grading schema), whereas round cell liposarcoma is a high-grade malignancy (Grade 3 in the POG schema). In Alaggio's series [125], adverse features such as metastases or local recurrence occurred in only 1 of 41 grade 1 liposarcomas but affected 7 of 9 patients with high-grade tumors. Seven of 10 patients with pleomorphic myxoid liposarcoma died of disease.

Well-Differentiated/Dedifferentiated Liposarcoma

Definition: Well-differentiated and dedifferentiated liposarcoma are morphologically divergent tumors of malignant lipoblasts, both characterized by amplification of chromosome 12q13-14.

Clinical Features and Epidemiology

In contrast to myxoid/round cell liposarcomas, well differentiated and dedifferentiated liposarcomas (WD/DDL) are rare in children. Of four adolescent patients described by Alaggio et al. [125], two were male and two were female, with ages ranging from 12 to 19 years. The lesions all involved deep soft tissues. An intriguing report suggests a relationship between constitutional *TP53* mutation and pediatric well-differentiated liposarcoma [161].

In adults, common locations of well-differentiated liposarcoma include the lower extremities (50 %), retroperitoneum (20–33 %), upper extremity (14 %), and trunk (12 %). Extremity lesions are commonly intramuscular but may be intermuscular and subcutaneous. The most common clinical presentation is a patient with a painless, soft tissue mass that has grown slowly over months to years. Retroperitoneal lesions are typically large at diagnosis and have a high local recurrence rate after surgical resection [152].

Imaging Features

WD/DDL may be apparent as a soft tissue mass on plain film radiography. Fat is often seen on plain films of large extremity lesions but is rarely seen in retroperitoneal masses. Calcification is present on radiography or CT in 10–30 % of tumors. Bony involvement is very rare [152].

Sonography typically demonstrates a heterogeneous, multilobulated, well-defined mass. The identification of hyperechoic fat within WD/DDL on ultrasound is not sensitive or specific, as other pediatric tumors, such as germ cell tumor and lipoblastoma, contain fat [152].

On CT and MRI, well-differentiated liposarcoma usually appears as a predominantly (about 75 %) lipomatous mass containing non-fat components. such as thick septa

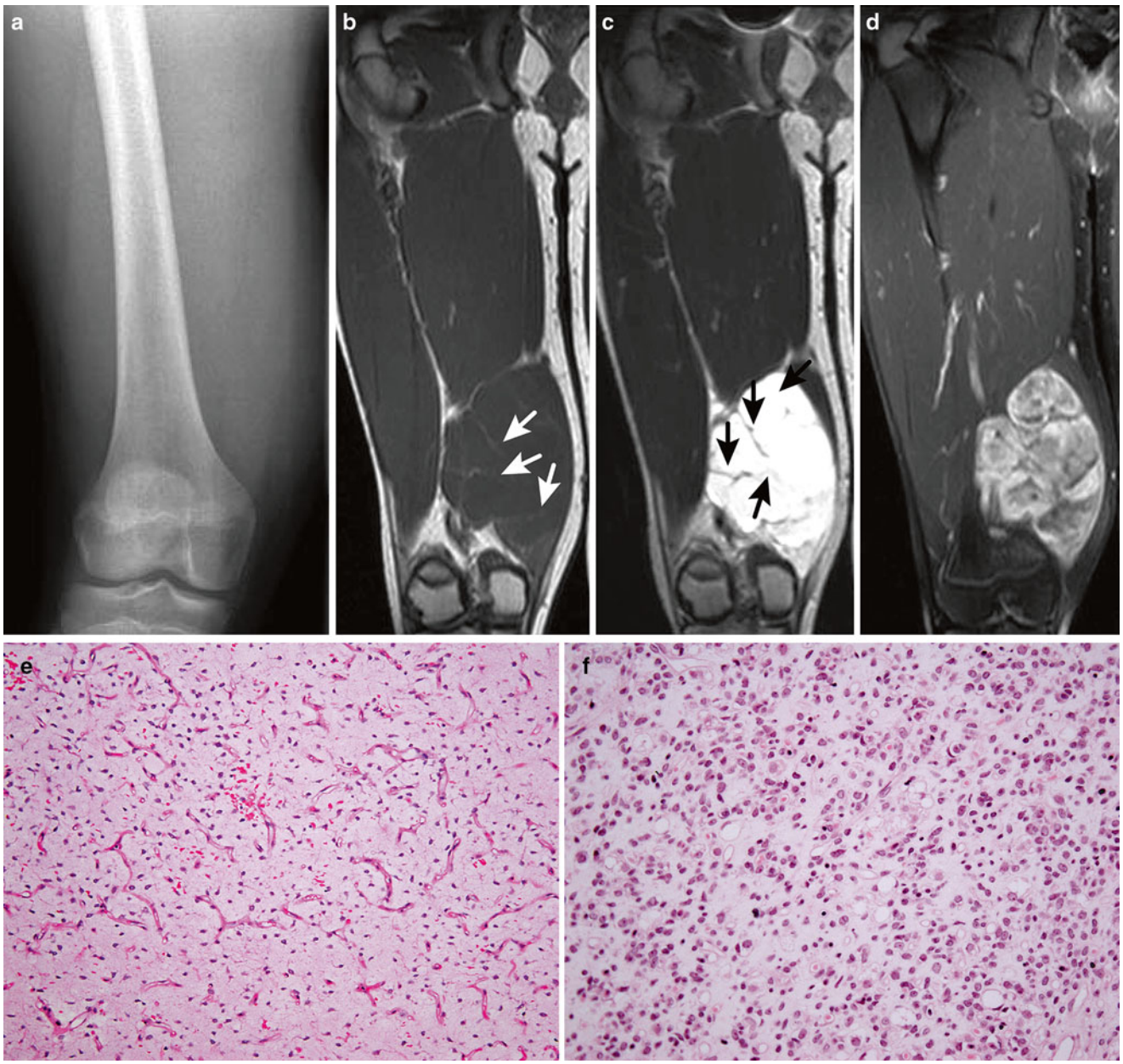

Fig. 3.11 Myxoid liposarcoma. (**a**–**d**) A 14-year-old boy presented with a firm thigh mass, noted 1 year prior, with recent increase in size. (**a**) Anteroposterior radiograph shows fullness in the distal medial thigh soft tissues without bony abnormality or soft tissue calcifications. The density of the soft tissues is the same as muscle. (**b**, **c**) Coronal non-contrast MR through the same region shows a multilobulated soft tissue mass whose signal intensity is the same as muscle on T1-weighted sequence (**b**) but intensely bright signal on STIR sequence (**c**). The mass lacks a significant fat component which would manifest as bright signal on T1-weighted imaging (similar to the white subcutaneous fat) and dark on STIR and fat saturated contrast-enhanced T1. Note multiple septae within the mass (*arrows*). (**d**) With administration of intravenous contrast, heterogeneous enhancement within the nodules is noted. (**e**) Myxoid liposarcoma containing a bland, mucinous stroma with scattered lipoblasts, intersected by a rich plexus of arcuate capillaries. (**f**) Round cell liposarcoma with increased cellular density and less stroma. The cells appear undifferentiated, but lipoblastic differentiation with cytoplasmic lipid vacuoles can be noted on close inspection

that may be nodular. Focal nodular or globular non-fat components, usually measuring less than 2 cm in size, suggest well-differentiated liposarcoma. After administration of gadolinium contrast agent, the septa demonstrate moderate to marked enhancement [152]. On PET-CT, well-differentiated liposarcoma demonstrates minimal FDG avidity, reflecting the low-grade nature of this malignancy [152, 162].

Molecular Genetics

Both well-differentiated and dedifferentiated liposarcoma exhibit genetic amplification affecting the chromosome 12q13-14 region. This leads to overexpression of protooncogenes such as *MDM2, CDK4, GLI, CHOP,* and *SAS* [126, 163]. The resultant genomic instability is potentiated by mutations of *TP53* [164].

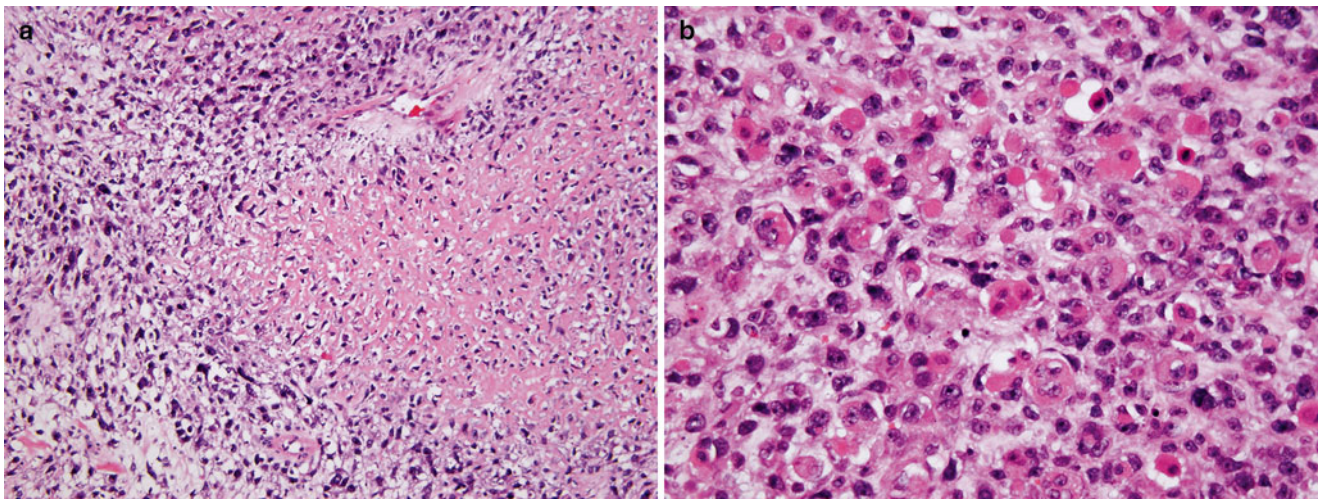

Fig. 3.12 Dedifferentiated liposarcoma. (**a**) This lesion contains large cells with angulated, hyperchromatic nuclei. Tumor cells show lipoblastic differentiation with lipid vacuoles. Prominent in the *right central portion* of the figure is a wedge-shaped area of osteoid production. (**b**) In another portion of the lesion, there is prominent rhabdomyoblastic differentiation. Cells contain abundant, brightly eosinophilic cytoplasm

Microscopic Features

Well-differentiated liposarcomas and atypical lipomatous tumors histologically and genetically comprise the same lesion, distinguished by the deep location of the former lesion and the superficiality of the latter [165]. These lesions largely consist of mature fat containing interspersed cells with enlarged, hyperchromatic, atypical nuclei. Conversely, dedifferentiated liposarcomas typically contain little fat and primarily comprise a high-grade storiform lesion resembling UPS. Low-grade spindle cell forms should not be confused with spindle cell lipoma [166]. Dedifferentiated liposarcomas often contain foci of heterologous differentiation into chondrosarcoma, osteosarcoma (Fig. 3.12a), and/or rhabdomyosarcoma (Fig. 3.12b). Often, tumors are mixed, with dedifferentiated liposarcoma foci abruptly merging with well-differentiated liposarcoma.

Immunohistochemistry and Other Special Stains

Immunostains for MDM2 and CDK4 may be used to confirm the overexpression of these proteins resulting from genetic amplication [167].

Molecular Diagnostic Features and Cytogenetics

Cytogenetically, the genetic amplication of well-differentiated/ dedifferentiated liposarcoma is characterized by ring or marker chromosomes. *MDM2* amplification may be detected by FISH [163], and overexpression is seen with immunohistochemistry. However, immunostains of pediatric lesions may demonstrate MDM2-negativity and p53-positivity [161].

Prognostic Features

The rare reports of well-differentiated/dedifferentiated liposarcoma in children suggest that they have a good outcome if completely excised [125].

Malignant Myogenous Tumors

Two myogenous sarcomas occur in children: rhabdomyosarcoma and leiomyosarcoma. Rhabdomyosarcoma is the most common pediatric soft tissue sarcoma and comprises more than one-half of all soft tissue malignancies. Leiomyosarcomas conversely are unusual in children. Pediatric rhabdomyosarcomas are classified by histology into two main types: embryonal and alveolar. Adult pleomorphic rhabdomyosarcomas are practically nonexistent in children [168].

Embryonal Rhabdomyosarcoma

Definition: Embryonal rhabdomyosarcomas (ERMS) are malignant soft tissue neoplasms arising from primitive mesenchymal cells and showing a variable capacity for neoplastic myogenesis. They form a morphologically diverse group of neoplasms that encompasses several subtypes.

Clinical Features and Epidemiology

ERMS occur most frequently among rhabdomyosarcomas and indeed among pediatric sarcomas in general. They show a pronounced proclivity to occur in younger children and are

infrequent in patients over the age of 5 years. They occur at every body site and are somewhat more common in males. Typical sites of origin are the genitourinary tract (including the scrotal sac), head, and neck. Other sites include the abdomen, the biliary tree, and the extremities, the latter site being relatively uncommon.

The anatomic diversity of ERMS is matched by a corresponding plethora of presenting signs and symptoms, related to space-occupying masses occurring in hollow viscera and body cavities. Common presentations include exophthalmos in orbital tumors, nasal obstruction in sinonasal tumors, jaundice in biliary tumors, and urinary obstruction in bladder and prostate lesions.

Imaging Features

Imaging ERMS by plain radiograph is of limited use; it may appear as a soft tissue mass similar to muscle. If diagnosed early, then no osseous abnormality is seen, however, if diagnosed later, these tumors may have adjacent extensive osseous destruction that may be seen on radiography. Gray-scale ultrasound images show a slightly hypoechoic or hyperechoic, often inhomogeneous, soft tissue mass, sometimes with markedly increased blood flow on color Doppler, although cases with low vascular density have been documented. When ERMS occurs at the bladder base (from the bladder or prostate), it usually appears as an intraluminal hyper- or hypoechoic mass protruding into the bladder lumen resembling a cluster of grapes (Fig. 3.13a). Tumors at the bladder base may cause bladder outlet obstruction and be associated with nonspecific bladder-wall thickening and hydronephrosis [6, 122, 123].

CT evaluation of ERMS usually shows a heterogeneous soft tissue lesion that is nonspecific and vigorously enhances after the administration of contrast (Fig. 3.13b). ERMS in the orbital region usually appears homogeneous and isodense to muscle. Intratumoral hemorrhage has a heterogeneous appearance on CT images. Destruction of underlying bone is seen in one-fourth of tumors, with periostitis, bone destruction, sclerosis, and bony remodeling visible on CT and plain radiographic images. ERMS have nonspecific features on MR images. These tumors are usually isointense or hyperintense to muscle on T1-weighted images. On T2-weighted images, they have high signal that heterogeneously enhances after gadolinium administration (Fig. 3.13c). Tumor necrosis and cystic areas, if present, appear as low signal on T1-weighted images and high signal on T2-weighted images. Orbital ERMS may extend intracranially or to the adjacent paranasal sinuses [122]. These lesions usually appear to be heterogeneous, with signal that is low or isointense to surrounding brain on T1-weighted images. Surrounding bony destruction, if present, is poorly delineated by MRI, and CT may be required to assess any osseous involvement. Extraorbital head and neck ERMS have similar imaging features; however, it is important to assess parameningeal extension, which affects the surgical approach and resectability. Post-contrast T1-weighted imaging with fat suppression is useful to assess cranial nerve involvement.

Molecular Genetics

On gene expression array studies, ERMS shows a diversity of molecular perturbations that significantly vary among tumors [169]. However, epigenetic studies reveal a striking loss of heterozygosity for portions of chromosome 11p, particularly evident at 11p15.5 [170, 171]. This appears to result primarily from uniparental disomy, resulting in altered expressed of imprinted genes ones [172].

Gross and Microscopic Features

Grossly, ERMS forms a fleshy, lobulated, grey-tan mass that may show areas of necrosis and hemorrhage. The botryoid variant of ERMS exhibits characteristic grape-like polyps that protrude from the epithelial surface of a hollow viscus (Fig. 3.13d). The spindle cell variant on section displays the whorled, firm, scar-like features of a fibromatous lesion.

Embryonal rhabdomyosarcoma, as the name implies, recapitulates the stages of embryonal myogenesis. The stage of myogenesis varies among tumors and even among microscopic fields. Some lesions contain the primitive mesenchymal stem cell features of post-somitic cells with slightly oblong, small, hyperchromatic nuclei and variable amounts of amphophilic cytoplasm bounded by stellate to elongate contours. These may produce a mucoid intercellular stroma or cluster together in dense packets. Tumors, especially on limited biopsies, thus may appear loosely cellular, dense, or loose and dense, the latter pattern resembling early limb musculature formation (Fig. 3.13e).

As embryonal musculature ages, cells acquire progressively more eosinophilic cytoplasm and assume a pinker hue to form rhabdomyoblasts. Rhabdomyoblasts are also a feature of RMS, and they become more prominent and numerous with successful therapy as tumor cells are forced either to die or to differentiate. Like density, this quality is highly variable in ERMS, and one observes either few or no rhabdomyoblasts in some tumors or a rhabdomyoma-like plethora in others. In rare tumors, particularly in the uterocervical region, cartilage may also be observed. With terminal differentiation, rhabdomyoblasts become multinucleated, nuclei sometimes arranged in tandem. As a result of this differentiation process, the cytological content of ERMS varies, and odd cellular contours give rise to names such as "strap cell," "tadpole cell," "racquet cell," "spider cell," and "broken straw sign" (Fig. 3.13f).

Subtypes of ERMS include botryoid, spindle cell, and anaplastic variants. Botryoid rhabdomyosarcoma (BRMS)

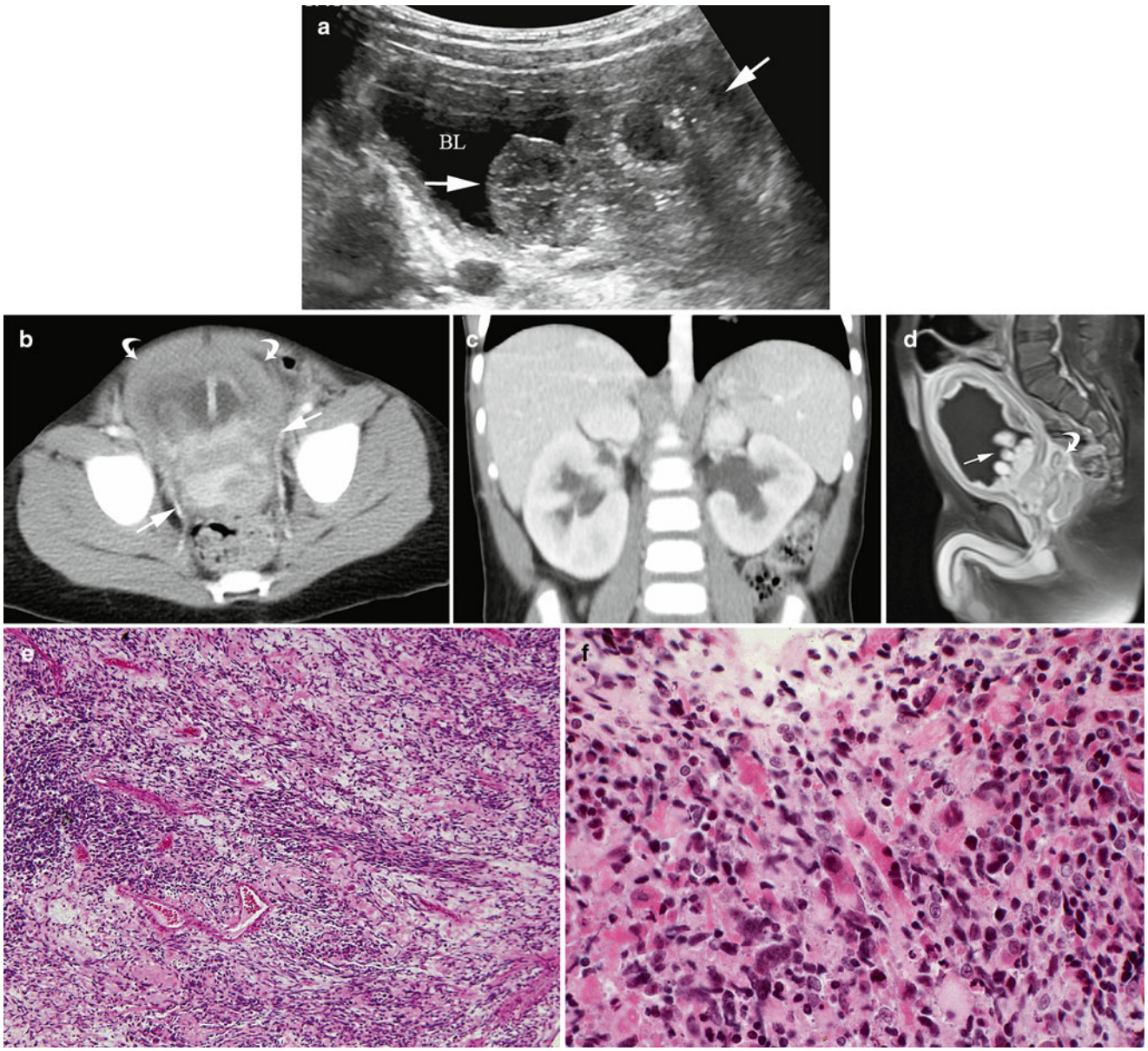

Fig. 3.13 Embryonal rhabdomyosarcoma. (**a**–**d**) This 2-year-old boy with embryonal rhabdomyosarcoma of the bladder base and prostate presented with abdominal pain and urinary dribbling. (**a**) Sagittal ultrasound image shows a lobulated, solid mass (*arrows*) in the bladder lumen (BL). (**b**) Post-contrast axial CT shows a heterogeneously enhancing mass at the bladder base and in the prostate (*straight arrows*) and diffuse bladder wall thickening (*curved arrows*) likely due to chronic bladder outlet obstruction. (**c**) Coronal CT image shows bilateral hydronephrosis secondary to bladder outlet obstruction. (**d**) Post-contrast T1W sagittal MR image shows the classic "cluster of grapes" appearance of the bladder tumor (*straight arrow*) as well as the prostate mass (*curved arrow*) and diffuse bladder wall thickening. (**e**) A low power photomicrograph of embryonal rhabdomyosarcoma shows a mixture of densely compacted cells and loose, myxoid zones. (**f**) At higher power, tumor cells show rhabdomyoblastic differentiation, with peripheralized nuclei, elongate, strap-shaped profiles, and brightly eosinophilic cytoplasm.

forms grape-like polyps by extrusion from a mucosal surface (Fig. 3.13d), whose epithelium abuts a dense cellular lamina known as the "cambium layer." Spindle cell rhabdomyosarcoma (SCRMS), considered a separate subtype by some, comprises dense fascicles of smooth muscle-like cells arranged in whorls or herring bones. SCRMS should contain rhabdomyoblasts on close inspection, separating them from leiomyosarcoma, and they usually occur in the paratesticular region or head and neck. Pediatric SCRMS often co-exist with ERMS foci.

Anaplasia, defined by enlarged, hyperchromatic nuclei and multipolar mitoses, occurs as single isolated cells in some ERMS and as prominent clonal populations in others. These are thus divided into "focal" and "diffuse" types,

Table 3.8 IRSG staging of rhabdomyosarcoma

Stage	Site	Size	Node status (N)	Metastasis (M)
1	Orbit	Any	N0, N1, or NX	M0
	Non-parameningeal head and neck			
	GU non-bladder, non-prostate			
	Biliary tract/liver			
2	Bladder/prostate	<5 cm	N0 or NX	M0
	Extremity			
	Cranial parameningeal			
	Other sites			
3	Extremity	<5 cm	N1	M0
	Cranial parameningeal			
	Other sites	>5 cm	N0, N1 or NX	
4	Any	Any	Any	M1

N0 negative lymph nodes by clinical or radiological examination, *N1* enlarged lymph nodes by clinical or radiological examination, *NX* indeterminate lymph nodes, *M0* no distant metastasis, *M1* distant metastasis

respectively. The latter may resemble adult pleomorphic rhabdomyosarcoma, particularly when occurring in SCRMS, but pleomorphic rhabdomyosarcomas occur rarely in children, if at all.

Immunohistochemistry and Other Special Stains

All variants of RMS, including ERMS, express muscle proteins analogous to their normal cellular counterparts. The most commonly used include desmin, muscle-specific actin (the epitope recognized by clone HHF-35), myogenin (myf4), and MyoD (myf3) [173]. Myoglobin can be used to highlight differentiated cells, which may be useful following chemotherapy. For nuclear transcription factors such as MyoD and myogenin, the staining should be nuclear and not cytoplasmic, which is nonspecific.

Immunohistochemistry also aids in RMS classification, as ERMS shows a relatively heterogeneous myogenin expression, instead of the strong diffuse myogenin expression typical of alveolar rhabdomyosarcoma (ARMS) [174]. Newer markers include HMGA2 [169], which typically stains ERMS and fails to stain fusion-positive ARMS, and AP2β [175], which shows diffuse positivity in ARMS and negative staining in ERMS.

Molecular Diagnostic Features and Cytogenetics

Standard karyotyping studies of ERMS have generally been non-revealing, but comparative genomic hybridization shows a recurring pattern of chromosomal loss and gain [176].

Microarray-based studies show a rather heterogeneous pattern of gene expression, likely related to the diversity of morphology and differences in myodifferentiation among tumors, as well as variable chromosomal loss and gain [169].

Table 3.9 IRSG grouping of rhabdomyosarcoma

Group 1: Completely resected
(A) Confined to organ of origin
(B) Spread to contiguous structures
Group 2: Grossly resected with
(A) Microscopic residual disease
(B) Involved nodes completely resected
(C) Involved node with evidence of microscopic residua or involvement of most distant node
Group 3: Gross residual disease
(A) Biopsy only
(B) Gross major resection of >50 % of tumor volume
Group 4: Distant metastasis (fluid cytologic involvement may be used as evidence)

Prognostic Features

Prognostication of ERMS is a somewhat confusing affair based on stage, group, and age. Intergroup Rhabdomyosarcoma Study Group (IRSG) staging depends on clinical and radiological factors that include site and clinical evidence of lymph node or distant metastasis (Table 3.8) [177]. Grouping depends on pathological evaluation of adequacy of excision and lymph node metastasis (Table 3.9). Age is an independent predictor of ERMS outcome [178], which is worse in adolescents and infants. All of these factors have been used with histological classification to separate patients treated by COG protocols into three subgroups: low risk, intermediate risk, and high risk. Among current published protocols, low-risk patients have overall survival of 80–90 % at 5 years [177], whereas intermediate risk patients have 4-year failure-free survivals of approximately 70 % [179]. High-risk patients, who primarily have ARMS, fare much worse, with an overall 4-year survival of 23 % [180].

Alveolar Rhabdomyosarcoma

Definition: Alveolar rhabdomyosarcoma (ARMS) is an aggressive, high-grade malignancy composed of uniform round cells with arrested early myogenic differentiation. Some feel that ARMS is best defined by genetic features rather than histology [181].

Clinical Features and Epidemiology

In contrast to ERMS, ARMS cases predominate in the extremities and parameningeal regions. Other favored sites include the sinonasal regions and perineum. Outside of the sinonasal tract, relatively few ARMS occur in sites favored by ERMS, such as genitourinary tract, biliary tree, orbit, and middle ear. Unusual presentations include breast metastases and leukemic disease with no apparent primary tumor.

In contradistinction to ERMS, ARMS occurs within a wide age range, making it more common in older children and adolescents. It occurs less frequently than ERMS and comprises about 20–30 % of RMS cases in most series. The frequency decreases further if only fusion-positive cases are considered.

Typically, ARMS presents as a growing, expansive mass that may invade adjacent structures such as bone. The patients may suffer from progressive loss of weight and energy prior to diagnosis, and extensive metastases may be found at diagnosis. Metastatic sites include bone marrow, lymph nodes, and lungs.

Imaging Features

Alveolar rhabdomyosarcoma (ARMS) is most commonly seen in the extremities, presenting as a painless soft tissue mass. Plain radiographic images are nonspecific and may show soft tissue swelling. Ultrasound images may show a hypoechoic or hyperechoic, often inhomogeneous, soft tissue mass. Color Doppler images show multiple vessels within the lesion. These tumors are very aggressive, and extensive involvement of adjacent structures is often seen at the time of diagnosis. CT usually shows a nonspecific enhancing lesion and is helpful in assessing for underlying osseous involvement and lymphadenopathy at the time of diagnosis [6, 122]. CT is important for assessing the extent of parameningeal involvement and invasion into surrounding structures, especially in orbital and extraorbital parameningeal ARMS. On MR images, the characteristics of ARMS are nonspecific, appearing as intermediate signal on T1-weighted images and intermediate to high signal on T2-weighted images. Enhancement is vigorous, and prominent high-flow vessels might be observed (Fig. 3.14a–c). MRI is useful to determine if there is vascular encasement [7, 69, 122]. CT and MRI are helpful in detecting nodal disease [122] (Fig. 3.14a–c).

Molecular Genetics

ARMS are characterized by the translocations t(2;13)(q35;q14) and t(1;13)(p36;q14). These fuse *FOXO1* (formerly *FKHR*) with the homeobox genes *PAX3* and *PAX7*, respectively. The highly expressed *PAX3*-FOXO1 fusion affects numerous downstream targets, whereas the *PAX7-FOXO1* usually becomes overexpressed because of gene amplification. *PAX3-FOXO1*-positive tumors also show gene amplification affecting other regions, including the 12p12-14 region that includes the *CDK4*, *MDM2*, and *GLI* protooncogenes and the 2p region that includes *N-MYC* [182].

A variable subset of tumors with ARMS histology show no evidence of PAX fusions. A few of these are "low expressors" that have evidence of DNA fusion but lack detectable fusion gene product for RNA-based assays. Rarely, they contain alternate fusions that substitute *NCOA1*, *NCOA2*, or *AFX* for *FOXO1* or *FGFR* for a *PAX* gene. However, the majority show a gene expression pattern more characteristic of ERMS than ARMS [182].

Gross and Microscopic Features

ARMS forms an infiltrative, soft tissue mass, frequently intramuscular, with nonencapsulated boundaries and a fleshy, grey-tan cut surface. On a low power objective, one is struck by the monotony of ARMS cells, which present the typical pattern of the "undifferentiated small round blue cell tumor." There are two basic histological patterns: the classic alveolar pattern, as originally described by Riopelle and Thériault [183], and the solid pattern [184]. In tumors with classical ARMS histology (Fig. 3.14d), delicate fibrovascular septa subtend the primitive cells into a pseudo-alveolar arrangement, heightened by the tendency of the cells to dissociate with the septa and form "floating clusters." However, a row of single cells maintains a septal attachment in a picket row fashion. Usually, histologically obvious myogenesis is scant, but some tumors form multinucleate giant cells analogous to the fused myoblasts seen in embryos.

Solid variant ARMS lacks septa but instead forms solid, patternless sheets of primitive round cells that usually lack obvious differentiation (Fig. 3.14e). Both forms of ARMS contain monomorphous nuclei with smooth nuclear contours, variably clumped chromatin, and mildly conspicuous nucleoli. Cytoplasm is scant, and cytoplasmic boundaries may be indistinct. On cytological preparations, there may be cytoplasmic vacuoles, and ARMS cells may mimic neoplastic B cells [185]. A rim of eosinophilic cytoplasm, a sign of early myogenesis, may be present in some cells.

Some RMS contain histologic foci resembling both ARMS and ERMS [186]. These "mixed RMS" have been considered ARMS cases in recent years [168, 187], but it has become apparent that most do not have the biological features of ARMS.

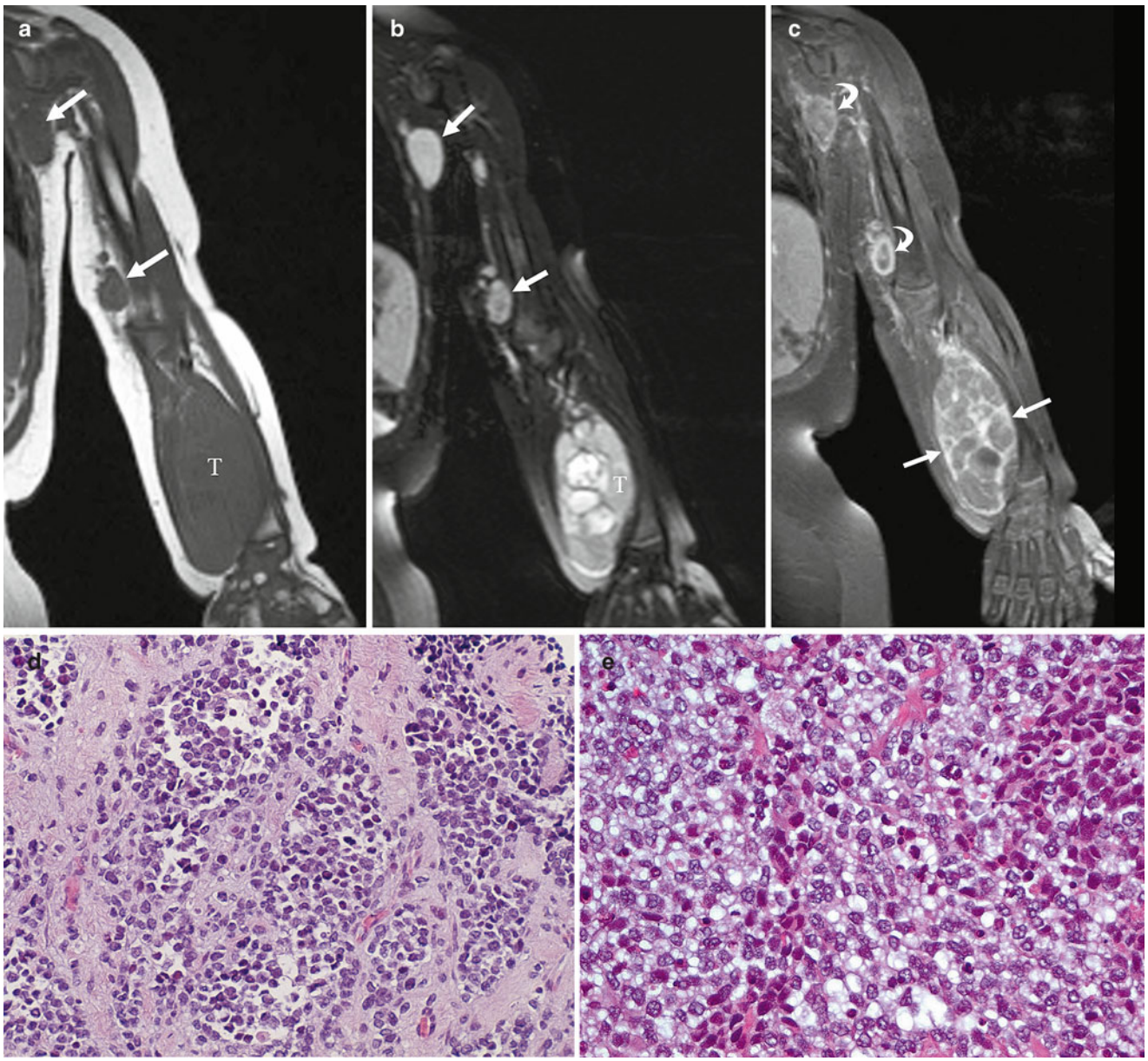

Fig. 3.14 Alveolar rhabdomyosarcoma. (**a**–**c**) A 2-year-old boy with forearm alveolar rhabdomyosarcoma. (**a**) Coronal non-contrast-enhanced T1W MR image shows the primary tumor (T) to be isointense to muscle. Epitrochlear and axillary lymphadenopathy is evident (*arrows*). (**b**) Coronal short tau inversion recovery MRI shows the tumor (T) to be heterogeneous. Nodal spread is again noted (*arrows*). (**c**) On this post-contrast T1W MR image the tumor (*straight arrows*) shows inhomogeneous enhancement with non-enhancing areas consistent with necrosis. The involved nodes also enhance (*curved arrows*). (**d**) Classical alveolar rhabdomyosarcoma histology, with fibrous septa dividing discohesive nests of primitive cells. (**e**) Solid variant alveolar rhabdomyosarcoma showing no fibrous septa but compromising patternless sheets of undifferential small round cells. In spite of the seeming lack of differentiation, there was strong, diffuse myogenin expression (not shown)

Immunohistochemistry and Other Special Stains

Like ERMS, ARMS typically expresses markers of primitive myogenesis, particularly desmin, myogenin, and MyoD. The latter two immunostains show strong, diffuse, nuclear positivity, not the heterogeneous, speckled positivity of ERMS. Cytoplasmic staining should not be considered positive for MyoD or myogenin [188]. A variant of SCRMS, the sclerosing RMS, has ARMS-like features such as thick fibrous septa and strong MyoD positivity, but myogenin positivity is typically weak or even absent.

Newer immunohistochemical markers of ARMS have been developed as a result of expression array analysis. AP2β and beta-cadherin appear to be particularly potent markers of fusion-positive ARMS [189].

Molecular Diagnostic Features and Cytogenetics

PAX3-FOXO1 and *PAX7-FOXO1* fusions can be successfully detected using either RT-PCR [190, 191] or FISH [192]. FISH of *PAX7-FOXO1* often shows amplification with a multitude of nuclear signals. Either of these methods yields sensitive, specific results, but one should carefully mark definite ARMS foci prior to FISH in order to prevent false negative testing. ARMS often shows tetraploidy on routine karyotypes, flow cytometry [193], and FISH studies.

Prognostic Features

ARMS acts in aggressive fashion, with worse outcomes than ERMS [194]. As a result, COG studies have not included ARMS cases in low-risk protocols [177]. In intermediate risk trials [179], ARMS patients showed a 4-year survival of 52–68 % for Stage 2/3 or Group II/III and 77–88 % for l Stage 1 or Group 1. ARMS patients comprise the majority of high-risk patients, who suffered an overall survival rate of 23 % at 5 years.

For PAX fusion-positive patients, survival is even worse [195]. Fusion positivity imparts a distinctive biological signature that associates with aggressive tumor behavior and poor survival [189, 196, 197]. However, in one series, ARMS patients with *PAX7-FOXO1* fusions showed better survival than those with *PAX3-FOXO1* fusions or fusion negativity [198].

Leiomyosarcoma

Definition: Leiomyosarcomas are malignant spindle cell neoplasms comprised of neoplastic smooth muscle. There is diagnostic overlap with myofibrosarcoma, but leiomyosarcomas should show more advanced differentiation.

Clinical Features and Epidemiology

Leiomyosarcomas predominately occur in adults and are relatively rare in children. In the POG series, they comprised only 7 % of 133 non-rhabdomyosarcomatous soft tissue sarcomas [5]. Well-defined series of pediatric leiomyosarcomas [199–201] report a wide age range including both infants and late adolescents [201]. Surprisingly, there is no gender predominance as observed in adults [199].

Leiomyosarcomas have interesting clinical associations, such as their predilection for occurring in unusual sites in pediatric AIDS patients [202]. AIDS-associated leiomyosarcomas appear to be EBV-driven and can occur in other forms of immunodeficiency, such as organ transplantation or primary genetic diseases. Secondary leiomyosarcomas occur in patients with other childhood malignancies.

Childhood leiomyosarcomas occur in a variety of sites [202]. As with adults, primary sites include skin, soft tissue, and gastrointestinal tract. It is critical to separate the latter lesions from gastrointestinal stromal tumors (GIST), as treatment is dramatically different.

Imaging Features

Leiomyosarcoma may arise in the deep soft tissues (within muscle or between muscles), superficial soft tissues, in the retroperitoneum, the genitourinary tract, or gastrointestinal (GI) tract. It is the most common sarcoma to arise from large vessels. Extremity tumors often present as a painless, slowly enlarging mass, most commonly involving the thigh. Tumors in the peritoneum and retroperitoneum can progress silently and often are very large at the time of diagnosis. Gastrointestinal tumors typically exhibit an extraluminal growth pattern resulting in large masses that cause only late obstruction and, therefore, are large at the time of diagnosis [203]. Metastasis occurs most frequently in the lung followed by the liver and peritoneal surfaces [77, 204].

About 17 % of extremity leiomyosarcomas show mineralization that is evident on plain film radiography and CT [205]. On sonography, retroperitoneal tumors appear solid with cystic spaces that have irregular walls. The solid component may appear isoechoic to liver or hyperechoic. The cystic components may contain internal low-level echoes or may be anechoic. The true extent of tumor is difficult to assess by ultrasound and additional cross-sectional imaging is required.

On CT retroperitoneal leiomyosarcomas form large, solid masses with cystic areas due to necrosis. Hyperdense foci, due to hemorrhage, may be present. There may be discordance between the sonographic and CT appearance of retroperitoneal tumors. Computed tomography may suggest large necrotic areas that appear solid on ultrasound. These areas are felt to represent nonliquified necrotic or avascular areas of tumor [206]. Smaller masses may be entirely solid on CT imaging [206]. Leiomyosarcomas arising from the GI tract are also generally large masses that are inhomogeneous on CT. Air or air-fluid levels may be present in GI tumors, reflecting communication with the bowel lumen [207].

On MRI the solid component of leiomyosarcoma is typically isointense to muscle on T1-weighted sequences, variably hyperintense on T2W images, and demonstrates prominent contrast enhancement (Fig. 3.15a–c) [77]. Areas of necrosis appear hypointense on T1W images. On T2W images necrotic areas show intermediate to high signal intensity due to water content. Hemorrhage, when present, may produce fluid-fluid levels [206]. The imaging features of leiomyosarcoma overlap those of GIST, and these tumors cannot be distinguished based on imaging. GISTs are far more common in the GI tract than leiomyosarcomas [208].

Molecular Genetics

Leiomyosarcomas typically contain a range of cytogenetic aberrations, with imbalance of chromosome 9 [209], overrepresentation of genes on 12q13-15 [210], and hypermethylation of *RASSF1A* [211]. EBV-associated leiomyosarcomas

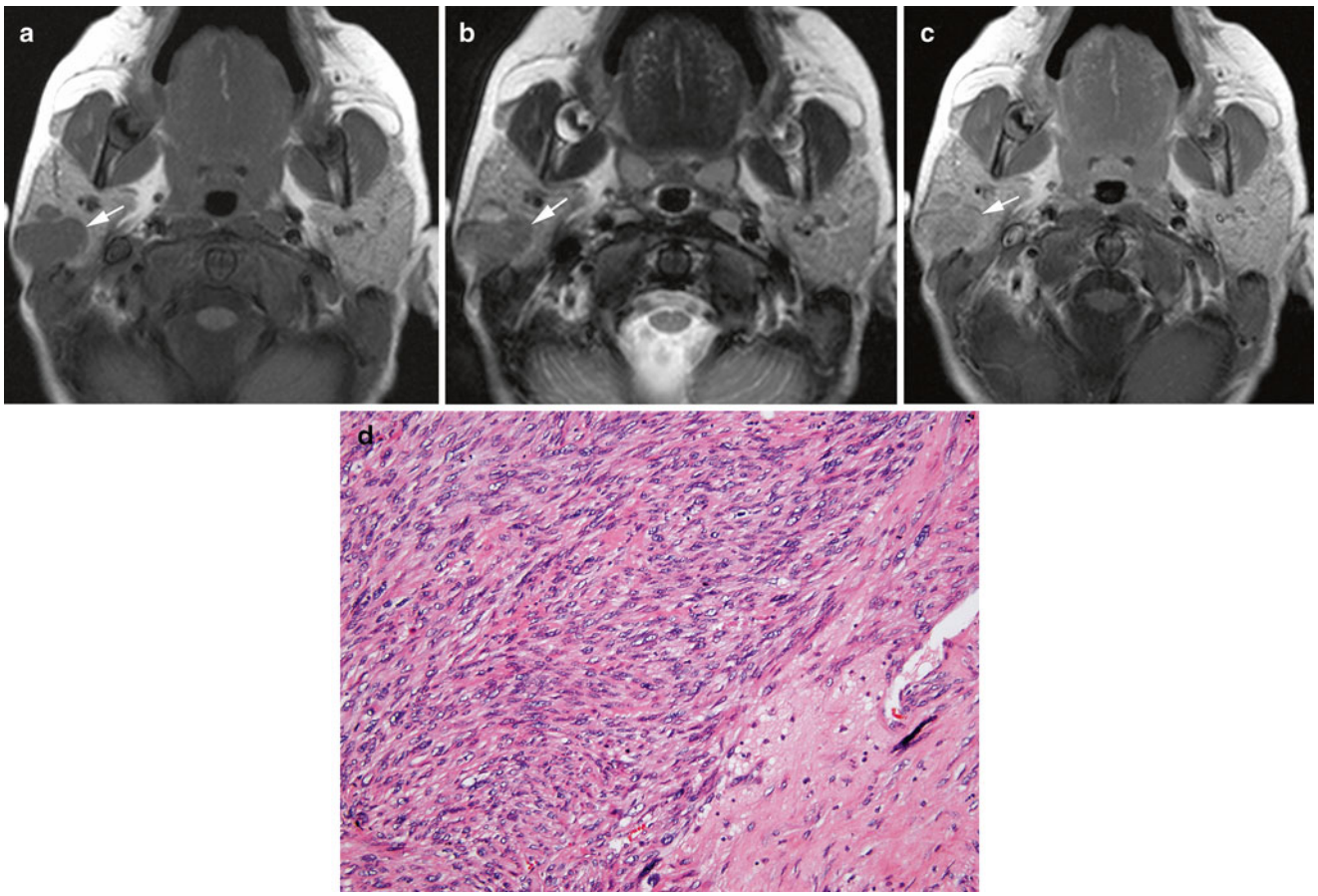

Fig. 3.15 Leiomyosarcoma. A 6-year-old HIV+boy with painful lump in area of right parotid. (**a**) T1W axial MR image shows a well-circumscribed right parotid mass (*arrow*) that is isointense to muscle. (**b**) T2W axial MR shows the mass (*arrow*) to be slightly hyperintense to muscle. (**c**) Post-contrast T1W MR image shows prominent enhancement of the tumor (*arrow*). (**d**) A photomicrograph of pediatric leiomyosarcoma illustrates tight fascicles of fusiform cells containing blunt-ended nuclei, moderately eosinophilic cytoplasm, and occasional vacuoles

show multiclonality that suggests multiple infection events rather than metastasis [212].

Gross and Microscopic Features

Leiomyosarcomas are malignant lesions that show the hypercellularity, interwoven and streaming arrangement, and mitotic activity characteristic of spindle cell sarcomas. Grossly, they are infiltrative, nonencapsulated tumors with bulging, firm, pale tan surfaces, often with zones of necrosis and hemorrhage. Cytologically, they characteristically contain blunted, cigarlike nuclei with perinuclear vacuoles (Fig. 3.15d). Their cytoplasm usually stains variably eosinophilic, but bright eosinophilia may indicate rhabdomyosarcoma (which should always be excluded).

Smooth muscle tumors associated with EBV infection may contain primitive small cell foci and T-lymphocyte infiltrates. They may lack pleomorphism, and histology does not appear to correlate with outcome [212].

Immunohistochemistry and Other Special Stains

Typically, leiomyosarcomas contain abundant microfilaments, giving them strong positivity with smooth muscle actin and muscle specific actin. However, a small percentage of embryonal rhabdomyosarcomas are also smooth muscle actin-positive [213]. To exclude spindle cell rhabdomyosarcoma, myogenin, myoglobin, and MyoD are thus useful. Smooth muscle actin positivity is also shared by a variety of myofibroblastic and myoepithelial tumors, so it should not be used as a sole diagnostic marker. To this end, additional markers of smooth muscle such as desmin and caldesmon are useful to support the diagnosis [45]. Stains for c-kit should be negative, which is important to exclude GIST.

Molecular Diagnostic Features and Cytogenetics

EBV testing should be performed on patients with various forms of immunodeficiency. This can be accomplished by in situ hybridization for EBV early RNAs (EBER) [212].

Prognostic Features

Although a tumor grade based on mitoses, pleomorphism, and necrosis may be assigned to leiomyosarcomas, their behavior does not always correlate with these parameters. As a result, factors such as tumor size, depth, resectability, and site must be considered [200].

Extraosseous Lesions Usually Occurring in Bone

A variety of bone neoplasms, including Ewing sarcoma, chondrosarcoma, giant cell tumor, aneurysmal bone cyst, and osteosarcoma, on occasion occur within extraosseous sites as primary lesions. Of these, the most frequently recurring childhood soft tissue sarcomas include Ewing sarcoma and mesenchymal chondrosarcoma. These are more fully covered in the chapter on bone sarcomas. Suffice it to say that soft tissue sarcomas that invade bone, and vice versa, can be a source of diagnostic and therapeutic uncertainty, and careful radiographic studies are of utmost importance in these situations.

Malignant Tumors of Indeterminate Histogenesis

Synovial Sarcoma

Definition: Synovial sarcomas are tumors of uncertain cell lineage, showing variable epithelial differentiation and cytogenetically characterized by the t(X;18) translocation.

Clinical Features and Epidemiology

Synovial sarcoma are relatively common in pediatrics and are the third most frequent soft tissue sarcoma, following rhabdomyosarcoma and soft tissue Ewing sarcoma [214]. In the Kiel Pediatric Tumor Registry, it accounted for 6 % of all soft tissue sarcomas [214], and in the POG and COG studies, it has been the most common "non-rhabdomyosarcoma soft tissue sarcoma" NRSTS [5].

Among children, synovial sarcoma primarily occurs in adolescents, with a median age of 13–14 years. However, the age range is wide, and lesions may occur in children as young as 14 months [214]. The primary site widely varies, although lower extremity lesions predominate. Other soft tissue sites include upper extremities, head and neck, and intra-abdominal and intrathoracic locations. Visceral tumors occasionally arise in organs such as the kidney and heart [215]. Rare intraneural lesions invite confusion with malignant peripheral nerve sheath tumors [216, 217].

Imaging Features

Although synovial sarcoma can occur in the head, neck, and trunk; approximately 85 % are extremity tumors that are para-articular in location. This tumor may arise from tendon sheaths, bursae, or joint capsules, but is seldom intra-articular and typically does not arise from synovium [218–220]. Patients most commonly present with a painless mass that has been present for weeks to years in the soft tissues of the lower extremity [219]. Other patterns of presentation include a pretumor phase of pain and tenderness without a mass, acute arthritis or bursitis, a chronic joint contracture, or a mass noted after trauma [219].

About one-third of synovial sarcomas contain calcification that may be apparent on radiographs or CT but can be overlooked on MRI [218, 221, 222]. Plain film radiography, CT, or MRI may also demonstrate cortical thinning, erosion, or invasion of adjacent bone, which occurs in 10–20 % of cases [221]. On MR images, synovial sarcomas tend to be large, rounded, or lobulated lesions (Fig. 3.16a); in one study the mean diameter was 9 cm [220]. Tumors often have fairly sharply defined margins and may be largely cystic. Subsequently, synovial sarcoma has been reported to be the most common malignant tumor to be misdiagnosed as a benign lesion (such as ganglion cyst or hematoma) based on MRI [223]. On imaging, synovial sarcomas tend to displace adjacent structures, such as muscle, fat, and tendons, but may encase the neurovascular bundle [220, 222]. In a review of MR imaging features of 34 synovial sarcomas, a triple-signal intensity on T2-weighted images was seen in 35 % of cases. This pattern consisted of mixtures of high signal intensity similar to fluid; intermediate signal intensity that was iso- or slightly hyperintense to fat; and slightly lower signal intensity, resembling fibrous tissue (Fig. 3.16b). In the same study, tumors less than 5 cm in diameter had homogeneously low-signal intensity on T1-weighted images and marked heterogeneity on T2-weighted images [220] (Fig. 3.16a, b). Others have described a heterogeneous, multiloculated appearance with various degrees of internal septations, with or without fluid-fluid levels probably due to internal hemorrhage [222]. After administration of contrast material there is usually prompt and heterogeneous enhancement, which may demonstrate nodularity within a cystic lesion (Fig. 3.16c). The presence of nodularity should raise suspicion of synovial sarcoma, and biopsy should be directed toward the solid nodule [77].

Molecular Genetics

Synovial sarcomas contain a reciprocal translocation, the t(X;18)(p11;q11), which fuses the *SS18* (alias *SYT*) gene on chromosome 18q11 with one of several *SSX* genes on chromosome Xp11. The *SSX* genes comprise contiguous loci that include *SSX1*, *SSX2*, and *SSX4*.

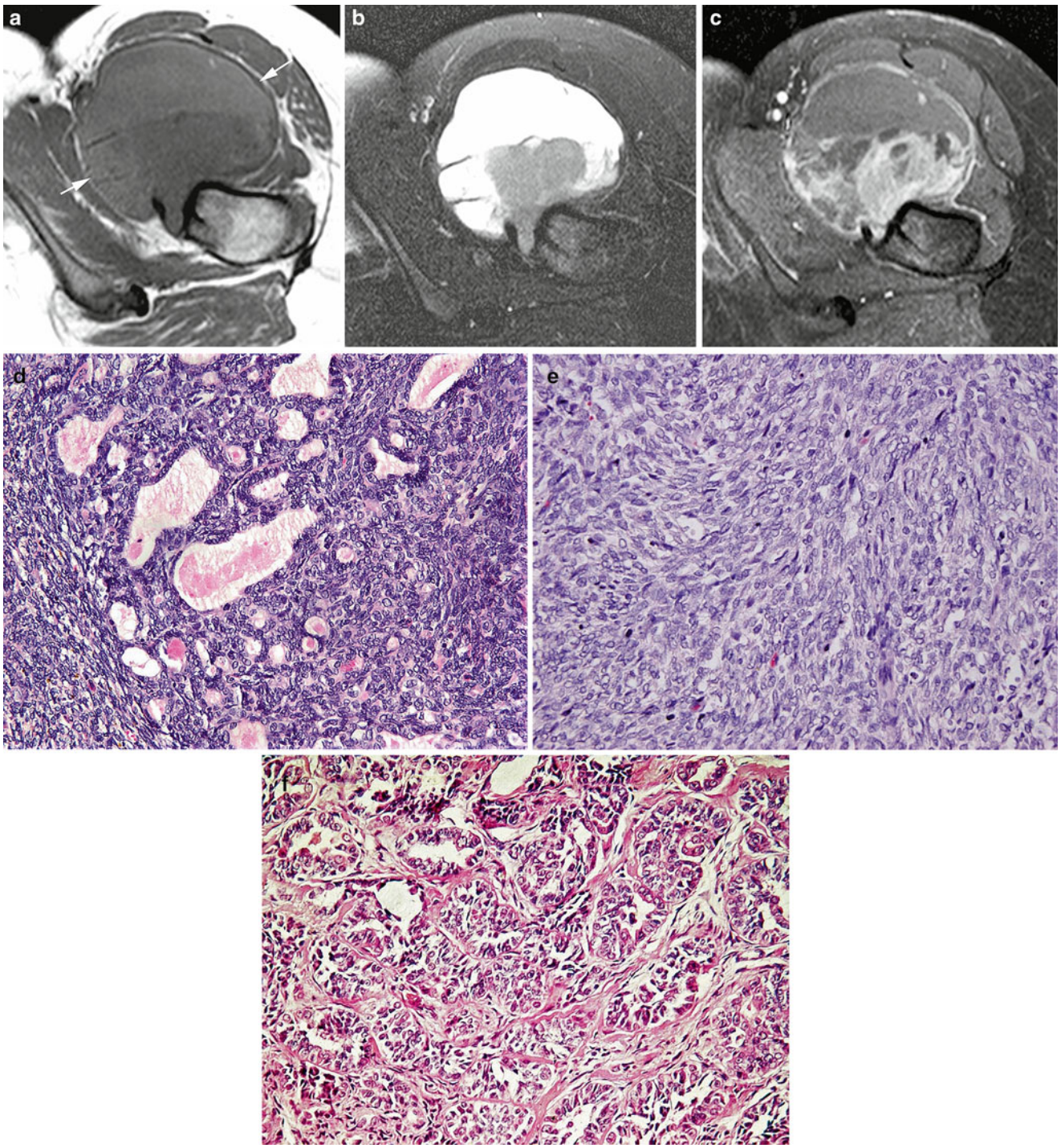

Fig. 3.16 Synovial sarcoma. A 14-year-old girl with intermittent left hip pain for 1 year. (**a**) T1W axial MR image shows a large, sharply defined, complex cystic mass (*arrows*) near the left hip joint. (**b**) T2W axial image shows the triple-signal intensity often seen with synovial sarcoma on T2W images; high signal consistent with fluid, intermediate signal that is iso- or slightly hyperintense to fat and slightly lower signal resembling fibrous tissue. (**c**) T1W post-contrast-enhanced image shows enhancement of a nodular component of this largely cystic tumor. (**d**) The typical biphasic histologic appearance of synovial sarcoma comprises well-formed glands embedded within dense fascicles of slender spindle cells. (**e**) Monophasic spindle cell synovial sarcoma contains only spindle cells, with vague epithelioid features such as loose clusters of cells with increased amounts of cytoplasm and large nuclei. (**f**) Monophasic epithelioid synovial sarcoma comprises mainly well-formed epithelial cells, with little intervening spindle cell component

Gross and Microscopic Features

Synovial sarcomas form infiltrative, nonencapsulated masses that permeate adjacent tissues and have a tendency to spread along fascial planes. Bony invasion may invite confusion with osseous neoplasms. Low-grade tumors may undergo cystic degeneration. The tumors have a pale grey-tan, fibrous surface and may be gritty if microcalcification is present.

A biphasic pattern with well-formed glands embedded within a dense spindle cell stroma comprises the prototypic form of synovial sarcoma (Fig. 3.16d). The epithelial component typically shows only mild to moderate nuclear atypia, whereas the spindle cells form elongated, intertwining cellular bundles akin to fibrosarcoma, with significant hypercellularity and nuclear hyperchromasia. Mitotic count varies, depending on nuclear grade, and grade 2 lesions may contain surprisingly few. This parameter seems to vary inversely with mast cell content, which may be prominent in low-grade tumors. Microcalcifications may be noted.

Synovial sarcomas show a variety of histological appearances. Monophasic spindle cell synovial sarcomas contain no glands or well-formed epithelial cells (Fig. 3.16e). However, vague epithelioid aggregates with rounded cellular contours and slightly more cytoplasm comprise common but often subtle features. Poorly differentiated monophasic synovial sarcomas primarily contain sheets of undifferentiated round cells that invite confusion with Ewing sarcoma and other round cell neoplasms. They typically show a brisk mitotic rate and are high-grade neoplasms.

Rarely, the epithelial component of synovial sarcoma predominates, forming anastomosing glands, canals, and cellular aggregates (Fig. 3.16f). An inconspicuous interglandular spindle cell component may be found with careful examination.

Immunohistochemistry and Other Special Stains

Positivity for cytokeratin and/or EMA typifies the majority of synovial sarcomas [214, 224]. EMA is a more sensitive marker than cytokeratin. BCL2 is usually positive but relatively nonspecific. A new marker of synovial sarcoma, TLE1, was discovered via gene array studies, but its specificity has been questioned [225]. S100 is often positive, negating its utility in distinction of S100 from nerve sheath tumors [224]. Similarly, frequent CD99 positivity renders it useless in separating synovial sarcomas from Ewing sarcomas [224].

Molecular Diagnostic Features and Cytogenetics

Routine karyotyping detects the t(X;18) of synovial sarcomas, but ancillary genetic testing is more commonly used today. Testing for *SSX-SS18* fusions can be performed using PCR-based methods [226] or FISH, the latter typically with a break-apart *SS18* (*SYT*) approach [227].

Prognostic Features

Grading is an important part of evaluating synovial sarcomas and is used for separation of treatment groups with COG protocols. Mitosis counting is the most commonly used parameter [5]. A variety of other parameters, including mast cell content, rhabdoid cells, and calcification, have also been used [228].

Alveolar Soft Part Sarcoma

Definition: Alveolar soft part sarcoma (ASPS) is a rare malignant soft tissue neoplasm of unknown histogenesis, containing cells with distinctive organoid histology, characteristic cytoplasmic crystals, and an *ASPL-TFE3* genetic fusion.

Clinical Features and Epidemiology

ASPS primarily occurs in the extremities of young adults, but the age range includes young children and older adults. In pediatrics, mostly adolescents are affected. The age range spanned from 2 to 71 years in one large study, with medians of 22 for females and 27 for males [229]. In patients less than 20 years, there appears to be a female predominance, but not in older patients [229].

ASPS typically occurs within skeletal muscle or fascia. Areas affected include the extremities, buttocks, and abdominal and chest wall; mostly frequently tumors arise from the thigh and buttocks [229]. Head and neck tumors also occur, particularly in children and in the tongue [230]. Tumors may arise in unexpected [231] locations. The presenting symptoms are generally those of a growing mass, and ASPS may grow very slowly.

Imaging Features

Alveolar soft part sarcoma typically presents as a painless, soft, slow-growing soft tissue mass and is commonly seen in girls, usually arising in the head and neck, trunk, and extremities in children and adolescents. Smaller tumor size is typically associated with a better outcome, although this association is controversial and indolent progression is the rule. Unenhanced CT images show that alveolar soft part sarcoma is less attenuated than muscle. On post-contrast CT there is significant peripheral enhancement, with central low-density necrosis or uniform isodensity or hyperdensity [7, 122]. These tumors appear to be well-circumscribed on MR images (Fig. 3.17a–c) and, unlike many soft tissue sarcomas, are of moderate- to high-signal intensity on T1-weighted images, perhaps because of abundant but slow blood flow through tumor vessels (Fig. 3.17a). This sarcoma is heterogeneously hyperintense on T2-weighted images (Fig. 3.17b) [69]. Dilated vessels in and around the lesion account for serpiginous areas of signal void. Enhancement is vigorous (Fig. 3.17c).

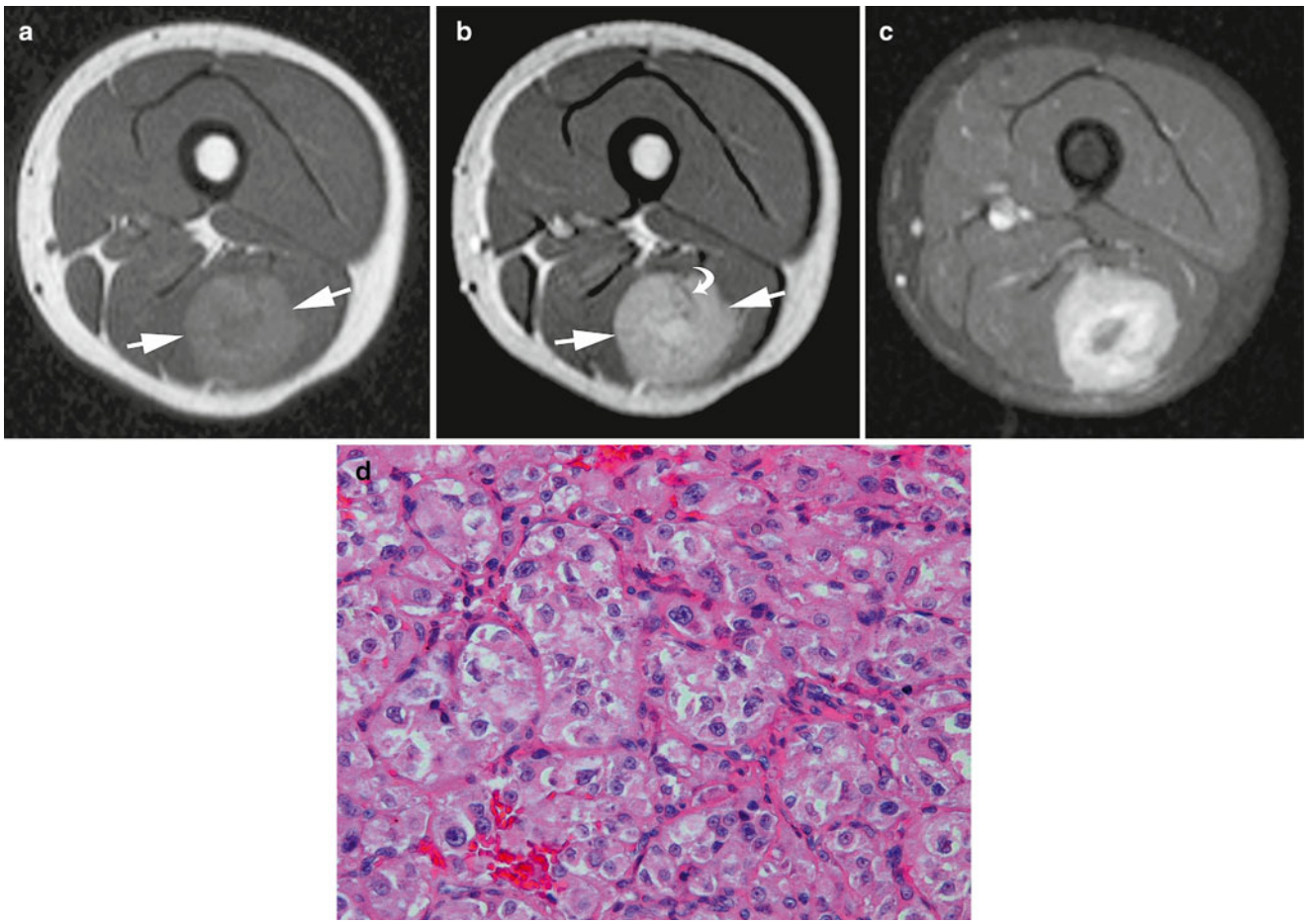

Fig. 3.17 Alveolar soft part sarcoma. A 9-year-old girl with alveolar soft part sarcoma of the left thigh. (**a**) Axial non-contrast-enhanced T1W MR image shows the well-defined, deeply seated mass (*arrows*) to be slightly hyperintense to muscle with a hypointense center. (**b**) Axial T2W MR shows the mass to be hyperintense to muscle with a more hyperintense central focus suggesting necrosis. Several small vessels within the mass are evident as flow voids (*curved arrow*). (**c**) Axial contrast-enhanced T1W MR shows fairly intense diffuse enhancement except centrally, consistent with central necrosis. High T1W signal intensity, well-defined margins, central necrosis, and intratumoral vessels are imaging features known to be associated with ASPS. (**d**) Photomicrograph of alveolar soft part sarcoma, illustrating clusters of polygonal cells with eosinophilic cytoplasm and uniform round nuclei, transected by a fine capillary network

Molecular Genetics

ASPS characteristically contains an unbalanced translocation, the der(17)t(X;17)(p11.2;q25), which fuses the *TFE3* gene on chromosome 17 with the *ASPL* gene on chromosome X [232]. The resultant *ASPL-TFE3* fusion gene acts as an aberrant transcription factor that promotes neoplastic transformation and proliferation. *TFE3* encodes a basic helix-loop-helix leucine zipper protein, and *ASPL-TFE3* fusion leaves the coding region intact, indicating upstream promoter dysregulation [232].

Gross and Microscopic Features

On cut section ASPS forms firm, bulging masses, with a variegated yellow-tan color alternating with frequent necrosis and hemorrhage. It may appear to be encapsulated, but this observation is usually false on microscopic examination. Tumor sizes show a wide range.

The histological features of ASPS show constant repetition, an observation unique in soft tissue pathology [232]. These include uniform, organoid clusters of cells separated by a rich fibrovascular framework and forming the characteristic alveolar histology (Fig. 3.17d). The polygonal tumor cells within these clusters contain eccentric round nuclei and granular, moderately eosinophilic cytoplasm, somewhat reminiscent of weakly staining rhabdomyoblasts but lacking fibrils or striations. The resultant epithelioid appearance may also resemble carcinoma, particularly when the cells contain clear cytoplasm. Pediatric tumors may lack the characteristic organoid appearance and instead display patternless sheets of cells lacking fibrovascular septa but showing similar cytological features [232].

ASPS characteristically contains cytoplasmic needle shaped crystals that are accentuated by diastase-resistant PAS staining. By electron microscopy, the crystals comprise

large rhomboidal structures with a periodic substructure. Some ASPS however lack crystals, so these structures cannot be relied upon for diagnosis in all cases, and careful prolonged search may be necessary in other cases [233]. Similar structures may be observed in intrafusal muscle spindle cells and in other tumors [234].

Immunohistochemistry and Other Special Stains

Staining for muscle markers [235] and neural markers [236] has led to competing hypotheses on the histogenesis of ASPS [237]. However, desmin, actin, and synaptophysin positivity are inconstant features and cannot be used for diagnosis. In particular, globular appearing cytoplasmic MyoD positivity is common [238]. However, cytoplasmic MyoD expression is a nonspecific common finding in a variety of sarcomas [174].

Of more practical use are antibodies against TFE protein, which uniformly decorate ASPS nuclei in a sensitive and specific manner [232]. A similar phenomenon occurs in translocation carcinoma of the kidney, which also contains an *ASPL-TFE3* fusion. TFE3 expression also occurs in a distinctive subset of PEComas and limits its use in differentiating these two neoplasms [239].

Molecular Diagnostic Features and Cytogenetics

ASPL-TFE3 fusion may be detected by both RT-PCR and FISH [240].

Prognostic Features

ASPS acts in a relatively indolent but inexorable manner, leading to long-term survival but eventual demise [229]. In the Memorial Sloan Kettering series [229], patients with localized tumors had survival rates of 77 % at 2 years, 60 % at 5 years, 38 % at 10 years, and 15 % at 20 years (median 6 years). Children appear to show better survival than adults [230], but this phenomenon may be deceptive in light of the slow growth of these lesions. Complete surgical resection holds the best chance for cure, as ASPS shows chemoresistance to current therapy. In the POG grading schema, all pediatric ASPS are high grade (grade 3), regardless of histological features [5].

Perivascular Epithelioid Cell Tumor (PEComa)/Myomelanocytic Tumor

Definition: PEComas comprise a group of clinically divergent neoplasms characterized by their content of a unique cell type, the perivascular epithelioid cell, which coexpresses a myogenic and melanocytic phenotype but does not exist as a non-neoplastic entity. One type of PEComa, the clear cell myomelanocytic tumor, shows a propensity to occur in soft tissue and bone.

Clinical Features and Epidemiology

Included in the PEComa category are renal angiomyolipoma, epithelioid angiomyolipoma of liver and kidney, lymphangioleiomyomatosis, clear cell tumor ("sugar tumor") of the lung, and clear cell myomelanocytic tumors of soft tissue, bone, and a variety of viscera. The last category most commonly occurs in soft tissue, but it is the rarest subtype of PEComa and lacks the association with tuberous sclerosis seen with the other forms. As such, it is an exceedingly rare neoplasm.

For some undefined reason, clear cell myomelanocytic tumor shows a strong propensity to occur in the ligamentum teres or falciform ligament of children [241]. In a series of six patients reported by Folpe et al. [241], ages ranged from 3 to 21 years, with a median of 11 years. Patients presented with abdominal pain, an abdominal mass, or both. Similar lesions are reported in bone [242, 243] and other soft tissue sites, particularly in the retroperitoneum, viscera, abdomen, and pelvis [244]. Outside of tumors arising in the ligamentum teres and falciform ligament or in occasional adolescents, soft tissue PEComas rarely affect children.

Imaging Features

The imaging features of soft tissue PEComas have not been well described.

Molecular Genetics

PEComas of bone and soft tissue described to date have not been found to contain a recurring genetic alteration, outside of a small subset that harbors *TFE3* fusions [245]. Sporadic single reports of translocations have appeared [242].

Gross and Microscopic Features

PEComas of the ligamentum teres or falciform ligament measured 5–20 cm [241]. They have firm, grey-tan cut surfaces with focal hemorrhage and cystic degeneration.

PEComas of bone and soft tissue contain a rich, arborizing vasculature that should be apparent under a low power objective. This vasculature is analogous to that seen in angiomyolipomas, but a fatty component is lacking. The vessels subtend PEComa cells into a fascicular or nested pattern resembling renal cell carcinoma and clear cell sarcoma (Fig. 3.18). These cells contain a clear to lightly eosinophilic cytoplasm with epithelioid or spindled contours and distinct boundaries. Nuclei are generally round with even membranes and chromatin, but pleomorphism and occasional giant cells may be apparent, the latter sometimes resembling the "spider cells" of rhabdomyoma. Some tumors show perivascular hyalinization that accentuates the nested pattern [244]. Rare examples contain a sparse amount of melanin pigment. Tumor cellularity is variable but generally low to moderate.

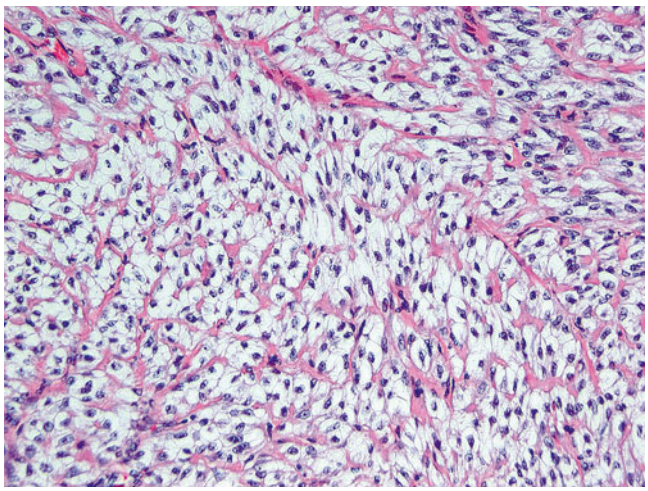

Fig. 3.18 Clear cell myomelanocytic tumor (PEComa), containing uniform epithelioid cells with clear cytoplasm, clustered by a richly arborizing microvasculature

Immunohistochemistry and Other Special Stains

Coexpression of melanocytic markers, particularly HMB45, and muscle markers, particularly smooth muscle actin and myosin, characterizes PEComas. Other melanoma markers such as melan A and MiTF may be positive, but S100 and desmin are typically negative. TFE3 positivity, perhaps related to genetic fusion [245], is seen in a small subset. CD34 should be negative.

Prognostic Features

A variably benign behavior characterizes PEComas as a group, but malignancy is exhibited by a subset of non-renal, non-pulmonary cases [246]. Folpe et al. have published a set of criteria for predicting PEComa clinical behavior [247]. They separate lesions into "benign," "uncertain," and "malignant" categories. Benign PEComas are smaller than 5 cm, contain non-infiltrative borders, have a low to intermediate nuclear grade and cellularity, show a mitotic rate of ≤1/50 hpf, and lack either necrosis or vascular invasion. PEComas of uncertain malignant features may show nuclear pleomorphism, contain giant cells, or measure >5 cm, but otherwise should have similar findings. Malignant PEComas exhibit two or more worrisome features, i.e., size >5 cm, mitotic rate >1/50 hpf, infiltrative borders, high nuclear grade or cellularity, necrosis, or vascular invasion.

Rhabdoid Tumor of Soft Tissue

Definition: Rhabdoid tumor is a high-grade, aggressive infantile sarcoma that occurs in viscera and soft tissue. A related tumor, the atypical teratoid-rhabdoid tumor, occurs in the CNS. It contain is characteristic cytoplasmic inclusions and genetic deletions affecting chromosome 22q11.

Clinical Features and Epidemiology

Rhabdoid tumors primarily occur in infants, and the diagnosis should be suspect in older patients. That said, their morphological and genetic features overlap with a variety of other neoplasms that usually occur in older patients; particularly noteworthy in this latter group is proximal epithelioid sarcomas. This has led to confusion in the literature, and it is well accepted that a variety of carcinomas and sarcoma may show rhabdoid features [248].

Fortunately, rhabdoid tumors are relatively rare entities, considering their aggressive behavior and dismal prognosis. Most commonly, they occur in the kidney, but they also occur in various visceral organs and soft tissue. Axially based neoplasms form a prominent component of soft tissue tumors [249], suggesting an association with axial embryogenesis. Extremity-based rhabdoid tumors are usually proximal. The lesions often grow rapidly and may reach an alarming size, but superficial cutaneous rhabdoid tumors may be discovered in sufficient time to allow complete excision, the best chance for cure [250].

Imaging Features

Most common in the kidney, rhabdoid tumors also have been described in the liver, brain, tongue, neck, chest, heart, pelvis, extremities, and other sites [251, 252].

The imaging characteristics of soft tissue rhabdoid tumors are not well known, largely because of the rarity of these tumors [251]. In the largest reported case series, no specific imaging features were observed that could prove diagnostic for these tumors; however, soft tissue rhabdoid tumors have a tendency to be large and hypodense on CT images and show heterogeneous hyperintensity on T2-weighted MR images (Fig. 3.19a–c) [251].

Molecular Genetics

Rhabdoid tumors characteristically contain variable deletions of chromosome 22q11 that affect a common region, *INI1* (also known as *SMARCB1*, *hSNF5*, or *BAF47*). This gene encodes a protein that forms part of a histone-binding SWI-SNF complex which is important in chromosomal maintenance [253]. Normal cells ubiquitously express INI1, as do most neoplasms [254]. A subset of patients with rhabdoid tumors show constitutional deletions and are at risk for multiple tumors [255].

Gross and Microscopic Features

Beckwith and Palmer [256] initially termed rhabdoid tumors "rhabdomyosarcomatoid forms of Wilms tumor" because of their classic rhabdomyosarcoma-like appearance, which comprises patternless sheets of cells with moderately abundant eosinophilic cytoplasm and eccentric nuclei. The nuclei often contain a large, prominent nucleolus, and the cytoplasm typically contains a hyaline inclusion made of whorled

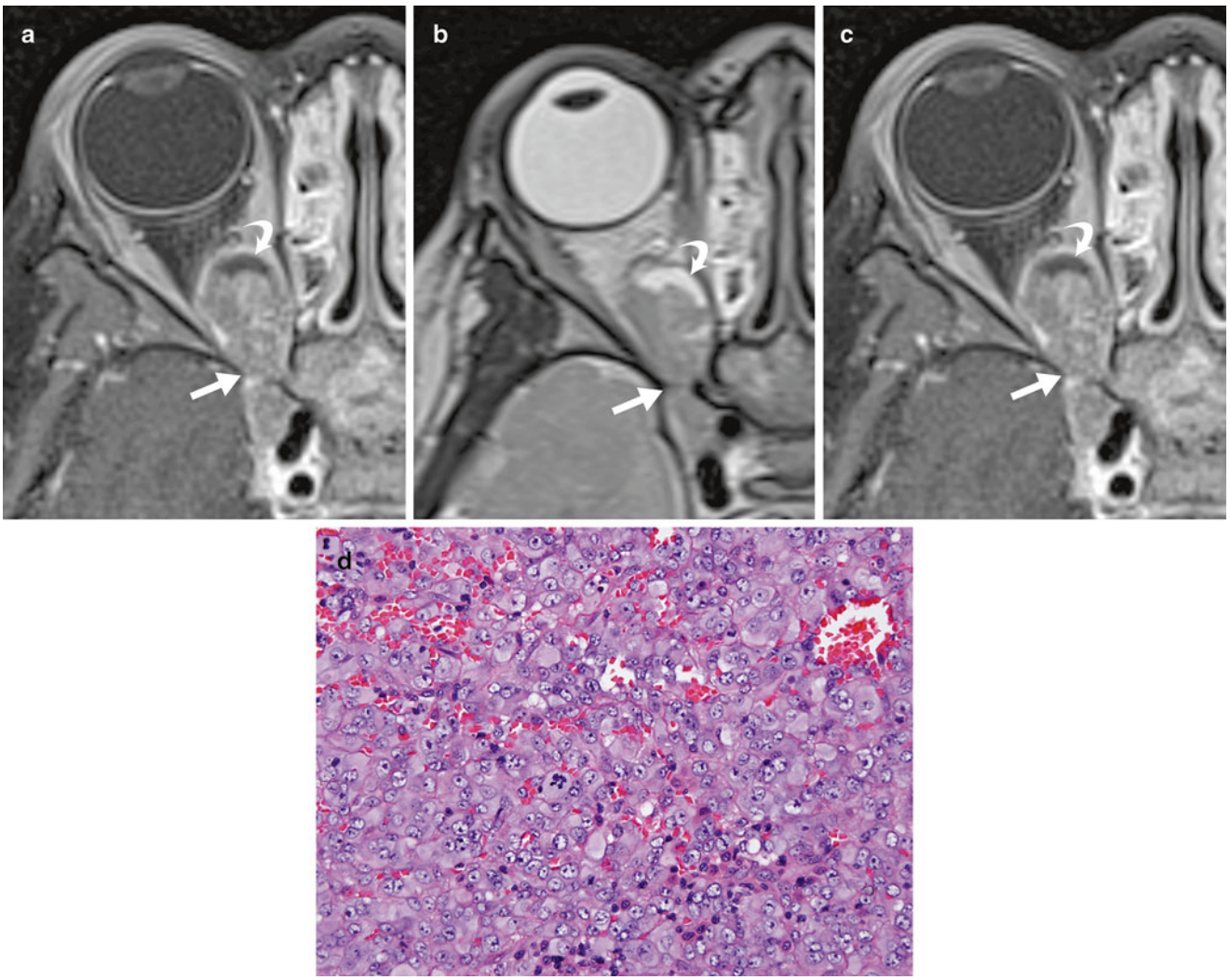

Fig. 3.19 Rhabdoid tumor. A 2-year-old girl with right orbital rhabdoid tumor. (**a**) Non-contrast-enhanced T1W image shows the tumor to be predominantly solid and isointense to muscle. The anterior aspect is hypointense on this sequence, is bright on (**b**) T2W images, and (**c**) non-enhancing on post-contrast T1W imaging, consistent with a cystic or necrotic component (*curved arrows*). Note heterogeneous contrast enhancement of solid component. The tumor extends through the optic canal (*straight arrows*). (**d**) Patternless sheets of epithelioid cells usually characterize this lesion. The tumor cells contain eccentric nuclei and variable eosinophilic cytoplasm, usually with ovoid paranuclear inclusions. Although they show no obvious differentiation, polyphenotypia is usually noted with immunochemistry (not shown)

masses of intermediate filaments (Fig. 3.19d) [257]. There is considerable histological variation [258], including small round blue cell forms that resemble lymphoma or histocytic sarcoma. Lesions with characteristic clinical, immunohistochemical, and/or genetic findings may lack the classical histology of this tumor [254].

Immunohistochemistry and Other Special Stains

Characteristically, rhabdoid tumors co-express a variety of intermediate filaments, particularly vimentin and cytokeratin [249]. Their epithelial nature is confirmed by EMA staining, but a confusing array of polyphenotypia may occur, with positive neural markers and CD99 [249]. Recently, INI1 has emerged as a major diagnostic marker, in that rhabdoid tumors generally show negative staining that contrasts with normal cells and the majority of other tumors [254, 259]. However, a growing list of other INI1-negative tumors is emerging [253].

Molecular Diagnostic Features and Cytogenetics

Early cytogenetic studies seemed to indicate that rhabdoid tumors show minimal karyotypic alterations [260], but monosomy 22 appeared frequent in atypical teratoid rhabdoid tumors. Additional work indicated that lesions lacking karyotypic abnormalities probably contained submicroscopic deletions of chromosome 22q11 and many showed loss of expression without apparent gene deletion [261]. Translocations may involve this region [262]. *BCR*, the gene

translocated in chronic myelogenous leukemia, abuts the *INI1* locus and may be useful as a surrogate deletion marker in FISH studies [263].

Prognostic Features

Malignant rhabdoid tumors have a well-deserved reputation for clinical aggressiveness and dismal outcome [264]. Although occasional case reports document cures with combination chemotherapy [265], the best chance for survival remains complete excision [249].

Epithelioid Sarcoma

Definition: Epithelioid sarcoma is a malignant soft tissue lesion showing squamous epithelial cell differentiation and immunophenotypic characteristics.

Clinical Features and Epidemiology

Epithelioid sarcoma is primarily a lesion of older children and adolescents, although some are described in young children [266]. There may be some overlap in the latter cases with rhabdoid tumor of soft tissue [253]. Most epithelioid sarcomas occur in distal soft tissues, particularly that of the upper extremity and hand [267]. The proximal variant of epithelioid sarcoma shows a tendency to occur in more axial locations [268]. Epithelioid sarcomas form infiltrative lesions that spread along tendons and aponeuroses. The primary lesion may be inconspicuous, leading to diagnosis only with the appearance of lymph nodal metastasis [267]. Nodal metastasis occurs in about 40 % of patients [266]. Some lesions are relatively indolent, but others grow quickly. There may be a clinical resemblance to ganglion cyst. Most patients are male. Symptoms include pain and nerve compression.

Imaging Features

Epithelioid sarcoma may present as single or multiple nodules, sometimes elevated on the skin or as deep infiltrative lesions. Necrosis or hemorrhage may develop. On radiographs, calcifications are seen in about 20 % of cases [72, 269]. Deep, longer-standing lesions may cause secondary changes in adjacent bone such as cortical thickening [269, 270].

MR characteristics are nonspecific and widely variable but reflect areas of hemorrhage, fibrosis, and varying degrees of cellularity (Fig. 3.20a–c). Peritumoral edema is common [269]. The infiltrative growth pattern of epithelioid sarcoma can be readily defined by MR. These tumors are characterized by T1-weighted signal that is isointense with muscle, heterogeneous T2-weighted signal, and enhancement with intravenous gadolinium contrast administration [269, 270].

The limited experience available to date with 18F FDG in imaging epithelioid sarcoma suggests a role in the staging of primary disease and detection of distant metastases [270].

Molecular Genetics

Deletions of the *INI1* gene characterize both conventional and proximal subtypes of epithelioid sarcoma [268]. Some tumors lack *INI1* deletions, suggesting alternate methods of gene inactivation [261].

Gross and Microscopic Features

Gross features of epithelioid sarcoma include one or more firm, unencapsulated nodules, poorly circumscribed margins, and sometimes foci of caseous necrosis. The overlying skin may be ulcerated, with draining sinus tracts. Low power examination of epithelioid sarcomas, particularly the conventional type, often reveals central foci of necrosis surrounded by cuffs of epithelioid cells, resembling tubercles. The tumor cells can show prominent squamous differentiation, replete with polygonal outlines, eosinophilic cytoplasm, and desmosomal junctions (Fig. 3.20d). Occasional giant cells may be seen, and calcification may be present. Recruitment of myofibroblasts within the tumor leads to intercellular collagen deposition. At times the lesion looks deceptively bland, very much like deep granuloma annulare. Occasional lesions may resemble epithelioid angiosarcoma. Rare examples have a fibroma-like appearance that can be confused with spindle cell tumors [271].

The proximal variant of epithelioid sarcoma typically shows features of a higher grade tumor (Fig. 3.20e) and contains many rhabdoid cells [253]. This latter feature has led to confusion in the literature between epithelioid sarcoma and rhabdoid tumor [272], but the two neoplasms comprise distinct clinicopathologic entities [253].

Immunohistochemistry and Other Special Stains

Co-expression of vimentin, cytokeratin, and EMA characterizes epithelioid sarcomas. About one-half express CD34, which can help diagnose tumors with aberrant staining [273]. Like rhabdoid tumor, some cases show polyphenotypia and expression of unexpected cell markers [274]. INI1 negativity is seen in both proximal and classical forms [268].

Molecular Diagnostic Features and Cytogenetics

With cytogenetic study, epithelioid sarcomas may show deletions or translocations involving chromosome 22q11 [253, 275]. *INI1* loss may be demonstrated with FISH probes [276].

Prognostic Features

In general, proximal epithelioid sarcomas show an aggressive behavior, with worse outcomes than distal ones [277]. Other indicators of poor prognosis include lymph node metastasis and vascular invasion [277–279]. Factors associated with better outcome include lower grade, female sex, younger age, size <2 cm, and presence of lymphocytic infiltration [280].

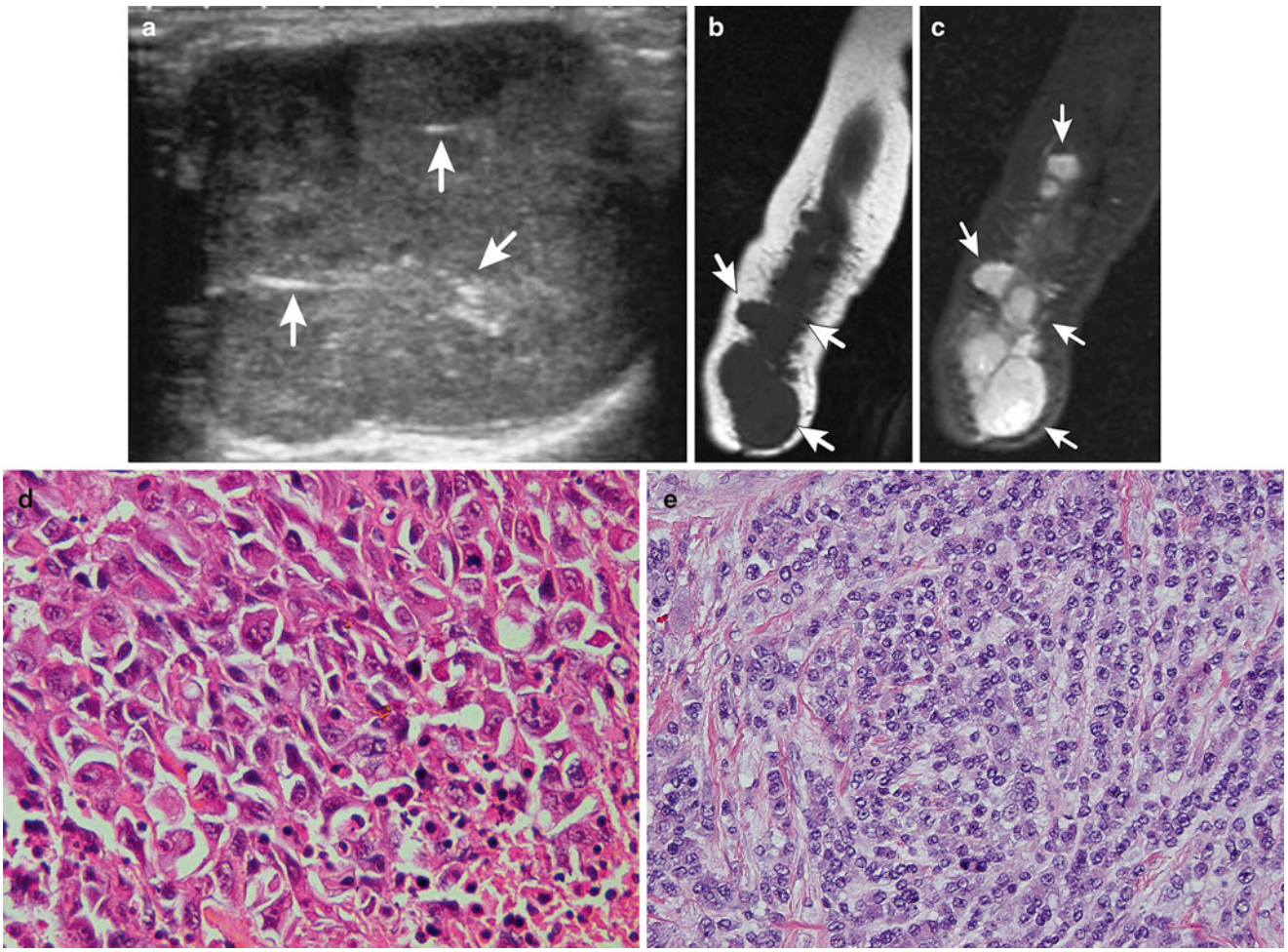

Fig. 3.20 Epithelioid sarcoma. (**a**–**c**) Recurrent epithelioid sarcoma in a 5-month-old boy born with a golf ball-sized mass right forearm. At diagnosis, ultrasound image (**a**) shows a well-circumscribed solid subcutaneous mass with scattered central strands of fibrosis (*arrows*). The surgical margins were positive for residual tumor. At presentation of disease recurrence, sagittal T1-weighted (**b**) and short tau inversion recovery (STIR; **c**) show multiple subcutaneous nodules tracking from the primary site of disease proximally to the elbow, sparing involvement of bone. On T1-weighted sequence (**b**), the nodules are isointense with muscle. On STIR (**c**), they demonstrate increased signal (*arrows*). (**d**) On histological examination, classical epithelioid sarcomas show squamous differentiation and resemble carcinoma. Note the zonal necrosis in the lower figure. (**e**) Proximal variant of epithelioid sarcoma comprises sheets of rhabdoid cells with eosinophilic cytoplasm and paranuclear inclusions. This example has a primitive, small cell appearance and forms epithelioid strands of tumor cells

Clear Cell Sarcoma of Soft Tissue (Melanoma of Soft Parts)

Definition: Clear cell sarcoma of soft parts is a fully malignant soft tissue sarcoma showing melanocytic features and containing a characteristic *EWS* translocation. It should not be confused with the unrelated clear cell sarcoma of the kidney.

Clinical Features and Epidemiology

Clear cell sarcoma occurs only rarely, and is even rarer in the pediatric population. Among 185 patients entered on POG soft tissue sarcoma trials, only 5 (3.8 %) had a clear cell sarcoma [5]. There is a slight male predominance (1.5:1), and the median age was 30 in one large series, with the youngest patient being 13 years old [281]. Lesions typically appear in the foot, ankle, leg, and knee [282], although some arise in the trunk. Patients often complain of pain of long duration [283].

Imaging Features

Up to 40 % of clear cell sarcomas occur near the Achilles tendon or plantar aponeurosis. Radiographs may reveal a soft tissue mass. Although involvement of adjacent bone is occasionally encountered, calcification is rare. On MR images, clear-cell sarcomas are typically sharply demarcated and homogeneous and are not often associated with intratumoral necrosis or osseous destruction. These tumors are slightly

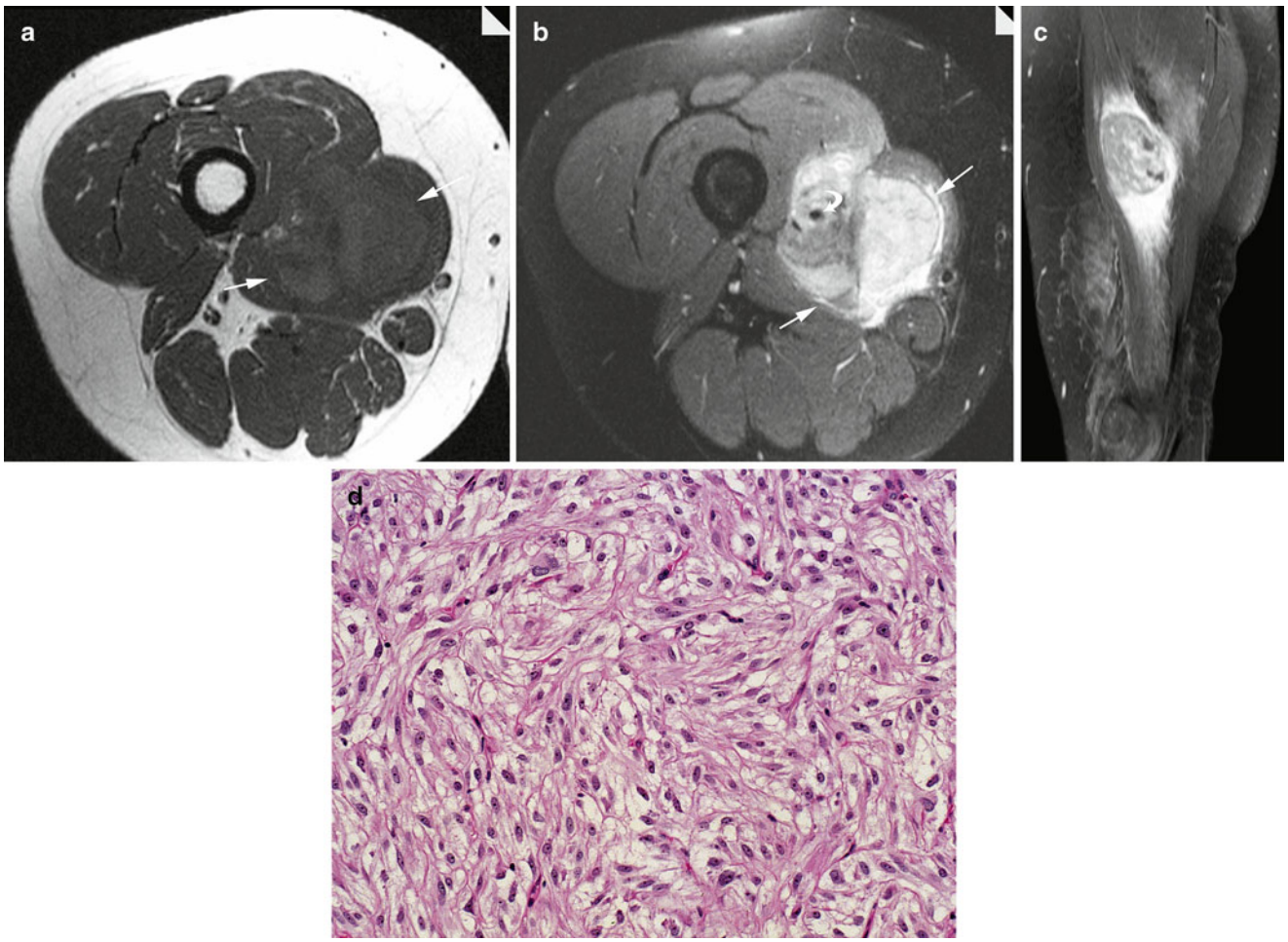

Fig. 3.21 Clear cell sarcoma of soft parts. (**a**–**c**) An 11-year-old girl with clear cell sarcoma of the right thigh. (**a**) Axial non-contrast-enhanced T1W MR image shows the tumor (*arrows*) to be slightly hyperintense to muscle but difficult to visualize. (**b**) Axial T2W MR image shows the tumor (*straight arrows*) to be sharply marginated and very heterogeneous. Low-signal areas within the tumor partially correspond to hyperintense areas seen in 1a and are probably due to melanin. The tumor encases the neurovascular bundle (*curve arrow*) making surgical resection difficult. (**c**) Sagittal contrast-enhanced T1W image shows minimal tumor enhancement with extensive surrounding edema. Non-enhancing foci within the tumor likely represent areas of necrosis. (**d**) Microscopic image of clear cell sarcoma, containing epithelioid cells in whorled clusters. The cells contain clear cytoplasm. They co-expressed smooth muscle actin and HMB-45 (not shown)

hyperintense to skeletal muscle on T1-weighted MR images [284], perhaps because of the presence of melanin (Fig. 3.21a). Areas of low-signal intensity relative to muscle on T2-weighted images, are also presumably due to melanin content (Fig. 3.21b); however, most lesions are of intermediate to high signal intensity on this sequence. The tumors demonstrate enhancement after administration of gadolinium (Fig. 3.21c).

Molecular Genetics

Characteristically, clear cell sarcoma of soft tissue contains a reciprocal translocation, the t(12;22)(q13;q12) [283]. The resultant *EWS-ATF1* gene produces a chimeric protein containing the transactivation locus of *EWS* and the basic leucine zipper region of *ATF1*. This fusion frees ATF1 protein from the control of cAMP and produces aberrant DNA transcription, with upregulation of MiTF and other melanocytic proteins [285]. The genetic features of clear cell sarcoma distinctly differ from those of melanoma [283].

Gross and Microscopic Features

Grossly, clear cell sarcomas form deep-seated, infiltrative masses, intimately bound to adjacent tendons and aponeuroses. Lesions may infiltrate into overlying dermis but do not ulcerate the skin. They display a firm, fleshy, grey cut surface, sometimes with necrosis, hemorrhage, cystic change, and/or brown to black pigment.

The tumor cells form a nested to fascicular packet-forming growth pattern, outlined by fibrovascular septa (Fig. 3.21d), at times reminiscent of alveolar rhabdomyosarcoma [282, 283].

Others show a more diffuse epithelioid appearance, contain lymphocytic infiltrates, and resemble seminoma. The lesions typically contain uniform cells with round to oval nuclei, vesicular chromatin, and prominent red nucleoli. The cytoplasm is moderately abundant and usually clear, although slight eosinophilia and even rhabdoid cells may be seen. Occasional giant cell formation and pleomorphism are not unusual features. Some clear cell sarcomas contain melanin pigment, which can be accentuated by the Fontana melanin stain [283].

Immunohistochemistry and Other Special Stains

Melanocytic marker expression characterizes clear cell sarcoma and reflects its content of premelanomes and melanosomes on ultrastructural examination. Melanocytic proteins expressed by clear cell sarcoma include S100 (the most sensitive marker), HMB45, MiTF, and melan A. The latter proteins may be found focally in some cases and not at all in a few others [281, 282]. Positive staining may also be present for bcl2 (most tumors), synaptophysin and CD57 (about one-half of cases), and CD56, CD117, EMA, cytokeratin, and CD34 (occasional). Muscle markers such as desmin and actin are negative [281].

Molecular Diagnostic Features and Cytogenetics

The characteristic *EWS-ATF1* of clear cell sarcoma may be detected by RT-PCR [281], and *EWS* rearrangement may be demonstrated by FISH [160]. The latter test is potentially useful in separating clear cell sarcoma from melanoma. However, one should keep alternate translocations such as the t(2;22) in mind when interpreting these results.

Prognostic Features

Regional lymph node and/or distant metastases are feared consequences of clear cell sarcoma and occur in over one-half of patients [283]. Prognostic factors predictive of metastases have been controversial; some authors find no value in pathological findings, whereas others have found tumor size and necrosis to be prognostic [283]. Nevertheless, a slow progression characterizes clear cell sarcoma, and in one recent study the survival rate drops from 63 % at 5 years to 25 % at 10 years [281, 286]. Radical excision is the treatment of choice, as chemotherapy offers little benefit [286].

Myoepithelial Tumor of Soft Tissues (Parachordoma)

Definition: Myoepithelial tumors of soft tissue (also known as mixed tumor; formerly known as parachordoma or chordoid sarcoma [287]) comprise a group of benign and malignant lesions that show a myoepithelial phenotype and occur in deep and superficial soft tissues.

Clinical Features and Epidemiology

The recent description of myoepithelial tumor as a soft tissue lesion precludes adequate epidemiology, but its predecessor parachordoma was a distinctly rare and unusual neoplasm—only three cases had been reported as late as 1995 [287]! These are mainly adult tumors, but about one quarter of them arise in children [288]. Patient ages have ranged from newborn to 17 years, with a median of 9 years. No gender predilection is apparent. Reported Lesions arose in a variety of locations, including extremities (14 cases), trunk (6 cases), head and neck (4 cases), mediastinum (3 cases), retroperitoneum (1 case), and heart (1 case). Symptoms arose from a growing mass, with or without pain.

Imaging Features

There are few articles describing the imaging features of myoepithelial tumor of soft tissue. On CT imaging this tumor has been described as a well-defined, diffusely enhancing homogenous or slightly heterogeneous tumor that generally lacks calcification, fat, or bony involvement. On MRI myoepithelial tumors of soft tissue may appear hypo- to isointense on T1W images, hyperintense on T2W images, and diffusely enhancing after contrast administration [289].

Molecular Genetics

No single molecular alteration characterizes myoepithelial tumors of soft tissue. Deletion of *INI1* is a recurring but not universal theme [253], and *EWS* rearrangement occurs in almost one-half of cases [290].

Gross and Microscopic Features

A thin pseudocapsule often circumscribes myoepithelial tumors of soft tissue. In one series, sizes of pediatric myoepithelial carcinomas ranged from 1.3 to 12 cm (median 4.7 cm) [288], whereas in a larger series that included adults, tumors ranged from 1.7 to 20 cm (median 4.7 cm) [291]. Cut surfaces showed a considerable heterogeneity that included fleshy, gelatinous, and gritty features, with variable degrees of necrosis.

Low power microscopic examination of soft tissue myoepithelial tumors reveals a distinctly lobular or multinodular appearance. Lobules show peripheral cellular condensation and contain myxoid to hyaline stroma enmeshing cells in a variety of histological patterns, including reticular, trabecular, nested, and solid features (Fig. 3.22a). Variable proportions of epithelioid, clear, spindle, and plasmacytoid cells constitute these tumors. Some have a small blue round cell appearance, and occasional examples contain ducts, cartilage, bone, or calcification [288]. Like the physaliferous cells of chordoma, cells may contain numerous vacuoles (Fig. 3.22b), hence the older term "parachordoma" [287].

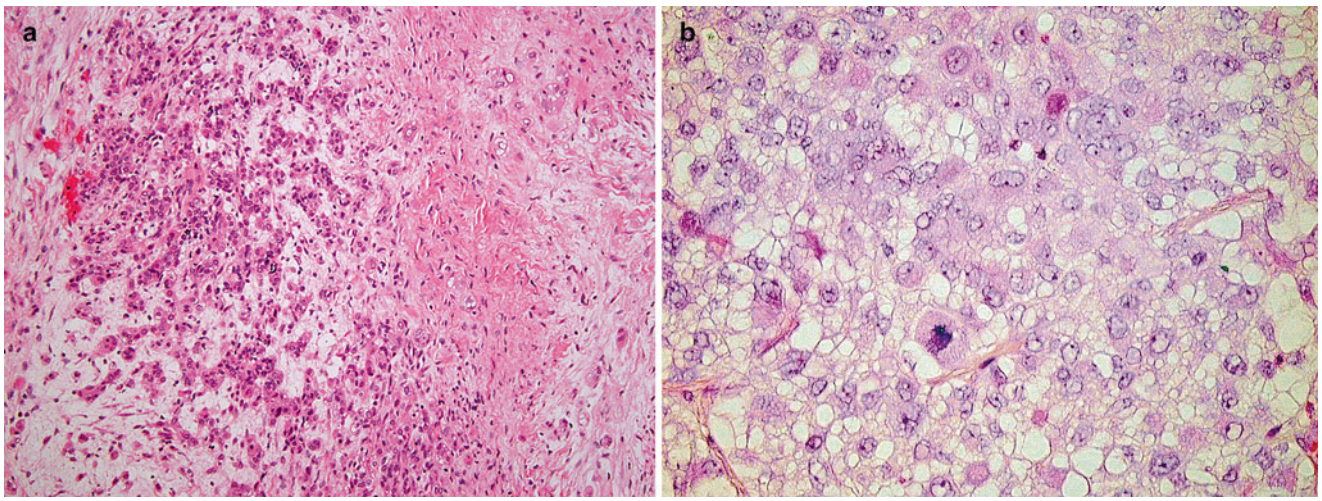

Fig. 3.22 Myoepithelial tumor of soft tissues (parachordoma). (**a**) Poorly defined aggregates of epithelioid cells are separated by myxoid stroma on the *left*. Dense collagen is noted on the *right*. (**b**) Higher power photograph highlights cytoplasmic vacuoles resembling those of physaliferous cells seen in chordoma

Immunohistochemistry and Other Special Stains

Like mixed tumors of salivary glands, myoepithelial tumors of soft tissue co-express cytokeratin, actin, and S100. Cytokeratin expression is a ubiquitous finding, but different antibodies give differing results [291]. Most cases also show positivity for EMA, S100, or GFAP. Smooth muscle markers actin and calponin are positive in most tumors, whereas desmin is usually negative [291]. CD34 is also typically negative, but CD99 is often positive. INI1 expression is lost in about one-half of tumors [291]. Brachyury expression is absent [292].

Molecular Diagnostic Features and Cytogenetics

A variety of cytogenetic abnormalities have been recorded with pediatric myoepithelial carcinoma of soft tissue. A recent study found *EWS* rearrangement in about one-half by FISH [290]. *EWS* fuses with *POU5F1*, *PBX1*, or *ZNF444*. Cases with *EWS-POU5F1* contain cells with clear cytoplasm.

Prognostic Features

About one-half of pediatric myoepitheliomas recur, in spite of clean surgical margins [288]. Almost all with marginal involvement recur, whereas wide margins predict good outcome. In one series of 23 patients, 12 developed metastases to a variety of locations, mostly lung and lymph node, and 10 had died after 10 days to 39 months (median 9 months) [288]. There was no correlation of survival with age, site, or mitotic rate. In a larger series of 101 patients from all ages and histologies, no clinical or histological parameters correlated with outcome [291].

Desmoplastic Small Round Cell Tumor

Definition: Desmoplastic small round cell tumor (DSRCT) is a highly malignant primitive sarcoma that shows a profound tendency for intra-abdominal origin, polyphenotypic expression of cell markers, and fusion of *EWS* and *WT1* genes.

Clinical Features and Epidemiology

In pediatrics, DSRCT primary arises in adolescents. Among 51 patients from Mayo Clinic [293] and Memorial Sloan Kettering Cancer Center [294], patient ages ranged from 6 to 54 years. DSRCT shows a marked predilection for males, with M:F ratios of 29:3 and 16:3 in the aforementioned series. Almost all DSRCTs arise in the abdomen, usually within the abdominal cavity. However, rare lesions arise in intrascrotal, pleural, and even CNS and extremity locations.

Symptoms and signs of DSRCTs usually relate to their predominately abdominal location and include abdominal pain, weight loss, hernia, ascites, increased girth, constipation, and hepatosplenomegaly [293]. Laparotomy typically reveals peritoneal implants, often with hepatic involvement.

Fortunately, DSRCTs are rare neoplasms; only 32 were seen at Mayo Clinic over an 8-year period [293].

Imaging Features

Because most DSRCTs arise in the abdomen or pelvis and spread diffusely throughout the peritoneum, the most common imaging finding is peritoneal thickening, nodules and bulky masses arising from the omentum or mesentery. Solitary, primary peritoneal masses, however, can occur without peritoneal spread. Peritoneal primary tumors tend to

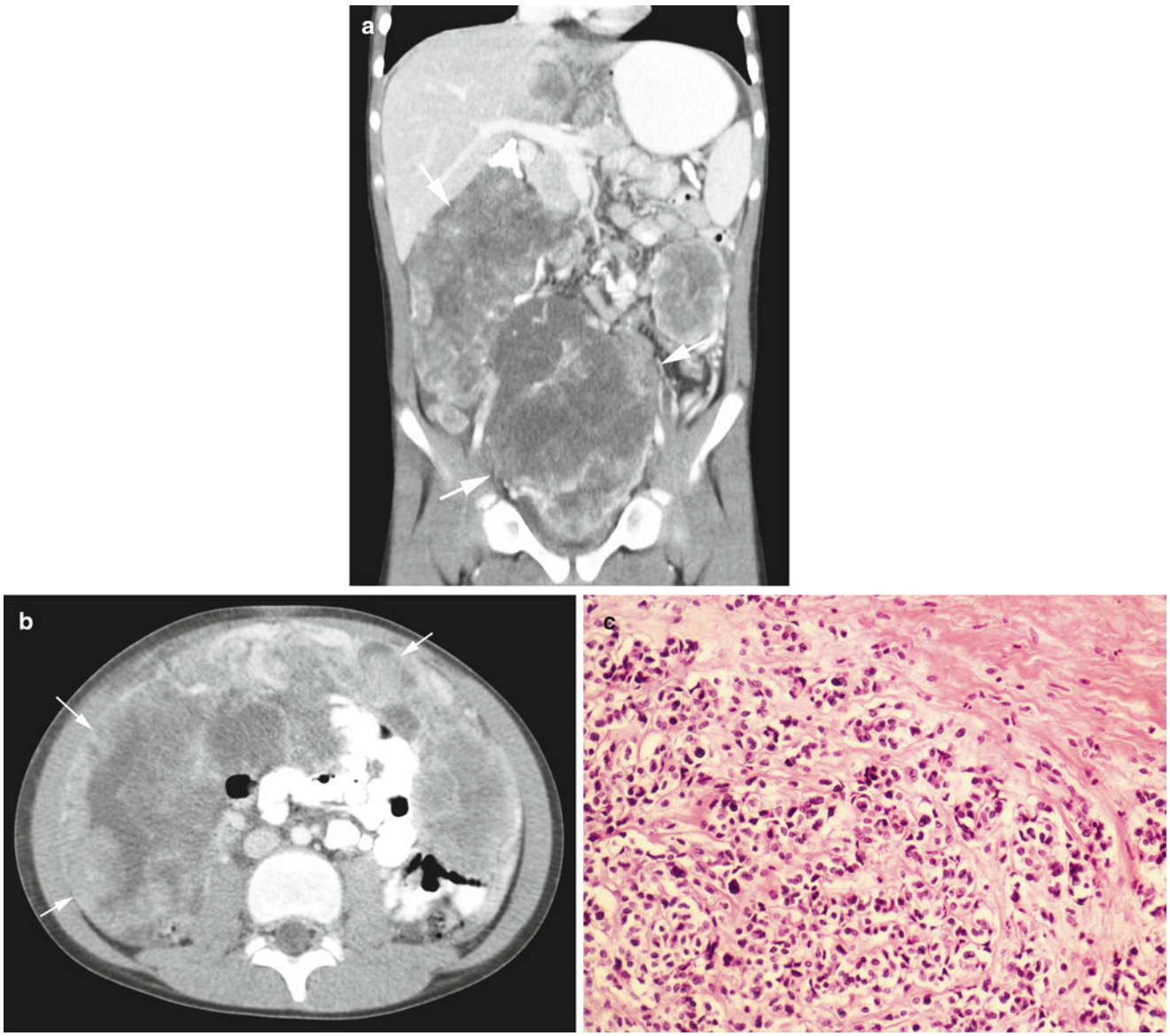

Fig. 3.23 Desmoplastic small round cell tumor. An 11-year-old boy presented with abdominal pain and mass. (**a**) Reconstructed coronal post-contrast CT image shows large, lobulated and partially necrotic peritoneal and pelvic masses (*arrows*). (**b**) Axial post-contrast CT image shows omental caking (*arrows*) typical of this tumor. (**c**) Variably sized nests of primitive round cells are embedded within a collagenous stroma in this intra-abdominal neoplasm. The lesion was positive for EMA, cytokeratin, S100, NSE, vimentin, and desmin (not shown)

be large, often 10 cm or larger at the time of diagnosis (Fig. 3.23a, b). Tumor masses displace adjacent structures but may cause bowel and ureteral obstruction. Masses are usually heterogeneous on CT and often contain central hypodense areas reflecting hemorrhage or necrosis. Tumors may contain punctuate calcification. Associated malignant ascites is a common finding [295, 296].

On MRI, DSRCTs demonstrate a heterogeneous signal, predominantly hypointense on T1W images and hyperintense on T2W sequences, with inhomogeneous enhancement after administration of contrast material. In one report, tumors contained areas that were hypointense on T2W images and enhanced mildly after contrast administration. These areas were felt to represent densely desmoplastic tissue. Also noted was the presence of fluid-fluid levels on T2W images and hyperintense foci on T1W images due to intratumoral hemorrhage [296]. Lymphatic and hematogenous (lung, liver, bone) metastasis occurs in about 50 % of patients at presentation, and careful attention should be paid to the bones, solid organs, and nodal basins for evidence of metastatic disease [295, 296]. A preliminary report of the value of FDG PET-CT found that DSRCTs are FDG avid, and this modality can reveal occult sites of disease not detected by conventional imaging [296].

Molecular Genetics

DSRCT contains a reciprocal translocation, the t(11;22)(p13;q12), which produces an *EWS-WT1* fusion [297]. The resultant protein transactivates the zinc finger region of WT1 and thus dysregulates DNA transcription.

Gross and Microscopic Features

DSRCT produces firm, multinodular masses with a grey-tan, solid cut surface, usually with attached mesentery or omentum.

Histologically, a dense collagenous stroma contains variably sized and contoured nests of cohesive small round cells (Fig. 3.23c), which sometimes occur in nests or sheets. The tumor cells generally contain round hyperchromatic nuclei, inconspicuous nucleoli, and modest amounts of ill-defined cytoplasm. Some cells contain more abundant, epithelioid cytoplasm, sometime producing rhabdoid cells. Occasional tubules, glands, and rosettes may be found [298]. Central geographic necrosis commonly occurs.

If one uses the *WT1-EWS* as a diagnostic standard, then a wider range of unexpected findings emerge including variations in cellularity, architecture, and immunoreactivity. About one-third of cases show unexpected findings, such as spindle cells, a lack of significant desmoplasia, or a zellballen or carcinoid-like appearance [299, 300].

Immunohistochemistry and Other Special Stains

Polyphenotypia, with expression of epithelial, neural, and mesenchymal markers, characterizes DSRCT [294]. These markers include cytokeratin and EMA (epithelium), neuron-specific enolase and CD57 (nerve), and desmin and vimentin (mesenchyme). Although negative in some cases, desmin stains characteristically produce a globoid or dot-like pattern of staining. Other variably positive markers include CD99, NB84, synaptophysin, CD15, actin, myoglobin, and chromogranin [293, 300]. WT1 stains are positive, if the antibody is directed against the carboxyl portion of the fusion protein [293]. INI1 stains show nuclear staining, differentiating DSRCT from rhabdoid tumor and epithelioid sarcoma.

Molecular Diagnostic Features and Cytogenetics

The t(11;22)(p13;q12) may be demonstrated by routine karyotype [301], and the *EWS-WT1* fusion can be shown by RT-PCR or FISH [293].

Prognostic Features

DSRCT carries a dismal prognosis, with survival rates of 30 % at 5 years, persistent disease after therapy, and widespread abdominal seeding similar to ovarian carcinoma [294]. However, recent reports suggest a better outcome with multimodality therapy, dependent upon neoadjuvant chemotherapy, complete surgical resection (including implants), and judicious adjuvant radiation [302].

Undifferentiated Sarcomas

Definition: The term "undifferentiated sarcoma" currently encompasses a wide array of neoplasms with considerable histological and molecular heterogeneity. It is primarily based on absence of cytological differentiation, indefinite nature of immunophenotypic features, and lack of a defining genetic aberration such as a well-characterized gene fusion or deletion. The lesion should have definite features of malignancy, such as hypercellularity, mitotic activity (with atypical figures), nuclear pleomorphism, and geographic necrosis.

Clinical Features and Epidemiology

Because of the lack of clear cut clinicopathological definition of undifferentiated sarcoma, characterization of clinical features becomes difficult. In a review of 34 undifferentiated sarcomas that were treated on IRSG protocols [303], ages ranged from 0 to 20 years, with a mean of 9 years. There was a slight male predominance, and most occurred in the extremities. The remainder arose in a variety of axial soft tissue and visceral locations. Most measured more than 5 cm and were either Group 3 or Group 4 (see Table 3.9). Undifferentiated sarcomas comprised less than 10 % of all IRSG cases.

Imaging Features

The imaging features of undifferentiated sarcomas have not been described.

Molecular Genetics

By definition, undifferentiated sarcomas should have no defining genetic features. However, *CIC-DUX4* fusions have been described in some [304].

Gross and Microscopic Features

For lack of a better method of delineation, undifferentiated sarcomas may be separated into spindle cell lesions, which coincide with pleomorphic sarcoma (formerly MFH; see above) and small cell lesions resembling Ewing sarcoma. Undifferentiated infantile sarcomas with myxoid features have been described as an entity by Alaggio et al. [29]. Unclassified sarcomas comprise a large portion of tumors in the current COG study of non-rhabdomyosarcomatous soft tissue sarcomas (NRSTS) [unpublished data]. Of these, many lack sufficient immunohistochemical and genetic data to exclude defined lesions, whereas others appear to be bona fide "undifferentiated sarcomas." Additional studies will soon be forthcoming on these enigmatic neoplasms. Recent publications suggest that *CIC-DUX4* fusion sarcomas have characteristic morphological features such as extensive necrosis, mild nuclear pleomorphism, coarse chromatin, prominent nucleoli, and foci of clear cells and myxoid matrix [305]. Lymph node metastasis, an unusual feature with Ewing sarcoma, also appears to be a distinctive feature of *CIC-DUX4* sarcomas [306].

Immunohistochemistry and Other Special Stains

By definition, lesions should not show features of a differentiating phenotype, i.e., myogenic, epithelial, or neural features. However, it is well accepted that certain markers are non specific, so they do not necessarily exclude this diagnosis. Examples include CD99, vimentin, neuron-specific enolase, CD56, CD68, and alpha-1-antitrysin. In particular, variable CD99 expression may occur with *CIC-DUX4* fusion tumors [307, 308], as well as occasional expression of cytokeratin and S100 [305, 306].

Molecular Diagnostic Features and Cytogenetics

By definition, no specific genetic features may be present, although undifferentiated sarcomas may show chromosomal deletions and additions. *CIC-DUX6* fusion has been reported in some [304] and may be detected by RT-PCR [306, 307].

Prognostic Features

In older IRSG studies that preceded the COG, undifferentiated sarcoma was an aggressive tumor that behaved more aggressively than ERMS and more like ARMS. Unfortunately, because they preceded modern genetic lesions, this group of neoplasms suffers from probable heterogeneity and likely includes lesions such as poorly differentiated synovial sarcoma. Prognosis was improved in a later review that included modern diagnostic techniques [303]. Current COG studies place undifferentiated sarcomas into a treatment category separate from rhabdomyosarcoma. Some data indicate that *CIC-DUX4* fusions impart a poor prognosis [307], but this has not been tested with COG data.

Acknowledgment The authors thank Ali Nael, M.D. for editorial review of this chapter.

References

1. Fletcher CD. The evolving classification of soft tissue tumours: an update based on the new WHO classification. Histopathology. 2006;48:3–12.
2. Parham D, Pao W, Pratt C, et al. A histological grading system of prognostic significance for childhood – adolescent soft tissue sarcomas other than rhabdomyosarcoma. Mod Pathol. 1990;3:78A.
3. Pratt CB, Maurer HM, Gieser P, et al. Treatment of unresectable or metastatic pediatric soft tissue sarcomas with surgery, irradiation, and chemotherapy: a Pediatric Oncology Group study. Med Pediatr Oncol. 1998;30:201–9.
4. Coindre JM, Trojani M, Contesso G, et al. Reproducibility of a histopathologic grading system for adult soft tissue sarcoma. Cancer. 1986;58:306–9.
5. Khoury JD, Coffin CM, Spunt SL, et al. Grading of nonrhabdomyosarcoma soft tissue sarcoma in children and adolescents: a comparison of parameters used for the Federation Nationale des Centers de Lutte Contre le Cancer and Pediatric Oncology Group Systems. Cancer. 2010;116:2266–74.
6. Navarro OM. Soft tissue masses in children. Radiol Clin North Am. 2011;49:1235–59, vi–vii.
7. Siegel MJ. Magnetic resonance imaging of musculoskeletal soft tissue masses. Radiol Clin North Am. 2001;39:701–20.
8. Stein-Wexler R. MR imaging of soft tissue masses in children. Magn Reson Imaging Clin N Am. 2009;17:489–507. vi.
9. Jadvar H, Connolly LP, Fahey FH, et al. PET and PET/CT in pediatric oncology. Semin Nucl Med. 2007;37:316–31.
10. Harms D. Soft tissue sarcomas in the Kiel Pediatric Tumor Registry. Curr Top Pathol. 1995;89:31–45.
11. Isaacs Jr H. Congenital and neonatal malignant tumors. A 28-year experience at Children's Hospital of Los Angeles. Am J Pediatr Hematol Oncol. 1987;9:121–9.
12. Kogon B, Shehata B, Katzenstein H, et al. Primary congenital infantile fibrosarcoma of the heart: the first confirmed case. Ann Thorac Surg. 2011;91:1276–80.
13. Vinnicombe SJ, Hall CM. Infantile fibrosarcoma: radiological and clinical features. Skeletal Radiol. 1994;23:337–41.
14. Canale S, Vanel D, Couanet D, et al. Infantile fibrosarcoma: magnetic resonance imaging findings in six cases. Eur J Radiol. 2009;72:30–7.
15. Fink AM, Stringer DA, Cairns RA, et al. Pediatric case of the day. Congenital fibrosarcoma (CFS). Radiographics. 1995;15:243–6.
16. Durin L, Jeanne-Pasquier C, Bailleul P, et al. Prenatal diagnosis of a fibrosarcoma of the thigh: a case report. Fetal Diagn Ther. 2006;21:481–4.
17. Eich GF, Hoeffel JC, Tschappeler H, et al. Fibrous tumours in children: imaging features of a heterogeneous group of disorders. Pediatr Radiol. 1998;28:500–9.
18. McCarville MB, Kaste SC, Pappo AS. Soft-tissue malignancies in infancy. AJR Am J Roentgenol. 1999;173:973–7.
19. Pousti TJ, Upton J, Loh M, et al. Congenital fibrosarcoma of the upper extremity. Plast Reconstr Surg. 1998;102:1158–62.
20. Knezevich SR, McFadden DE, Tao W, et al. A novel ETV6-NTRK3 gene fusion in congenital fibrosarcoma. Nat Genet. 1998;18:184–7.
21. Rubnitz JE, Downing JR, Pui CH, et al. TEL gene rearrangement in acute lymphoblastic leukemia: a new genetic marker with prognostic significance. J Clin Oncol. 1997;15:1150–7.
22. Yamashiro DJ, Nakagawara A, Ikegaki N, et al. Expression of TrkC in favorable human neuroblastomas. Oncogene. 1996;12:37–41.
23. Lannon CL, Sorensen PH. ETV6-NTRK3: a chimeric protein tyrosine kinase with transformation activity in multiple cell lineages. Semin Cancer Biol. 2005;15:215–23.
24. Lae M, Freneaux P, Sastre-Garau X, et al. Secretory breast carcinomas with ETV6-NTRK3 fusion gene belong to the basal-like carcinoma spectrum. Mod Pathol. 2009;22:291–8.
25. Alaggio R, Barisani D, Ninfo V, et al. Morphologic overlap between infantile myofibromatosis and infantile fibrosarcoma: a pitfall in diagnosis. Pediatr Dev Pathol. 2008;11:355–62.
26. Mandahl N, Heim S, Rydholm A, et al. Nonrandom numerical chromosome aberrations (+8, +11, +17, +20) in infantile fibrosarcoma. Cancer Genet Cytogenet. 1989;40:137–9.
27. Bourgeois JM, Knezevich SR, Mathers JA, et al. Molecular detection of the ETV6-NTRK3 gene fusion differentiates congenital fibrosarcoma from other childhood spindle cell tumors. Am J Surg Pathol. 2000;24:937–46.
28. Makretsov N, He M, Hayes M, et al. A fluorescence in situ hybridization study of ETV6-NTRK3 fusion gene in secretory breast carcinoma. Genes Chromosomes Cancer. 2004;40:152–7.
29. Alaggio R, Ninfo V, Rosolen A, et al. Primitive myxoid mesenchymal tumor of infancy: a clinicopathologic report of 6 cases. Am J Surg Pathol. 2006;30:388–94.
30. Nonaka D, Sun CC, Nonaka D, et al. Congenital fibrosarcoma with metastasis in a fetus. Pediatr Dev Pathol. 2004;7:187–91.

31. Russell H, Hicks MJ, Bertuch AA, et al. Infantile fibrosarcoma: clinical and histologic responses to cytotoxic chemotherapy. Pediatr Blood Cancer. 2009;53:23–7.
32. Meis-Kindblom JM, Kindblom LG, Enzinger FM. Sclerosing epithelioid fibrosarcoma. A variant of fibrosarcoma simulating carcinoma. Am J Surg Pathol. 1995;19:979–93.
33. Ossendorf C, Studer GM, Bode B, et al. Sclerosing epithelioid fibrosarcoma: case presentation and a systematic review. Clin Orthop Relat Res. 2008;466:1485–91.
34. Grunewald TG, Von LI, Weirich G, et al. Sclerosing epithelioid fibrosarcoma of the bone: a case report of high resistance to chemotherapy and a survey of the literature. Sarcoma. 2010;2010: 431627.
35. Rekhi B, Folpe AL, Deshmukh M, et al. Sclerosing epithelioid fibrosarcoma-a report of two cases with cytogenetic analysis of fus gene rearrangement by FISH technique. Pathol Oncol Res. 2011;17:145–8.
36. Guillou L, Benhattar J, Gengler C, et al. Translocation-positive low-grade fibromyxoid sarcoma: clinicopathologic and molecular analysis of a series expanding the morphologic spectrum and suggesting potential relationship to sclerosing epithelioid fibrosarcoma: a study from the French Sarcoma Group. Am J Surg Pathol. 2007;31:1387–402.
37. Donner LR, Clawson K, Dobin SM. Sclerosing epithelioid fibrosarcoma: a cytogenetic, immunohistochemical, and ultrastructural study of an unusual histological variant. Cancer Genet Cytogenet. 2000;119:127–31.
38. Mentzel T, Dry S, Katenkamp D, et al. Low-grade myofibroblastic sarcoma: analysis of 18 cases in the spectrum of myofibroblastic tumors. Am J Surg Pathol. 1998;22:1228–38.
39. Montgomery E, Goldblum JR, Fisher C. Myofibrosarcoma: a clinicopathologic study. Am J Surg Pathol. 2001;25:219–28.
40. Smith DM, Mahmoud HH, Jenkins JJ, et al. Myofibrosarcoma of the head and neck in children. Pediatr Pathol Lab Med. 1995; 112:275–81.
41. Fujiwara M, Yuba Y, Wada A, et al. Myofibrosarcoma of the nasal bone. Am J Otolaryngol. 2005;26:265–7.
42. Eyden B. The myofibroblast: an assessment of controversial issues and a definition useful in diagnosis and research. [Review] [97 refs]. Ultrastruct Pathol. 2001;25:39–50.
43. Fisher C. Myofibroblastic malignancies. [Review] [92 refs]. Adv Anat Pathol. 2004;11:190–201.
44. Montgomery E, Fisher C. Myofibroblastic differentiation in malignant fibrous histiocytoma (pleomorphic myofibrosarcoma): a clinicopathological study. Histopathology. 2001;38:499–509.
45. Hisaoka M, Wei-Qi S, Jian W, et al. Specific but variable expression of h-caldesmon in leiomyosarcomas: an immunohistochemical reassessment of a novel myogenic marker. Appl Immunohistochem Mol Morphol. 2001;9:302–8.
46. Cessna MH, Zhou H, Perkins SL, et al. Are myogenin and myoD1 expression specific for rhabdomyosarcoma? A study of 150 cases, with emphasis on spindle cell mimics. Am J Surg Pathol. 2001; 25:1150–7.
47. Cessna MH, Zhou H, Sanger WG, et al. Expression of ALK1 and p80 in inflammatory myofibroblastic tumor and its mesenchymal mimics: a study of 135 cases. Mod Pathol. 2002;15:931–8.
48. Bhattacharya B, Dilworth HP, Iacobuzio-Donahue C, et al. Nuclear beta-catenin expression distinguishes deep fibromatosis from other benign and malignant fibroblastic and myofibroblastic lesions. Am J Surg Pathol. 2005;29:653–9.
49. Vernon SE, Bejarano PA. Low-grade fibromyxoid sarcoma: a brief review. Arch Pathol Lab Med. 2006;130:1358–60.
50. Kaoutar Z, Benlemlih A, Taoufiq H, et al. Low-grade fibromyxoid sarcoma arising in the big toe. South Med J. 2011;104:241–3.
51. Bahrami A, Folpe AL. Adult-type fibrosarcoma: a reevaluation of 163 putative cases diagnosed at a single institution over a 48-year period. Am J Surg Pathol. 2010;34:1504–13.
52. Hwang S, Kelliher E, Hameed M. Imaging features of low-grade fibromyxoid sarcoma (Evans tumor). Skeletal Radiol. 2012;41: 1263–72.
53. Evans HL. Low-grade fibromyxoid sarcoma: a report of 12 cases. Am J Surg Pathol. 1993;17:595–600.
54. Lane KL, Shannon RJ, Weiss SW. Hyalinizing spindle cell tumor with giant rosettes: a distinctive tumor closely resembling low-grade fibromyxoid sarcoma. Am J Surg Pathol. 1997;21: 1481–8.
55. Doyle LA, Moller E, Dal Cin P, et al. MUC4 is a highly sensitive and specific marker for low-grade fibromyxoid sarcoma. Am J Surg Pathol. 2011;35:733–41.
56. Moller E, Hornick JL, Magnusson L, et al. FUS-CREB3L2/L1-positive sarcomas show a specific gene expression profile with upregulation of CD24 and FOXL1. Clin Cancer Res. 2011;17: 2646–56.
57. Matsuyama A, Hisaoka M, Shimajiri S, et al. Molecular detection of FUS-CREB3L2 fusion transcripts in low-grade fibromyxoid sarcoma using formalin-fixed, paraffin-embedded tissue specimens. Am J Surg Pathol. 2006;30:1077–84.
58. Downs-Kelly E, Goldblum JR, Patel RM, et al. The utility of fluorescence in situ hybridization (FISH) in the diagnosis of myxoid soft tissue neoplasms. Am J Surg Pathol. 2008;32:8–13.
59. Patel RM, Downs-Kelly E, Dandekar MN, et al. FUS (16p11) gene rearrangement as detected by fluorescence in-situ hybridization in cutaneous low-grade fibromyxoid sarcoma: a potential diagnostic tool. Am J Dermatopathol. 2011;33:140–3.
60. Mertens F, Fletcher CD, Antonescu CR, et al. Clinicopathologic and molecular genetic characterization of low-grade fibromyxoid sarcoma, and cloning of a novel FUS/CREB3L1 fusion gene. Lab Invest. 2005;85:408–15.
61. Bisogno G, Sotti G, Nowicki Y, et al. Soft tissue sarcoma as a second malignant neoplasm in the pediatric age group. Cancer. 2004;100:1758–65.
62. Horenstein MG, Prieto VG, Nuckols JD, et al. Indeterminate fibrohistiocytic lesions of the skin: is there a spectrum between dermatofibroma and dermatofibrosarcoma protuberans? Am J Surg Pathol. 2000;24:996–1003.
63. Rudolph P, Schubert B, Wacker HH, et al. Immunophenotyping of dermal spindle cell tumors: diagnostic value of monocyte marker Ki-M1p and histogenetic considerations. Am J Surg Pathol. 1997; 21:791–800.
64. Fletcher CDM. Pleomorphic malignant fibrous histiocytoma: fact or fiction? A critical reappraisal based on 159 tumors diagnosed as pleomorphic sarcoma. Am J Surg Pathol. 1992;16:213–28.
65. Brooks JJ. The significance of double phenotypic patterns and markers in human sarcomas: a new model of mesenchymal differentiation. Am J Pathol. 1986;125:113–23.
66. Garg MK, Yadav MK, Gupta S, et al. Dermatofibrosarcoma protuberans with contiguous infiltration of the underlying bone. Cancer Imaging. 2009;9:63–6.
67. Kransdorf MJ, Meis-Kindblom JM. Dermatofibrosarcoma protuberans: radiologic appearance. AJR Am J Roentgenol. 1994; 163:391–4.
68. Torreggiani WC, Al-Ismail K, Munk PL, et al. Dermatofibrosarcoma protuberans: MR imaging features. AJR Am J Roentgenol. 2002; 178:989–93.
69. Laffan EE, Ngan BY, Navarro OM. Pediatric soft-tissue tumors and pseudotumors: MR imaging features with pathologic correlation: part 2. Tumors of fibroblastic/myofibroblastic, so-called fibrohistiocytic, muscular, lymphomatous, neurogenic, hair matrix, and uncertain origin. Radiographics. 2009;29:e36.
70. Kim SD, Park JY, Choi WS, et al. Intracranial recurrence of the scalp dermatofibrosarcoma. Clin Neurol Neurosurg. 2007;109:172–5.
71. Abe T, Kamida T, Goda M, et al. Intracranial infiltration by recurrent scalp dermatofibrosarcoma protuberans. J Clin Neurosci. 2009;16:1358–60.

72. Morel M, Taieb S, Penel N, et al. Imaging of the most frequent superficial soft-tissue sarcomas. Skeletal Radiol. 2011;40:271–84.
73. Parajuly SS, Peng YL. Sonography of dermatofibrosarcoma protuberans in the skin over breast. J Med Ultrasound. 2010;18:130–5.
74. Liu SZ, Ho TL, Hsu SM, et al. Imaging of dermatofibrosarcoma protuberans of breast. Breast J. 2010;16:541–3.
75. Widmann G, Riedl A, Schoepf D, et al. State-of-the-art HR-US imaging findings of the most frequent musculoskeletal soft-tissue tumors. Skeletal Radiol. 2009;38:637–49.
76. Shin YR, Kim JY, Sung MS, et al. Sonographic findings of dermatofibrosarcoma protuberans with pathologic correlation. J Ultrasound Med. 2008;27:269–74.
77. Walker EA, Salesky JS, Fenton ME, et al. Magnetic resonance imaging of malignant soft tissue neoplasms in the adult. Radiol Clin North Am. 2011;49:1219–34, vi.
78. Riggs K, McGuigan KL, Morrison WB, et al. Role of magnetic resonance imaging in perioperative assessment of dermatofibrosarcoma protuberans. Dermatol Surg. 2009;35:2036–41.
79. Thornton SL, Reid J, Papay FA, et al. Childhood dermatofibrosarcoma protuberans: role of preoperative imaging. J Am Acad Dermatol. 2005;53:76–83.
80. Serra-Guillen C, Sanmartin O, Llombart B, et al. Correlation between preoperative magnetic resonance imaging and surgical margins with modified Mohs for dermatofibrosarcoma protuberans. Dermatol Surg. 2011;37:1638–45.
81. Djilas-Ivanovic D, Prvulovic N, Bogdanovic-Stojanovic D, et al. Dermatofibrosarcoma protuberans of the breast: mammographic, ultrasound, MRI and MRS features. Arch Gynecol Obstet. 2009; 280:827–30.
82. Basu S, Baghel NS. Recurrence of dermatofibrosarcoma protuberans in post-surgical scar detected by 18F-FDG-PET imaging. Hell J Nucl Med. 2009;12:68.
83. Maire G, Martin L, Michalak-Provost S, et al. Fusion of COL1A1 exon 29 with PDGFB exon 2 in a der(22)t(17;22) in a pediatric giant cell fibroblastoma with a pigmented Bednar tumor component. Evidence for age-related chromosomal pattern in dermatofibrosarcoma protuberans and related tumors. Cancer Genet Cytogenet. 2002;134:156–61.
84. Orndal C, Mandahl N, Rydholm A, et al. Supernumerary ring chromosomes in five bone and soft tissue tumors of low or borderline malignancy. Cancer Genet Cytogenet. 1992;60:170–5.
85. Pedeutour F, Simon MP, Minoletti F, et al. Translocation, t(17;22)(q22;q13), in dermatofibrosarcoma protuberans: a new tumor-associated chromosome rearrangement. Cytogenet Cell Genet. 1996;72:171–4.
86. Terrier-Lacombe MJ, Guillou L, Maire G, et al. Dermatofibrosarcoma protuberans, giant cell fibroblastoma, and hybrid lesions in children: clinicopathologic comparative analysis of 28 cases with molecular data – a study from the French Federation of Cancer Centers Sarcoma Group. Am J Surg Pathol. 2003;27:27–39.
87. Sigel JE, Bergfeld WF, Goldblum JR. A morphologic study of dermatofibrosarcoma protuberans: expansion of a histologic profile. J Cutan Pathol. 2000;27:159–63.
88. Tardio JC, Tardio JC. CD34-reactive tumors of the skin. An updated review of an ever-growing list of lesions. [Review] [171 refs]. J Cutan Pathol. 2009;36:89–102.
89. Haycox CL, Odland PB, Olbricht SM, et al. Immunohistochemical characterization of dermatofibrosarcoma protuberans with practical applications for diagnosis and treatment. [see comments.]. [Review] [38 refs]. J Am Acad Dermatol. 1997;37:438–44.
90. Goldblum JR, Reith JD, Weiss SW. Sarcomas arising in dermatofibrosarcoma protuberans: a reappraisal of biologic behavior in eighteen cases treated by wide local excision with extended clinical follow up. Am J Surg Pathol. 2000;24:1125–30.
91. Sachdev R, Sundram U. Expression of CD163 in dermatofibroma, cellular fibrous histiocytoma, and dermatofibrosarcoma protuberans: comparison with CD68, CD34, and Factor XIIIa. J Cutan Pathol. 2006;33:353–60.
92. Sozzi G, Minoletti F, Miozzo M, et al. Relevance of cytogenetic and fluorescent in situ hybridization analyses in the clinical assessment of soft tissue sarcoma. Hum Pathol. 1997;28:134–42.
93. Connelly JH, Evans HL. Dermatofibrosarcoma protuberans: a clinicopathologic review with emphasis on fibrosarcomatous areas. Am J Surg Pathol. 1992;16:921–5.
94. Marks LB, Suit HD, Rosenberg AE, et al. Dermatofibrosarcoma protuberans treated with radiation therapy. Int J Radiat Oncol Biol Phys. 1989;17:379–84.
95. Abrams TA, Schuetze SM, Abrams TA, et al. Targeted therapy for dermatofibrosarcoma protuberans. [Review] [39 refs]. Curr Oncol Rep. 2006;8:291–6.
96. Enzinger FM. Angiomatoid malignant fibrous histiocytoma: a distinct fibrohistiocytic tumor of children and young adults simulating a vascular neoplasm. Cancer. 1979;44:2147–57.
97. Costa MJ, Weiss SW. Angiomatoid malignant fibrous histiocytoma. A follow-up study of 108 cases with evaluation of possible histologic predictors of outcome. Am J Surg Pathol. 1990;14: 1126–32.
98. Thway K. Angiomatoid fibrous histiocytoma: a review with recent genetic findings. Arch Pathol Lab Med. 2008;132:273–7.
99. Hothi D, Brogan PA, Davis E, et al. Polyarteritis nodosa as a presenting feature of angiomatoid fibrous histiocytoma. Rheumatology (Oxford). 2004;43:245–6.
100. Fanburg-Smith JC, Miettinen M. Angiomatoid "malignant" fibrous histiocytoma: a clinicopathologic study of 158 cases and further exploration of the myoid phenotype. Hum Pathol. 1999;30: 1336–43.
101. Ajlan AM, Sayegh K, Powell T, et al. Angiomatoid fibrous histiocytoma: magnetic resonance imaging appearance in 2 cases. J Comput Assist Tomogr. 2010;34:791–4.
102. Petrey WB, LeGallo RD, Fox MG, et al. Imaging characteristics of angiomatoid fibrous histiocytoma of bone. Skeletal Radiol. 2011;40:233–7.
103. Raddaoui E, Donner LR, Panagopoulos I. Fusion of the FUS and ATF1 genes in a large, deep-seated angiomatoid fibrous histiocytoma. Diagn Mol Pathol. 2002;11:157–62.
104. Hallor KH, Mertens F, Jin Y, et al. Fusion of the EWSR1 and ATF1 genes without expression of the MITF-M transcript in angiomatoid fibrous histiocytoma. Genes Chromosomes Cancer. 2005;44:97–102.
105. Rossi S, Szuhai K, Ijszenga M, et al. EWSR1-CREB1 and EWSR1-ATF1 fusion genes in angiomatoid fibrous histiocytoma. Clin Cancer Res. 2007;13:7322–8.
106. Weinreb I, Rubin BP, Goldblum JR. Pleomorphic angiomatoid fibrous histiocytoma: a case confirmed by fluorescence in situ hybridization analysis for EWSR1 rearrangement. J Cutan Pathol. 2008;35:855–60.
107. Fletcher CDM. Angiomatoid "malignant fibrous histiocytoma": an immunohistochemical study indicative of myoid differentiation. Hum Pathol. 1991;22:563–8.
108. Tanas MR, Rubin BP, Montgomery EA, et al. Utility of FISH in the diagnosis of angiomatoid fibrous histiocytoma: a series of 18 cases. Mod Pathol. 2010;23:93–7.
109. Corpron CA, Black CT, Raney RB, et al. Malignant fibrous histiocytoma in children. J Pediatr Surg. 1996;31:1080–3.
110. Cole CH, Magee JF, Gianoulis M, et al. Malignant fibrous histiocytoma in childhood. Cancer. 1993;71:4077–83.
111. Chow LT, Allen PW, Kumta SM, et al. Angiomatoid malignant fibrous histiocytoma: report of an unusual case with highly aggressive clinical course. J Foot Ankle Surg. 1998;37:235–8.

112. Enzinger FM, Zhang RY. Plexiform fibrohistiocytic tumor presenting in children and young adults. An analysis of 65 cases. Am J Surg Pathol. 1988;12:818–26.
113. Jafarian F, McCuaig C, Kokta V, et al. Plexiform fibrohistiocytic tumor in three children. Pediatr Dermatol. 2006;23:7–12.
114. Leclerc-Mercier S, Pedeutour F, Fabas T, et al. Plexiform fibrohistiocytic tumor with molecular and cytogenetic analysis. Pediatr Dermatol. 2011;28:26–9.
115. Segura LG, Harris J, Wang B, et al. Plexiform fibrohistiocytic tumor: a rare low-grade malignancy of children and young adults. Arch Otolaryngol Head Neck Surg. 2002;128:966–70.
116. Taher A, Pushpanathan C. Plexiform fibrohistiocytic tumor: a brief review. Arch Pathol Lab Med. 2007;131:1135–8.
117. Zelger B, Weinlich G, Steiner H, et al. Dermal and subcutaneous variants of plexiform fibrohistiocytic tumor. Am J Surg Pathol. 1997;21:235–41.
118. Remstein ED, Arndt CA, Nascimento AG. Plexiform fibrohistiocytic tumor: clinicopathologic analysis of 22 cases. Am J Surg Pathol. 1999;23:662–70.
119. Jacobson-Dunlop E, White Jr CR, Mansoor A. Features of plexiform fibrohistiocytic tumor in skin punch biopsies: a retrospective study of 6 cases. Am J Dermatopathol. 2011;33:551–6.
120. Angervall L, Kindblom LG, Lindholm K, et al. Plexiform fibrohistiocytic tumor. Report of a case involving preoperative aspiration cytology and immunohistochemical and ultrastructural analysis of surgical specimens. Pathol Res Pract. 1992;188:350–6. discussion 356-359.
121. Alaggio R, Collini P, Randall RL, et al. Undifferentiated high-grade pleomorphic sarcomas in children: a clinicopathologic study of 10 cases and review of literature. Pediatr Dev Pathol. 2010;13:209–17.
122. Stein-Wexler R. Pediatric soft tissue sarcomas. Semin Ultrasound CT MR. 2011;32:470–88.
123. Colleran G, Madewell J, Foran P, et al. Imaging of soft tissue and osseous sarcomas of the extremities. Semin Ultrasound CT MR. 2011;32:442–55.
124. Palmer JL, Masui S, Pritchard S, et al. Cytogenetic and molecular genetic analysis of a pediatric pleomorphic sarcoma reveals similarities to adult malignant fibrous histiocytoma. Cancer Genet Cytogenet. 1997;95:141–7.
125. Alaggio R, Coffin CM, Weiss SW, et al. Liposarcomas in young patients: a study of 82 cases occurring in patients younger than 22 years of age. Am J Surg Pathol. 2009;33:645–58.
126. Coindre JM, Hostein I, Maire G, et al. Inflammatory malignant fibrous histiocytomas and dedifferentiated liposarcomas: histological review, genomic profile, and MDM2 and CDK4 status favour a single entity. J Pathol. 2004;203:822–30.
127. Sarkar M, Mulliken JB, Kozakewich HP, et al. Thrombocytopenic coagulopathy (Kasabach-Merritt phenomenon) is associated with Kaposiform hemangioendothelioma and not with common infantile hemangioma. Plast Reconstr Surg. 1997;100:1377–86.
128. Hsiao CC, Chen CC, Ko SF, et al. A case of axillary kaposiform hemangioendothelioma resembles a soft tissue sarcoma. J Pediatr Hematol Oncol. 2005;27:596–8.
129. Lalaji TA, Haller JO, Burgess RJ. A case of head and neck kaposiform hemangioendothelioma simulating a malignancy on imaging. Pediatr Radiol. 2001;31:876–8.
130. Zhu Y, Qiu G, Zhao H, et al. Kaposiform hemangioendothelioma with adolescent thoracic scoliosis: a case report and review of literature. Eur Spine J. 2011;20 Suppl 2:S309–13.
131. DeFatta RJ, Verret DJ, Adelson RT, et al. Kaposiform hemangioendothelioma: case report and literature review. Laryngoscope. 2005;115:1789–92.
132. Mukerji SS, Osborn AJ, Roberts J, et al. Kaposiform hemangioendothelioma (with Kasabach Merritt syndrome) of the head and neck: case report and review of the literature. Int J Pediatr Otorhinolaryngol. 2009;73:1474–6.
133. Dadras SS, Skrzypek A, Nguyen L, et al. Prox-1 promotes invasion of kaposiform hemangioendotheliomas. J Invest Dermatol. 2008;128:2798–806.
134. Le Huu AR, Jokinen CH, Rubin BP, et al. Expression of prox1, lymphatic endothelial nuclear transcription factor, in Kaposiform hemangioendothelioma and tufted angioma. Am J Surg Pathol. 2010;34:1563–73.
135. North PE. Pediatric vascular tumors and malformations. Surg Pathol Clin. 2010;2010:455–95.
136. Bien E, Stachowicz-Stencel T, Balcerska A, et al. Angiosarcoma in children – still uncontrollable oncological problem. The report of the Polish Paediatric Rare Tumours Study. Eur J Cancer Care (Engl). 2009;18:411–20.
137. Deyrup AT, Miettinen M, North PE, et al. Angiosarcomas arising in the viscera and soft tissue of children and young adults: a clinicopathologic study of 15 cases. Am J Surg Pathol. 2009;33:264–9.
138. Deyrup AT, Miettinen M, North PE, et al. Pediatric cutaneous angiosarcomas: a clinicopathologic study of 10 cases. Am J Surg Pathol. 2011;35:70–5.
139. Thompson WM, Levy AD, Aguilera NS, et al. Angiosarcoma of the spleen: imaging characteristics in 12 patients. Radiology. 2005;235:106–15.
140. Qiu LL, Yu RS, Chen Y, et al. Sarcomas of abdominal organs: computed tomography and magnetic resonance imaging findings. Semin Ultrasound CT MR. 2011;32:405–21.
141. Abbott RM, Levy AD, Aguilera NS, et al. From the archives of the AFIP: primary vascular neoplasms of the spleen: radiologic-pathologic correlation. Radiographics. 2004;24:1137–63.
142. Lalwani N, Prasad SR, Vikram R, et al. Pediatric and adult primary sarcomas of the kidney: a cross-sectional imaging review. Acta Radiol. 2011;52:448–57.
143. Chung EM, Lattin Jr GE, Cube R, et al. From the archives of the AFIP: pediatric liver masses: radiologic-pathologic correlation. Part 2. Malignant tumors. Radiographics. 2011;31:483–507.
144. Kaneko K, Onitsuka H, Murakami J, et al. MRI of primary spleen angiosarcoma with iron accumulation. J Comput Assist Tomogr. 1992;16:298–300.
145. Van Dyck P, Vanhoenacker FM, Vogel J, et al. Prevalence, extension and characteristics of fluid-fluid levels in bone and soft tissue tumors. Eur Radiol. 2006;16:2644–51.
146. Benz MR, Dry SM, Eilber FC, et al. Correlation between glycolytic phenotype and tumor grade in soft-tissue sarcomas by 18F-FDG PET. J Nucl Med. 2010;51:1174–81.
147. Vasanawala MS, Wang Y, Quon A, et al. F-18 fluorodeoxyglucose PET/CT as an imaging tool for staging and restaging cutaneous angiosarcoma of the scalp. Clin Nucl Med. 2006;31:534–7.
148. Freudenberg LS, Rosenbaum SJ, Schulte-Herbruggen J, et al. Diagnosis of a cardiac angiosarcoma by fluorine-18 fluordeoxyglucose positron emission tomography. Eur Radiol. 2002;12 Suppl 3:S158–61.
149. Shimada K, Nakamoto Y, Isoda H, et al. FDG PET for giant cavernous hemangioma: important clue to differentiate from a malignant vascular tumor in the liver. Clin Nucl Med. 2010;35:924–6.
150. Drevelegas A, Pilavaki M, Chourmouzi D. Lipomatous tumors of soft tissue: MR appearance with histological correlation. Eur J Radiol. 2004;50:257–67.
151. Sheah K, Ouellette HA, Torriani M, et al. Metastatic myxoid liposarcomas: imaging and histopathologic findings. Skeletal Radiol. 2008;37:251–8.
152. Murphey MD, Arcara LK, Fanburg-Smith J. From the archives of the AFIP: imaging of musculoskeletal liposarcoma with radiologic-pathologic correlation. Radiographics. 2005;25:1371–95.

153. Song T, Shen J, Liang BL, et al. Retroperitoneal liposarcoma: MR characteristics and pathological correlative analysis. Abdom Imaging. 2007;32:668–74.
154. van Vliet M, Kliffen M, Krestin GP, et al. Soft tissue sarcomas at a glance: clinical, histological, and MR imaging features of malignant extremity soft tissue tumors. Eur Radiol. 2009;19:1499–511.
155. Jelinek JS, Kransdorf MJ, Shmookler BM, et al. Liposarcoma of the extremities: MR and CT findings in the histologic subtypes. Radiology. 1993;186:455–9.
156. Sreekantaiah C, Karakousis CP, Leong SP, et al. Cytogenetic findings in liposarcoma correlate with histopathologic subtypes. Cancer. 1992;69:2484–95.
157. Kuroda M, Ishida T, Takanashi M, et al. Oncogenic transformation and inhibition of adipocytic conversion of preadipocytes by TLS/FUS-CHOP type II chimeric protein. Am J Pathol. 1997;151:735–44.
158. Panagopoulos I, Hoglund M, Mertens F, et al. Fusion of the EWS and CHOP genes in myxoid liposarcoma. Oncogene. 1996;12:489–94.
159. Bode-Lesniewska B, Frigerio S, Exner U, et al. Relevance of translocation type in myxoid liposarcoma and identification of a novel EWSR1-DDIT3 fusion. Genes Chromosomes Cancer. 2007;46:961–71.
160. Romeo S, Dei Tos AP. Soft tissue tumors associated with EWSR1 translocation. Virchows Arch. 2010;456:219–34.
161. Debelenko LV, Perez-Atayde AR, Dubois SG, et al. p53+/mdm2-atypical lipomatous tumor/well-differentiated liposarcoma in young children: an early expression of Li-Fraumeni syndrome. Pediatr Dev Pathol. 2010;13:218–24.
162. Schwarzbach MH, Dimitrakopoulou-Strauss A, Mechtersheimer G, et al. Assessment of soft tissue lesions suspicious for liposarcoma by F18-deoxyglucose (FDG) positron emission tomography (PET). Anticancer Res. 2001;21:3609–14.
163. Sirvent N, Coindre JM, Maire G, et al. Detection of MDM2-CDK4 amplification by fluorescence in situ hybridization in 200 paraffin-embedded tumor samples: utility in diagnosing adipocytic lesions and comparison with immunohistochemistry and real-time PCR. Am J Surg Pathol. 2007;31:1476–89.
164. Taubert H, Wurl P, Meye A, et al. Molecular and immunohistochemical p53 status in liposarcoma and malignant fibrous histiocytoma: identification of seven new mutations for soft tissue sarcomas. Cancer. 1995;76:1187–96.
165. Weiss SW, Rao VK. Well-differentiated liposarcoma (atypical lipoma) of deep soft tissue of the extremities, retroperitoneum, and miscellaneous sites. A follow-up study of 92 cases with analysis of the incidence of "dedifferentiation". Am J Surg Pathol. 1992;16:1051–8.
166. Hisaoka M, Morimitsu Y, Hashimoto H, et al. Retroperitoneal liposarcoma with combined well-differentiated and myxoid malignant fibrous histiocytoma-like myxoid areas. Am J Surg Pathol. 1999;23:1480–92.
167. Leach FS, Tokino T, Meltzer P, et al. p53 Mutation and MDM2 amplification in human soft tissue sarcomas. Cancer Res. 1993;53:2231–4.
168. Newton Jr WA, Gehan EA, Webber BL, et al. Classification of rhabdomyosarcomas and related sarcomas. Pathologic aspects and proposal for a new classification – an Intergroup Rhabdomyosarcoma Study. Cancer. 1995;76:1073–85.
169. Davicioni E, Anderson MJ, Finckenstein FG, et al. Molecular classification of rhabdomyosarcoma–genotypic and phenotypic determinants of diagnosis: a report from the Children's Oncology Group. Am J Pathol. 2009;174:550–64.
170. Scrable H, Witte D, Shimada H, et al. Molecular differential pathology of rhabdomyosarcoma. Genes Chromosomes Cancer. 1989;1:23–35.
171. Xia SJ, Pressey JG, Barr FG. Molecular pathogenesis of rhabdomyosarcoma. Cancer Biol Ther. 2002;1:97–104.
172. Anderson J, Gordon A, Pritchard-Jones K, et al. Genes, chromosomes, and rhabdomyosarcoma. Genes Chromosomes Cancer. 1999;26:275–85.
173. Morotti RA, Nicol KK, Parham DM, et al. An immunohistochemical algorithm to facilitate diagnosis and subtyping of rhabdomyosarcoma: the Children's Oncology Group experience. Am J Surg Pathol. 2006;30:962–8.
174. Folpe AL. MyoD1 and myogenin expression in human neoplasia: a review and update. Adv Anat Pathol. 2002;9:198–203.
175. Ebauer M, Wachtel M, Niggli FK, et al. Comparative expression profiling identifies an in vivo target gene signature with TFAP2B as a mediator of the survival function of PAX3/FKHR. Oncogene. 2007;26:7267–81.
176. Bridge JA, Liu J, Weibolt V, et al. Novel genomic imbalances in embryonal rhabdomyosarcoma revealed by comparative genomic hybridization and fluorescence in situ hybridization: an Intergroup Rhabdomyosarcoma Study. Genes Chromosomes Cancer. 2000;27: 337–44.
177. Raney RB, Walterhouse DO, Meza JL, et al. Results of the Intergroup Rhabdomyosarcoma Study Group D9602 protocol, using vincristine and dactinomycin with or without cyclophosphamide and radiation therapy, for newly diagnosed patients with low-risk embryonal rhabdomyosarcoma: a report from the Soft Tissue Sarcoma Committee of the Children's Oncology Group. J Clin Oncol. 2011;29:1312–8.
178. Joshi D, Anderson JR, Paidas C, et al. Age is an independent prognostic factor in rhabdomyosarcoma: a report from the Soft Tissue Sarcoma Committee of the Children's Oncology Group. Pediatr Blood Cancer. 2004;42:64–73.
179. Arndt CA, Stoner JA, Hawkins DS, et al. Vincristine, actinomycin, and cyclophosphamide compared with vincristine, actinomycin, and cyclophosphamide alternating with vincristine, topotecan, and cyclophosphamide for intermediate-risk rhabdomyosarcoma: Children's Oncology Group study D9803. J Clin Oncol. 2009;27:5182–8.
180. Lager JJ, Lyden ER, Anderson JR, et al. Pooled analysis of phase II window studies in children with contemporary high-risk metastatic rhabdomyosarcoma: a report from the Soft Tissue Sarcoma Committee of the Children's Oncology Group. J Clin Oncol. 2006;24:3415–22.
181. Wexler LH, Ladanyi M. Diagnosing alveolar rhabdomyosarcoma: morphology must be coupled with fusion confirmation. J Clin Oncol. 2010;28:2126–8.
182. Parham DM, Barr FG. Classification of rhabdomyosarcoma and its molecular basis. Adv Anat Pathol. 2013;20:387–97.
183. Riopelle JL, Theriault JP. An unknown type of soft part sarcoma: alveolar rhabdomyosarcoma. Ann Anat Pathol (Paris). 1956;1: 88–111.
184. Tsokos M, Webber BL, Parham DM, et al. Rhabdomyosarcoma. A new classification scheme related to prognosis. Arch Pathol Lab Med. 1992;116:847–55.
185. Pinto A, Tallini G, Novak RW, et al. Undifferentiated rhabdomyosarcoma with lymphoid phenotype expression. Med Pediatr Oncol. 1997;28:165–70.
186. Gonzalez-Crussi F, Black-Schaffer S. Rhabdomyosarcoma of infancy and childhood. Problems of morphologic classification. Am J Surg Pathol. 1979;3:157–71.
187. Harms D. Alveolar rhabdomyosarcoma: a prognostically unfavorable rhabdomyosarcoma type and its necessary distinction from embryonal rhabdomyosarcoma. Curr Top Pathol. 1995;89:273–96.
188. Wang NP, Marx J, McNutt MA, et al. Expression of myogenic regulatory proteins (myogenin and MyoD1) in small blue round cell tumors of childhood. Am J Pathol. 1995;147:1799–810.
189. Wachtel M, Runge T, Leuschner I, et al. Subtype and prognostic classification of rhabdomyosarcoma by immunohistochemistry. J Clin Oncol. 2006;24:816–22.

190. Barr FG, Smith LM, Lynch JC, et al. Examination of gene fusion status in archival samples of alveolar rhabdomyosarcoma entered on the Intergroup Rhabdomyosarcoma Study-III trial: a report from the Children's Oncology Group. J Mol Diagn. 2006;8:202–8.
191. Tobar A, Avigad S, Zoldan M, et al. Clinical relevance of molecular diagnosis in childhood rhabdomyosarcoma. Diagn Mol Pathol. 2000;9:9–13.
192. Nishio J, Althof PA, Bailey JM, et al. Use of a novel FISH assay on paraffin-embedded tissues as an adjunct to diagnosis of alveolar rhabdomyosarcoma. Lab Invest. 2006;86:547–56.
193. Shapiro DN, Parham DM, Douglass EC, et al. Relationship of tumor-cell ploidy to histologic subtype and treatment outcome in children and adolescents with unresectable rhabdomyosarcoma. J Clin Oncol. 1991;9:159–66.
194. Smith LM, Anderson JR, Qualman SJ, et al. Which patients with microscopic disease and rhabdomyosarcoma experience relapse after therapy? A report from the soft tissue sarcoma committee of the children's oncology group. J Clin Oncol. 2001;19:4058–64.
195. Douglass EC, Shapiro DN, Valentine M, et al. Alveolar rhabdomyosarcoma with the t(2;13): cytogenetic findings and clinicopathologic correlations. Med Pediatr Oncol. 1993;21:83–7.
196. Lae M, Ahn EH, Mercado GE, et al. Global gene expression profiling of PAX-FKHR fusion-positive alveolar and PAX-FKHR fusion-negative embryonal rhabdomyosarcomas. J Pathol. 2007;212:143–51.
197. Williamson D, Missiaglia E, de Reynies A, et al. Fusion gene-negative alveolar rhabdomyosarcoma is clinically and molecularly indistinguishable from embryonal rhabdomyosarcoma. J Clin Oncol. 2010;28:2151–8.
198. Sorensen PH, Lynch JC, Qualman SJ, et al. PAX3-FKHR and PAX7-FKHR gene fusions are prognostic indicators in alveolar rhabdomyosarcoma: a report from the children's oncology group. J Clin Oncol. 2002;20:2672–9.
199. de Saint Aubain Somerhausen N, Fletcher CD. Leiomyosarcoma of soft tissue in children: clinicopathologic analysis of 20 cases. Am J Surg Pathol. 1999;23:755–63.
200. Ferrari A, Bisogno G, Casanova M, et al. Childhood leiomyosarcoma: a report from the soft tissue sarcoma Italian Cooperative Group. Ann Oncol. 2001;12:1163–8.
201. Hwang ES, Gerald W, Wollner N, et al. Leiomyosarcoma in childhood and adolescence. Ann Surg Oncol. 1997;4:223–7.
202. Parham DM, Alaggio R, Coffin CM. Myogenic tumors in children and adolescents. Pediatr Dev Pathol. 2012;15:211–38.
203. Akwari OE, Dozois RR, Weiland LH, et al. Leiomyosarcoma of the small and large bowel. Cancer. 1978;42:1375–84.
204. McLeod AJ, Zornoza J, Shirkhoda A. Leiomyosarcoma: computed tomographic findings. Radiology. 1984;152:133–6.
205. Bush CH, Reith JD, Spanier SS. Mineralization in musculoskeletal leiomyosarcoma: radiologic-pathologic correlation. AJR Am J Roentgenol. 2003;180:109–13.
206. Hartman DS, Hayes WS, Choyke PL, et al. From the archives of the AFIP. Leiomyosarcoma of the retroperitoneum and inferior vena cava: radiologic-pathologic correlation. Radiographics. 1992;12:1203–20.
207. Megibow AJ, Balthazar EJ, Hulnick DH, et al. CT evaluation of gastrointestinal leiomyomas and leiomyosarcomas. AJR Am J Roentgenol. 1985;144:727–31.
208. Levy AD, Remotti HE, Thompson WM, et al. Gastrointestinal stromal tumors: radiologic features with pathologic correlation. Radiographics. 2003;23:283–304.
209. Sabah M, Cummins R, Leader M, et al. Leiomyosarcoma and malignant fibrous histiocytoma share similar allelic imbalance pattern at 9p. Virchows Arch. 2005;446:251–8.
210. Ragazzini P, Gamberi G, Pazzaglia L, et al. Amplification of CDK4, MDM2, SAS and GLI genes in leiomyosarcoma, alveolar and embryonal rhabdomyosarcoma. Histol Histopathol. 2004;19:401–11.
211. Seidel C, Bartel F, Rastetter M, et al. Alterations of cancer-related genes in soft tissue sarcomas: hypermethylation of RASSF1A is frequently detected in leiomyosarcoma and associated with poor prognosis in sarcoma. Int J Cancer. 2005;114:442–7.
212. Deyrup AT, Lee VK, Hill CE, et al. Epstein-Barr virus-associated smooth muscle tumors are distinctive mesenchymal tumors reflecting multiple infection events: a clinicopathologic and molecular analysis of 29 tumors from 19 patients. Am J Surg Pathol. 2006;30:75–82.
213. Parham DM, Reynolds AB, Webber BL. Use of monoclonal antibody 1H1, anticortactin, to distinguish normal and neoplastic smooth muscle cells: comparison with anti-alpha-smooth muscle actin and antimuscle-specific actin. Hum Pathol. 1995;26:776–83.
214. Schmidt D, Thum P, Harms D, et al. Synovial sarcoma in children and adolescents. A report from the Kiel Pediatric Tumor Registry. Cancer. 1991;67:1667–72.
215. Iyengar V, Lineberger AS, Kerman S, et al. Synovial sarcoma of the heart. Correlation with cytogenetic findings. Arch Pathol Lab Med. 1995;119:1080–2.
216. Zenmyo M, Komiya S, Hamada T, et al. Intraneural monophasic synovial sarcoma: a case report. Spine (Phila Pa 1976). 2001;26:310–3.
217. Chu PG, Benhattar J, Weiss LM, et al. Intraneural synovial sarcoma: two cases. Mod Pathol. 2004;17:258–63.
218. McCarville MB, Spunt SL, Skapek SX, et al. Synovial sarcoma in pediatric patients. AJR Am J Roentgenol. 2002;179:797–801.
219. Coffin C. Synovial-based tumors and synovial sarcoma. In: Coffin CMOSP, Dehner LP, editors. Pediatric soft tissue tumors: a clinical, pathological and therapeutic approach. Baltimore, MD: Williams and Wilkins; 1997. p. 295–310.
220. Jones BC, Sundaram M, Kransdorf MJ. Synovial sarcoma: MR imaging findings in 34 patients. AJR Am J Roentgenol. 1993;161:827–30.
221. Cadman NL, Soule EH, Kelly PJ. Synovial sarcoma; an analysis of 34 tumors. Cancer. 1965;18:613–27.
222. Morton MJ, Berquist TH, McLeod RA, et al. MR imaging of synovial sarcoma. AJR Am J Roentgenol. 1991;156:337–40.
223. Berquist TH, Ehman RL, King BF, et al. Value of MR imaging in differentiating benign from malignant soft-tissue masses: study of 95 lesions. AJR Am J Roentgenol. 1990;155:1251–5.
224. Folpe AL, Schmidt RA, Chapman D, et al. Poorly differentiated synovial sarcoma: immunohistochemical distinction from primitive neuroectodermal tumors and high-grade malignant peripheral nerve sheath tumors. Am J Surg Pathol. 1998;22:673–82.
225. Kosemehmetoglu K, Vrana JA, Folpe AL. TLE1 expression is not specific for synovial sarcoma: a whole section study of 163 soft tissue and bone neoplasms. Mod Pathol. 2009;22:872–8.
226. Fritsch MK, Bridge JA, Schuster AE, et al. Performance characteristics of a reverse transcriptase-polymerase chain reaction assay for the detection of tumor-specific fusion transcripts from archival tissue. Pediatr Dev Pathol. 2003;6:43–53.
227. Sun B, Sun Y, Wang J, et al. The diagnostic value of SYT-SSX detected by reverse transcriptase-polymerase chain reaction (RT-PCR) and fluorescence in situ hybridization (FISH) for synovial sarcoma: a review and prospective study of 255 cases. Cancer Sci. 2008;99:1355–61.
228. Oda Y, Hashimoto H, Tsuneyoshi M, et al. Survival in synovial sarcoma. A multivariate study of prognostic factors with special emphasis on the comparison between early death and long-term survival. Am J Surg Pathol. 1993;17:35–44.
229. Lieberman PH, Brennan MF, Kimmel M, et al. Alveolar soft-part sarcoma. A clinico-pathologic study of half a century. Cancer. 1989;63:1–13.

230. Pappo AS, Parham DM, Cain A, et al. Alveolar soft part sarcoma in children and adolescents: clinical features and outcome of 11 patients. Med Pediatr Oncol. 1996;26:81–4.
231. Guillou L, Lamoureux E, Masse S, et al. Alveolar soft-part sarcoma of the uterine corpus: histological, immunocytochemical and ultrastructural study of a case. Virchows Arch A Pathol Anat Histopathol. 1991;418:467–71.
232. Folpe AL, Deyrup AT. Alveolar soft-part sarcoma: a review and update. J Clin Pathol. 2006;59:1127–32.
233. Tucker JA. Crystal-deficient alveolar soft part sarcoma. Ultrastruct Pathol. 1993;17:279–86.
234. Carstens HB. Membrane-bound cytoplasmic crystals, similar to those in alveolar soft part sarcoma, in a human muscle spindle. Ultrastruct Pathol. 1990;14:423–8.
235. Sciot R, Dal Cin P, De Vos R, et al. Alveolar soft-part sarcoma: evidence for its myogenic origin and for the involvement of 17q25. Histopathology. 1993;23:439–44.
236. Heller DS, Frydman CP, Gordon RE, et al. An unusual organoid tumor. Alveolar soft part sarcoma or paraganglioma? Cancer. 1991;67:1894–9.
237. Ordonez NG. Alveolar soft part sarcoma: a review and update. Adv Anat Pathol. 1999;6:125–39.
238. Wang NP, Bacchi CE, Jiang JJ, et al. Does alveolar soft-part sarcoma exhibit skeletal muscle differentiation? An immunocytochemical and biochemical study of myogenic regulatory protein expression. Mod Pathol. 1996;9:496–506.
239. Wen MC, Jan YJ, Li MC, et al. Monotypic epithelioid angiomyolipoma of the liver with TFE3 expression. Pathology. 2010;42:300–2.
240. Pang LJ, Chang B, Zou H, et al. Alveolar soft part sarcoma: a bimarker diagnostic strategy using TFE3 immunoassay and ASPL-TFE3 fusion transcripts in paraffin-embedded tumor tissues. Diagn Mol Pathol. 2008;17:245–52.
241. Folpe AL, Goodman ZD, Ishak KG, et al. Clear cell myomelanocytic tumor of the falciform ligament/ligamentum teres: a novel member of the perivascular epithelioid clear cell family of tumors with a predilection for children and young adults. Am J Surg Pathol. 2000;24:1239–46.
242. Sawyer JR, Nicholas RW, Parham DM. A novel t(X;2)(q13;q35) in clear cell sugar tumor of bone. Cancer Genet Cytogenet. 2004;154:77–80.
243. Yamashita K, Fletcher CD. PEComa presenting in bone: clinicopathologic analysis of 6 cases and literature review. Am J Surg Pathol. 2010;34:1622–9.
244. Hornick JL, Fletcher CD. Sclerosing PEComa: clinicopathologic analysis of a distinctive variant with a predilection for the retroperitoneum. Am J Surg Pathol. 2008;32:493–501.
245. Cho HY, Chung DH, Khurana H, et al. The role of TFE3 in PEComa. Histopathology. 2008;53:236–49.
246. Hornick JL, Fletcher CD. PEComa: what do we know so far? Histopathology. 2006;48:75–82.
247. Folpe AL, Mentzel T, Lehr HA, et al. Perivascular epithelioid cell neoplasms of soft tissue and gynecologic origin: a clinicopathologic study of 26 cases and review of the literature. Am J Surg Pathol. 2005;29:1558–75.
248. Wick MR, Ritter JH, Dehner LP. Malignant rhabdoid tumors: a clinicopathologic review and conceptual discussion. Semin Diagn Pathol. 1995;12:233–48.
249. Parham DM, Weeks DA, Beckwith JB. The clinicopathologic spectrum of putative extrarenal rhabdoid tumors. An analysis of 42 cases studied with immunohistochemistry or electron microscopy. Am J Surg Pathol. 1994;18:1010–29.
250. Hsueh C, Kuo TT. Congenital malignant rhabdoid tumor presenting as a cutaneous nodule: report of 2 cases with review of the literature. Arch Pathol Lab Med. 1998;122:1099–102.
251. Abdullah A, Patel Y, Lewis TJ, et al. Extrarenal malignant rhabdoid tumors: radiologic findings with histopathologic correlation. Cancer Imaging. 2010;10:97–101.
252. Ferrari A, Orbach D, Sultan I, et al. Neonatal soft tissue sarcomas. Semin Fetal Neonatal Med. 2012;17:231–8.
253. Hollmann TJ, Hornick JL. INI1-deficient tumors: diagnostic features and molecular genetics. Am J Surg Pathol. 2011;35:e47–63.
254. Hoot AC, Russo P, Judkins AR, et al. Immunohistochemical analysis of hSNF5/INI1 distinguishes renal and extra-renal malignant rhabdoid tumors from other pediatric soft tissue tumors. Am J Surg Pathol. 2004;28:1485–91.
255. Eaton KW, Tooke LS, Wainwright LM, et al. Spectrum of SMARCB1/INI1 mutations in familial and sporadic rhabdoid tumors. Pediatr Blood Cancer. 2011;56:7–15.
256. Beckwith JB, Palmer NF. Histopathology and prognosis of Wilms tumors: results from the First National Wilms' Tumor Study. Cancer. 1978;41:1937–48.
257. Haas JE, Palmer NF, Weinberg AG, et al. Ultrastructure of malignant rhabdoid tumor of the kidney. A distinctive renal tumor of children. Hum Pathol. 1981;12:646–57.
258. Weeks DA, Beckwith JB, Mierau GW, et al. Rhabdoid tumor of kidney. A report of 111 cases from the National Wilms' Tumor Study Pathology Center. Am J Surg Pathol. 1989;13:439–58.
259. Perry A, Fuller CE, Judkins AR, et al. INI1 expression is retained in composite rhabdoid tumors, including rhabdoid meningiomas. Mod Pathol. 2005;18:951–8.
260. Douglass EC, Valentine M, Rowe ST, et al. Malignant rhabdoid tumor: a highly malignant childhood tumor with minimal karyotypic changes. Genes Chromosomes Cancer. 1990;2:210–6.
261. Biegel JA. Molecular genetics of atypical teratoid/rhabdoid tumor. Neurosurg Focus. 2006;20:E11.
262. Sawyer JR, Goosen LS, Swanson CM, et al. A new reciprocal translocation (12;22)(q24.3;q11.2-12) in a malignant rhabdoid tumor of the brain. Cancer Genet Cytogenet. 1998;101:62–7.
263. Bruch LA, Hill DA, Cai DX, et al. A role for fluorescence in situ hybridization detection of chromosome 22q dosage in distinguishing atypical teratoid/rhabdoid tumors from medulloblastoma/central primitive neuroectodermal tumors. Hum Pathol. 2001;32:156–62.
264. Gururangan S, Bowman LC, Parham DM, et al. Primary extracranial rhabdoid tumors. Clinicopathologic features and response to ifosfamide. Cancer. 1993;71:2653–9.
265. Jayaram A, Finegold MJ, Parham DM, et al. Successful management of rhabdoid tumor of the liver. J Pediatr Hematol Oncol. 2007;29:406–8.
266. Gross E, Rao BN, Pappo A, et al. Epithelioid sarcoma in children. J Pediatr Surg. 1996;31:1663–5.
267. Sugarbaker PH, Auda S, Webber BL, et al. Early distant metastases from epithelioid sarcoma of the hand. Cancer. 1981;48:852–5.
268. Hornick JL, Dal Cin P, Fletcher CD. Loss of INI1 expression is characteristic of both conventional and proximal-type epithelioid sarcoma. Am J Surg Pathol. 2009;33:542–50.
269. Hanna SL, Kaste S, Jenkins JJ, et al. Epithelioid sarcoma: clinical, MR imaging and pathologic findings. Skeletal Radiol. 2002;31:400–12.
270. Sakamoto A, Jono O, Hirahashi M, et al. Epithelioid sarcoma with muscle metastasis detected by positron emission tomography. World J Surg Oncol. 2008;6:84.
271. Mirra JM, Kessler S, Bhuta S, et al. The fibroma-like variant of epithelioid sarcoma. A fibrohistiocytic/myoid cell lesion often confused with benign and malignant spindle cell tumors. Cancer. 1992;69:1382–95.
272. Perrone T, Swanson PE, Twiggs L, et al. Malignant rhabdoid tumor of the vulva: is distinction from epithelioid sarcoma possible? A pathologic and immunohistochemical study. Am J Surg Pathol. 1989;13:848–58.

273. Arber DA, Kandalaft PL, Mehta P, et al. Vimentin-negative epithelioid sarcoma. The value of an immunohistochemical panel that includes CD34. Am J Surg Pathol. 1993;17:302–7.
274. Gerharz CD, Moll R, Meister P, et al. Cytoskeletal heterogeneity of an epithelioid sarcoma with expression of vimentin, cytokeratins, and neurofilaments. Am J Surg Pathol. 1990;14:274–83.
275. Cordoba JC, Parham DM, Meyer WH, et al. A new cytogenetic finding in an epithelioid sarcoma, t(8;22)(q22;q11). Cancer Genet Cytogenet. 1994;72:151–4.
276. Raoux D, Peoc'h M, Pedeutour F, et al. Primary epithelioid sarcoma of bone: report of a unique case, with immunohistochemical and fluorescent in situ hybridization confirmation of INI1 deletion. Am J Surg Pathol. 2009;33:954–8.
277. Chase DR, Enzinger FM. Epithelioid sarcoma. Diagnosis, prognostic indicators, and treatment. Am J Surg Pathol. 1985;9:241–63.
278. Prat J, Woodruff JM, Marcove RC. Epithelioid sarcoma: an analysis of 22 cases indicating the prognostic significance of vascular invasion and regional lymph node metastasis. Cancer. 1978;41: 1472–87.
279. Spillane AJ, Thomas JM, Fisher C. Epithelioid sarcoma: the clinicopathological complexities of this rare soft tissue sarcoma. Ann Surg Oncol. 2000;7:218–25.
280. Fisher C. Epithelioid sarcoma of Enzinger. Adv Anat Pathol. 2006;13:114–21.
281. Hisaoka M, Ishida T, Kuo TT, et al. Clear cell sarcoma of soft tissue: a clinicopathologic, immunohistochemical, and molecular analysis of 33 cases. Am J Surg Pathol. 2008;32:452–60.
282. Lucas DR, Nascimento AG, Sim FH. Clear cell sarcoma of soft tissues. Mayo Clinic experience with 35 cases. Am J Surg Pathol. 1992;16:1197–204.
283. Meis-Kindblom JM. Clear cell sarcoma of tendons and aponeuroses: a historical perspective and tribute to the man behind the entity. Adv Anat Pathol. 2006;13:286–92.
284. Stacy GS, Nair L. Magnetic resonance imaging features of extremity sarcomas of uncertain differentiation. Clin Radiol. 2007;62: 950–8.
285. Davis IJ, Kim JJ, Ozsolak F, et al. Oncogenic MITF dysregulation in clear cell sarcoma: defining the MiT family of human cancers. Cancer Cell. 2006;9:473–84.
286. Jones RL, Constantinidou A, Thway K, et al. Chemotherapy in clear cell sarcoma. Med Oncol. 2011;28:859–63.
287. Dabska M. Parachordoma: a new clinicopathologic entity. Cancer. 1977;40:1586–92.
288. Gleason BC, Fletcher CD. Myoepithelial carcinoma of soft tissue in children: an aggressive neoplasm analyzed in a series of 29 cases. Am J Surg Pathol. 2007;31:1813–24.
289. Huang CC, Cheng SM. Clinical and radiological presentations of pelvic parachordoma. Rare Tumors. 2012;4:e5.
290. Antonescu CR, Zhang L, Chang NE, et al. EWSR1-POU5F1 fusion in soft tissue myoepithelial tumors. A molecular analysis of sixty-six cases, including soft tissue, bone, and visceral lesions, showing common involvement of the EWSR1 gene. Genes Chromosomes Cancer. 2010;49:1114–24.
291. Hornick JL, Fletcher CD. Myoepithelial tumors of soft tissue: a clinicopathologic and immunohistochemical study of 101 cases with evaluation of prognostic parameters. Am J Surg Pathol. 2003;27:1183–96.
292. Tirabosco R, Mangham DC, Rosenberg AE, et al. Brachyury expression in extra-axial skeletal and soft tissue chordomas: a marker that distinguishes chordoma from mixed tumor/myoepithelioma/parachordoma in soft tissue. Am J Surg Pathol. 2008;32:572–80.
293. Lae ME, Roche PC, Jin L, et al. Desmoplastic small round cell tumor: a clinicopathologic, immunohistochemical, and molecular study of 32 tumors. Am J Surg Pathol. 2002;26:823–35.
294. Gerald WL, Miller HK, Battifora H, et al. Intra-abdominal desmoplastic small round-cell tumor. Report of 19 cases of a distinctive type of high-grade polyphenotypic malignancy affecting young individuals. Am J Surg Pathol. 1991;15:499–513.
295. Levy AD, Arnaiz J, Shaw JC, et al. From the archives of the AFIP: primary peritoneal tumors: imaging features with pathologic correlation. Radiographics. 2008;28:583–607. quiz 621–582.
296. Zhang WD, Li CX, Liu QY, et al. CT, MRI, and FDG-PET/CT imaging findings of abdominopelvic desmoplastic small round cell tumors: correlation with histopathologic findings. Eur J Radiol. 2011;80:269–73.
297. de Alava E, Ladanyi M, Rosai J, et al. Detection of chimeric transcripts in desmoplastic small round cell tumor and related developmental tumors by reverse transcriptase polymerase chain reaction. A specific diagnostic assay. Am J Pathol. 1995; 147:1584–91.
298. Ordonez NG. Desmoplastic small round cell tumor: I: a histopathologic study of 39 cases with emphasis on unusual histological patterns. Am J Surg Pathol. 1998;22:1303–13.
299. Alaggio R, Rosolen A, Sartori F, et al. Spindle cell tumor with EWS-WT1 transcript and a favorable clinical course: a variant of DSCT, a variant of leiomyosarcoma, or a new entity? Report of 2 pediatric cases. Am J Surg Pathol. 2007;31:454–9.
300. Zhang PJ, Goldblum JR, Pawel BR, et al. Immunophenotype of desmoplastic small round cell tumors as detected in cases with EWS-WT1 gene fusion product. Mod Pathol. 2003;16:229–35.
301. Sawyer JR, Tryka AF, Lewis JM. A novel reciprocal chromosome translocation t(11;22)(p13;q12) in an intraabdominal desmoplastic small round-cell tumor. Am J Surg Pathol. 1992;16:411–6.
302. Al Balushi Z, Bulduc S, Mulleur C, et al. Desmoplastic small round cell tumor in children: a new therapeutic approach. J Pediatr Surg. 2009;44:949–52.
303. Pawel BR, Hamoudi AB, Asmar L, et al. Undifferentiated sarcomas of children: pathology and clinical behavior – an Intergroup Rhabdomyosarcoma study. Med Pediatr Oncol. 1997;29:170–80.
304. Kawamura-Saito M, Yamazaki Y, Kaneko K, et al. Fusion between CIC and DUX4 up-regulates PEA3 family genes in Ewing-like sarcomas with t(4;19)(q35;q13) translocation. Hum Mol Genet. 2006;15:2125–37.
305. Choi EY, Thomas DG, McHugh JB, et al. Undifferentiated small round cell sarcoma with t(4;19)(q35;q13.1) CIC-DUX4 fusion: a novel highly aggressive soft tissue tumor with distinctive histopathology. Am J Surg Pathol. 2013;37:1379–86.
306. Machado I, Cruz J, Lavernia J, et al. Superficial EWSR1-negative undifferentiated small round cell sarcoma with CIC/DUX4 gene fusion: a new variant of Ewing-like tumors with locoregional lymph node metastasis. Virchows Arch. 2013;463:837–42.
307. Italiano A, Sung YS, Zhang L, et al. High prevalence of CIC fusion with double-homeobox (DUX4) transcription factors in EWSR1-negative undifferentiated small blue round cell sarcomas. Genes Chromosomes Cancer. 2012;51:207–18.
308. Kajtar B, Tornoczky T, Kalman E, et al. CD99-positive undifferentiated round cell sarcoma diagnosed on fine needle aspiration cytology, later found to harbour a CIC-DUX4 translocation: a recently described entity. Cytopathology. 2014;25:129–32.